Biochemical characterisation of Pfj2, a *Plasmodium falciparum* heat shock protein 40 chaperone potentially involved in protein quality control in the endoplasmic reticulum

A dissertation submitted in fulfilment of the requirements for the degree

of

MASTER OF SCIENCE IN BIOCHEMISTRY

of

RHODES UNIVERSITY

in the

FACULTY OF SCIENCE

DEPARTMENT OF BIOCHEMISTRY, MICROBIOLOGY AND BIOTECHNOLOGY

by

OMOLOLA AFOLAYAN

March 2012

Abstract

Plasmodium falciparum is a protozoan parasite that causes a severe form of malaria, a mosquito-borne infectious disease in humans. *P. falciparum* encodes a number of proteins to facilitate its life-cycle, including a type II heat shock protein 40 (Hsp40), Pfj2. Pfj2 shows a degree of homology to human ERdj5, a resident protein of the endoplasmic reticulum (ER) that promotes protein quality control by facilitating the degradation of misfolded proteins. The overall aim of this study was to further understand the function of Pfj2 in the *P. falciparum* cell by characterising it biochemically. A bioinformatic analysis of Pfj2 was carried out to enable the identification of a potential ER signal sequence and cleavage site. Furthermore, an analysis of Pfj2 protein sequence was performed to compare domain similarities and identities with typical type II Hsp40s namely, human ERdj5, *S. cerevisiae* Sis1, human Hsj1a and human DnaJB4. The method used included the insertion of the codon-optimised coding sequence for the processed ER form of Pfj2 into the prokaryotic expression vector, pQE30, to enable overproduction of a histidine-tagged protein. A 62 kDa His_6-Pfj2 was successfully expressed in *Escherichia coli* and purified using denaturing nickel affinity chromatography. ATPase assays were performed to determine the ability of His_6-Pfj2 to stimulate the chaperone activity of the ER Hsp70, also called immunoglobulin binding protein (BiP). Initial studies were conducted on readily available mammalian His_6-BiP as a control, which was shown to have an intrinsic activity of 12.07±3.92 nmolPi/min/mg. His_6-Pfj2 did not stimulate the ATPase activity of mammalian His_6-BiP, suggesting that it either could not act as a co-chaperone of mammalian His_6-BiP (specificity), or it required a misfolded substrate in the system. Therefore, ongoing studies are addressing the interaction of Pfj2 and misfolded substrates with *P. falciparum* BiP. The results of these studies will further our understanding of a poorly-studied parasite chaperone that represents a potential drug target for development of novel strategies for the control of a serious human disease.

Declaration

I, Omolola Afolayan, hereby declare that this thesis represents my own work and that I have not submitted it to this or any other institution in application for admission to a degree, diploma or any other qualification.

Acknowledgements

I would like to thank:

- My supervisor Professor Gregory Blatch for his guidance, dedication and for sharing his expertise with me throughout my study period.
- Co-supervisors, Dr Eva-Rachele Pesce for academic assistance and advice right through the duration of my study, and Dr Caroline Knox for her assistance in editing my dissertation and her willingness to help.
- Biomedical Biotechnology Research Unit (BioBRU) in the Department of Biochemistry, Microbiology and Biotechnology for providing facilities and technical support that enabled me to complete this project.
- National Research Foundation (NRF), Medical Research Council (MRC) and Japan Science and Technology Agency (JST) for funding.
- Professor Nagata's laboratory, Kyoto Sangyo University, Japan for collaborative inputs academically, financially and allowing me to do some experiment in their laboratory.
- My family, especially my sister Anthonia F Afolayan for continuous encouragement and constant support emotionally and financially.
- God for giving me the strength to complete my study.

Table of Contents

List of Figures

List of Tables

List of Abbreviations

α	Alpha
β	Beta
λ	Lambda
µg	Microgram
µl	Microlitre
µM	Micromolar
%	Percentage
° C	Degrees Centigrade
3-D	Three Dimensional
A_{600}	Absorbance at 600nm
ADP	Adenosine Diphosphate
Agt	*Agrobacterium tumefaciens*
Amp^R	Ampicillin Resistance
APS	Ammonium Persulphate
ATP	Adenosine triphosphate
bp	Base pairs
DNA	Deoxyribonucleic acid
DTT	Dithiothreitol
E. coli	*Escherichia coli*
EDTA	Ethylenediaminetetraacetic acid
ER	Endoplasmic reticulum
G/C	Guanine/cytosine
G/F	Glycine/phenylalanine
HCl	Hydrochloric acid
His	Histidine
HPD	Histidine, proline, aspartic acid
Hsp(s)	Heat shock protein(s)
Hsp40(s)	40 Kilodalton heat shock proteins(s)

Hsp70(s)	70 Kilodalton heat shock proteins(s)
HT	Host targeting signal
IPTG	Isopropyl-1-thio-β-D-galactopyranoside
KAHRP	Knob-associated histidine-rich protein
kDa	Kilodalton
LB	Liquid broth
MC(s)	Maurer's cleft(s)
mg	Milligram
ml	Millilitre
mM	Millimolar
mRNA	Messenger ribonucleic acid
Ms	*Medicago sativa*
NCBI	National Centre for Biotechnology Information
nm	Nanometres
P	Pellet
PBS	Phosphate buffered saline
PCR	Polymerase chain reaction
Pexel	*Plasmodium* export element
P. falciparum	*Plasmodium falciparum*
PfBiP	*Plasmodium falciparum* immunoglobulin binding protein
PfEMP1	*Plasmodium falciparum* erythrocyte membrane protein 1
PfHsp40	*Plasmodium falciparum* heat shock protein 40
PfHsp70	*Plasmodium falciparum* heat shock protein 70
PMSF	Phenylmethylsulfonyl fluoride
PV	Parasitophorous vacuole
RESA	Ring-infected erythrocyte surface antigen
RNA	Ribonucleic acid
S	Supernatant
S. cerevisiae	*Saccharomyces cerevisiae*

SDS	Sodium dodecyl sulphate
SDS-PAGE	Sodium dodecyl sulphate-polyacrylamide gel electrophoresis
Sis1	Yeast type II heat shock protein 40
TBE buffer	Tris, borate, EDTA buffer
TBS	Tris buffered saline
TBS-T	Tris buffered saline containing Tween-20
TEMED	N,N,N',N'-Tetramethylethylenediamine
TP	Total protein
Tris	Tris-2-amino-2-(hydroxymethyl)-1,3,propandiol
v/v	Volume per volume
w/v	Weight per volume
YT	Yeast/tryptone

CHAPTER 1
LITERATURE REVIEW

1.1. Malaria: A human health concern

Malaria is a mosquito-borne infectious disease caused by obligate intracellular protozoan parasites of the genus *Plasmodium*. Five *Plasmodium* species namely, *P. falciparum*, *P. knowlesi*, *P. malariae*, *P. ovale* and *P. vivax* are known to cause malaria in humans. *P. falciparum*, accounts for the majority of the 800, 000 malaria-associated human fatality cases each year. Most mortality cases are children under the age of five (World Health Organisation, 2012).

Malaria is one of the major health challenges facing developing countries and is responsible for high mortality rate with over 90% of cases occurring in Sub-Saharan Africa (World Health Organisation, 2012). Malaria is endemic mostly in the tropical and subtropical areas (Figure 1.1). In addition to Africa, areas with prevalent malaria transmission rate include South and Southeast Asia and Central and South America highlighted in maroon. The Middle East and the Caribbean, highlighted in pink, represents areas where malaria is largely eliminated while the remaining regions of the world, highlighted in green, are malaria-free areas. Examples of malaria-endemic countries thus include Brazil, Columbia, Kenya, Nigeria, Thailand, and Vietnam.

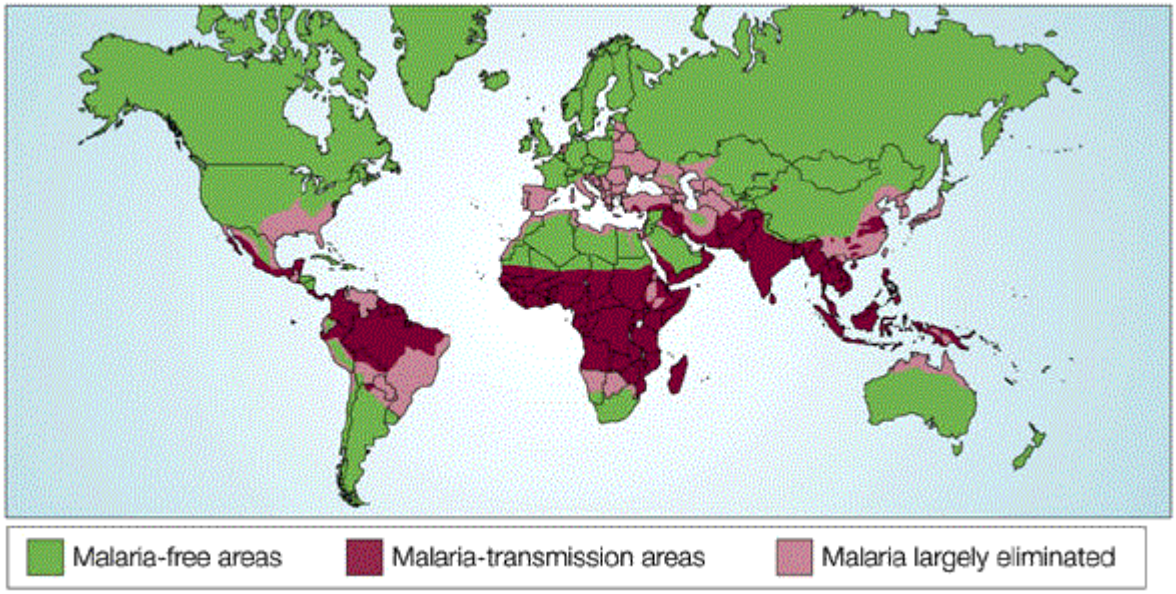

Figure 1.1: ***The geographical distribution of malaria*** (Sabeti, 2008). Green: Malaria-free areas; Maroon: Malaria-transmission areas; Pink: Areas where malaria is largely eliminated.

1.1.1. History of malaria

Malaria is an ancient disease that has been noted for over 4000 years. References to malaria related symptoms were documented in Chinese medical writing from about 2700 BC (Cox, 2010). There were speculations for over 2500 years that malaria fevers were caused by 'bad air' rising from swamps from the Italian the word 'mal'aria' which means spoiled air (Reiter, 2000). Studies on malaria intensified after the discovery of the parasite in the blood of malaria infected patients by a French scientist, Alphonse Laveran (Laveran, 1881). Ronald Ross, a British doctor, suggested that mosquito vectors are implicated in transmitting avian malaria (Ross, 1898). Italian malariologists discovered that anopheline mosquito vectors are responsible for transmission of human malaria parasite (Celli, 1933). Our understanding that the malaria parasite develops in the human liver prior to entering the blood stream was elucidated by Henry Short and Cyril Garnham in 1948 (Cox, 2010).

1.1.2. Symptoms of malaria

Malaria infections symptoms mostly manifest as fever, chills and mild anaemia (reviewed in Beare, 2006). Symptoms of high level of parasitemia, severe malaria, manifest with major signs of organ dysfunction including cerebral malaria, pulmonary edema and acute renal failure (Trampuz, 2003). Young children and pregnant women in particular are at high risk for severe malaria (Desai, 2007). A common manifestation of severe malaria in children includes seizures and hypoglycaemia whereas jaundice and renal failure are common in adults (White, 2004). Older children and adults are able to develop partial immunity after repeated infections, and are therefore at low risk for severe malaria (Desai, 2007). Although malaria can be treated and cured, many of the available antimalarial agents such as chloroquine are virtually ineffective due to the development of resistance by *P. falciparum.* (Guerin *et al*., 2002).

1.1.3. Malaria treatment

Existing approaches towards malaria control are the use of insecticides and prevention of contact with anopheline mosquito using screens and insecticide-treated bed nets (World Health Organisation, 2012). Antimalarial drugs such as chloroquine, doxycycline and

mefloquine are available but are partially or completely ineffective due to resistance (Jacquerioz and Croft, 2009). Uncontrolled use and poor quality drugs could also cause emergence of resistance (Guerin *et al*., 2002). The availability of fake artesunate and mefloquine has been reported throughout Southeast Asia (Newton *et al*., 2001; Rozendaal, 2001). A notable exception to resistance is the new class of antimalaria agents, artemisinins, which are natural products developed in China in the 1960s (Gamo *et al*., 2010; Woodrow *et al*., 2005). Artemisinins have rapid antiparasitic activity. However, artemisinins have short half-lives, hence these drugs are administered in combination with a longer acting agent and combination therapy is also used to avoid development of drug resistance. Examples of efficacious artemisinin-based combination are artesunate-mefloquine, artemether-lumefantrine and artesunate-amodiaquine (Gamo *et al*., 2010; Rosenthal, 2008). The intravenous and intramuscular administration of quinine has been the standard therapy for severe cases of *P. falciparum* malaria for many years however it is associated with toxic effects such as reversible hearing loss and hypoglycaemia (White, 1983). Nausea and vomiting are the common side effects relating to artemisinins, which could be as a result of acute malaria rather than the drug (Price *et al*., 1999). Correct use of chemoprophylaxis such as clindamycin and pyrimethamine could aid to prevent malaria. There is currently no available malaria vaccine. Malaria control is limited by drug resistance, therefore, there is an urgent need for novel drug development and strategies to tackle this disease.

1.2. The life cycle of *P. falciparum*

The *P. falciparum* life cycle takes place in two different hosts namely, insect vector and human. The genesis of the malaria parasite in the human host is as a result of inoculation of sporozoites into the bloodstream by an infected anopheline mosquito (Step 1) (Figure 1.2) (reviewed in Zuccala and Baum, 2011). The motile sporozoites within 14 days migrate to the liver invading the hepatocytes, and upon repeated replication, growth and transformation the hepatocytes rupture, releasing merozoites into the bloodstream (Step 2). The merozoites invade the host erythrocytes and undergo cellular division within 48 hours causing the erythrocytes to burst (Step 3). This asexual blood stage of the *P. falciparum* accounts for the clinical symptoms associated with malaria infection such as fever, anaemia and organ deterioration. As the infection progresses, merozoites develop into gametocytes that are

taken up by feeding anopheline mosquito. Gametocytes mature into male and female gametes, sexual reproduction occurs and a zygote (ookinete) is formed (Step 4). Further multiplication and development take place resulting in the formation of infectious sporozoites that migrate to the salivary glands of the mosquito and are injected into a new host (Step 5) (Chang *et al*., 2008; Cox, 2010).

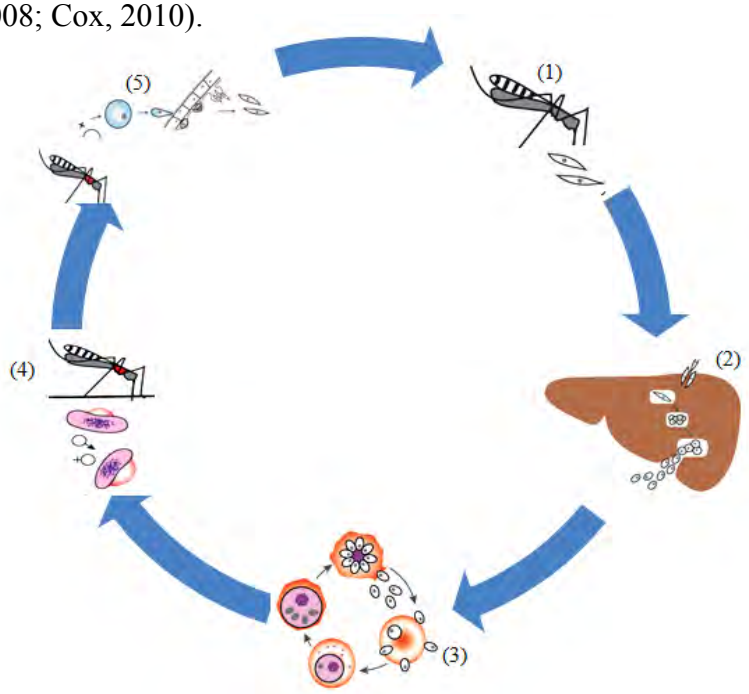

Figure 1.2: ***Schematic representation of P. falciparum life cycle*** (Adapted from Zuccala and Baum, 2011). (1) : Injection of sporozoites by infectious anopheline mosquito; (2) : Exoerythrocytic hepatic invasion by sporozoites resulting in merozoite production; (3) : Erythrocyte invasion by merozoite; (4) : Gametocytes taken up by mosquito; (5) : Production of infectious sporozoite in anopheline mosquito.

1.3. The biology of *P. falciparum* in human host erythrocytes

The human malarial parasite, *P. falciparum*, inhabits the human erythrocyte in a parasitophorous vacuole (PV) during the asexual stage life cycle (Sargeant *et al*., 2006). The PV develops during invasion of the host erythrocyte. The vacuolar membrane functions as a selective semi-permeable barrier between the parasite and the erythrocyte cytoplasm through which parasite-encoded proteins known as exportome are exported to the erythrocyte cytosol and membrane (Ansorge *et al*., 1996; Joiner, 1991). As the parasite intra-erythrocytic development progresses, membranous structures referred to as Maurer's clefts are formed in the erythrocyte cytoplasm. Maurer's clefts, usually located at the erythrocyte periphery,

extensively remodel the erythrocyte to form electron dense structures termed knobs. Examples of exported parasite proteins include knob-associated histidine-rich protein (KAHRP) (Pologe *et al*., 1987; Triglia *et al*., 1987) and *P. falciparum* erythrocyte membrane protein 1 (*Pf*EMP1) (Baruch *et al*., 1995; Kilejian and Jensen, 1977). *Pf*EMP1 in particular has been implicated in the cytoadherence of the parasite-infected erythrocyte to the endothelial receptor cells of the blood vessels thus preventing removal by the spleen in human host. The mode of export of parasite proteins into the host cells is thought to be dependent on a highly conserved *Plasmodium* export element (PEXEL) motif which has also been identified as host targeting (HT) signal (Hiller *et al*., 2004; Marti *et al*., 2004). A few other parasite proteins known to be present in the exportome are kinases, phosphatases and members of the molecular chaperones most especially the highly conserved heat shock proteins (Hsps) (Kooij *et al*., 2006; Sargeant *et al*., 2006). An example of exported molecular chaperones belonging to the hsp family include members of the Hsp40s namely, type I Hsp40s (J1), type II Hsp40s (J2), type III Hsp40s (J3) and type IV Hsp40s (J4) (Figure 1.3).

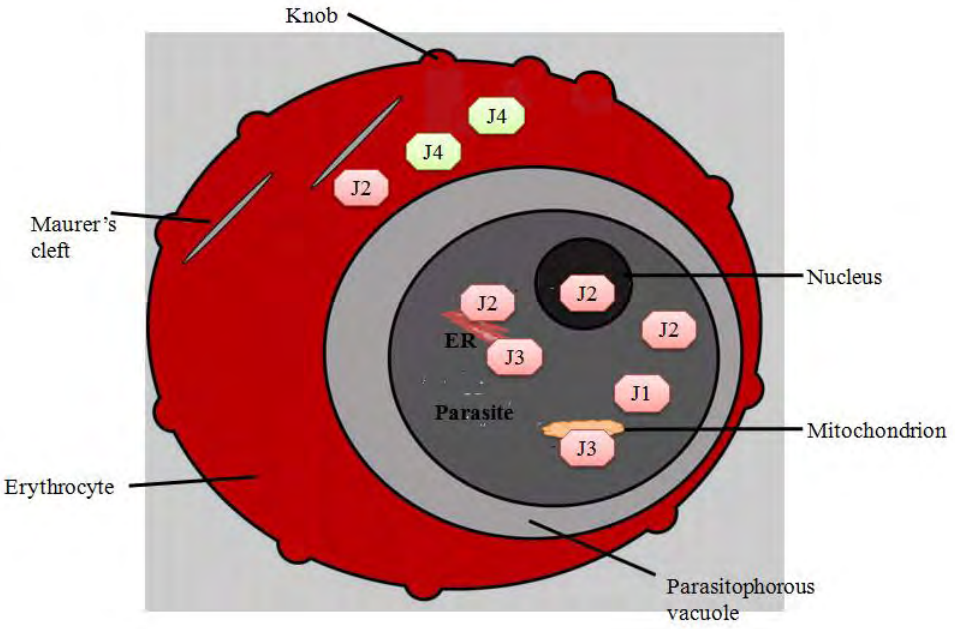

Figure 1.3: ***<u>The location of different PfHsp40s within the parasite and the erythrocyte</u>***. (Adapted from Rug and Maier, 2011). (J1) Type I Hsp40s; (J2) Type II Hsp40s; (J3) Type III Hsp40s; (J4) Type IV Hsp40s.

1.4. Molecular chaperones

Molecular chaperones are groups of proteins implicated in promoting quality control in a cell, including protein aggregation suppression and facilitating the folding of non-native proteins

into correct native conformations without being part of the final structure (Walter and Buchner, 2002; Borges and Ramos, 2005). In addition, molecular chaperones facilitate protein assembly, disassembly and protein transport to various subcellular compartments (Mayer and Bakau, 2005). The majority of the molecular chaperones identified belong to highly conserved Hsp family. A number of these heat shock proteins are known to increase in expression levels upon exposure to heat shock while some proteins are proposed to be constitutively expressed (Watanabe, 1997). For example, messenger RNA (mRNA) levels of Pfj1 are upregulated upon heat shock in *P. falciparum* infected erythrocytes whereas Pfj2 is proposed to be constitutively expressed in the erythrocytic stage parasite but decreases in expression upon heat shock (Watanabe, 1997). Hsp70 and Hsp40 molecular chaperones have been extensively studied (Botha *et al*., 2011; Shonhai *et al*., 2008).

1.4.1. Heat shock protein 70 (Hsp70)

Hsp70s, ubiquitous in cell compartments, are either constitutively expressed or inducible in response to cellular stress, for example an increase in temperature. Hsp70 possesses an N-terminal 44 kDa ATPase domain and a C-terminal peptide-binding domain subdivided into 18 kDa ß-substrate binding and 10 kDa α-helical domains respectively (Flaherty *et al*., 1990; Wang *et al*., 1993). The conserved C-terminal peptide sequence EEVD motif is involved in regulating the Hsp40 stimulated adenosine triphosphate (ATP) hydrolysis by Hsp70. Stimulation of ATP hydrolysis is crucial for the chaperone activity of Hsp70 (Szabo *et al*., 1994). In the ATP-bound state, Hsp70 has a low affinity for substrate protein whereas in the ADP-bound state Hsp70 has a high affinity for substrate (Suh *et al*., 1999). Nucleotide exchange factors (NEFs) mediate nucleotide exchange to replace ADP with ATP thereby inducing a conformational change to facilitate substrate release (Liberek *et al*., 1991). Hsp70 function in partnership with co-chaperone Hsp40 in mediating protein folding, assembly and transport (Feldman and Frydman, 2000; Fink, 1999).

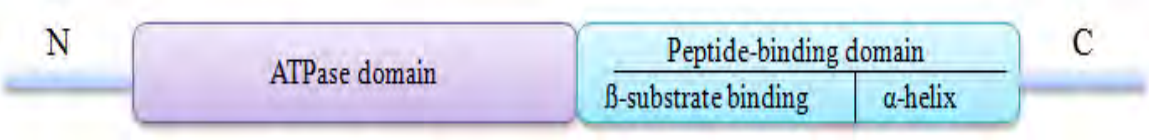

Figure 1.4: ***Diagrammatic representation of the domain organisation of Hsp70***. The domains shown are the ATPase domain and the peptide-binding domain that is subdivided into ß-substrate binding and α-helix subdomains.

1.4.2. Heat shock protein 40 (Hsp40)

Hsp40s are defined by the presence of a J-domain with approximately 70 amino acid region, similar to the J-domain of the *Escherichia coli* Hsp40 protein, DnaJ (Pellecchia *et al*., 1996). The J-domain structure has four α-helices (helices I-IV) and situated in a loop region between helices II and III is the highly conserved histidine-proline-aspartic acid (HPD) tripeptide motif (Figure 1.5) (Botha *et al*., 2007). This domain is orientated such that charged residues in helix II can interact correctly with the ATPase domain of partner Hsp70 (Hennessy *et al*., 2005; Tsai and Douglas, 1996). Mutations in the HPD motif result in loss of functional interactions between Hsp40 and Hsp70 (Hennessy *et al*., 2005; Laufen *et al*., 1999; Mayer and Bukau, 2005; Tsai and Douglas, 1996; Wittung-Stafshede *et al*., 2003). The HPD motif is essential for J-domain-based stimulation of the ATPase activity of Hsp70, resulting in the stabilisation of the substrate-bound form of Hsp70. Helices II and III mediate domain interaction with Hsp70 whereas helix IV may modulate the specificity or affinity of the Hsp70-Hsp40 chaperone partnership (Hennessy *et al*., 2005).

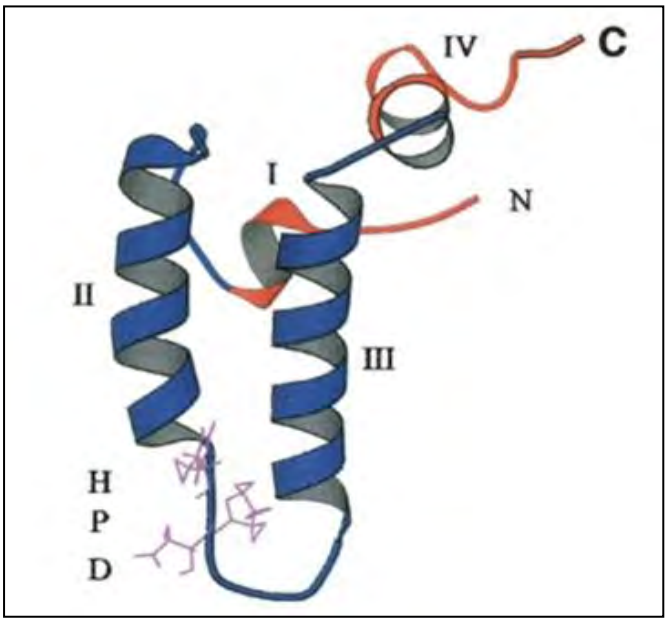

***Figure 1.5:* <u>*Ribbon representation of the J domain of E. coli DnaJ*</u> <u>**(1XBL)**</u>** (Pellecchia *et al*., 1996). The conserved HPD motif is represented in purple sticks. Helices I-IV are labelled. N represents the amino terminus. C represents carboxyl terminus.

1.4.2.1. Classification of Hsp40s

Hsp40s are classified into four groups based on their domain organisation (Figure 1.6). Type I Hsp40s consist of an N-terminal J-domain with a highly conserved HPD motif, a glycine/phenylalanine (G/F)-rich region, a cysteine-rich zinc finger domain and a less conserved C-terminal substrate-binding domain. Type II Hsp40s contain all the domains typical of type I Hsp40s except that the zinc-finger region is absent. Types III Hsp40s only possess a J-domain with conserved HPD motif. Type IV Hsp40s are characterised by the presence of a J-domain but the HPD motifs are not conserved (Cheetham and Caplan, 1998; Botha *et al*., 2007). Type I and type II Hsp40s, in partnership with Hsp70, are involved in processes which include protein folding, refolding of misfolded proteins, assembly of proteins and protein degradation. Type III Hsp40s, tend to perform more highly specialised functions such as regulation of other chaperone (Cheetham and Caplan, 1998; Walsh *et al*., 2004). Since the normally conserved HPD motif of the J-domain in the type IV Hsp40s varies, it is suggested that this variation may hinder interaction between Hsp40 and Hsp70, and thus this class of Hsp40s seem to function in an unknown manner (Botha *et al*., 2007).

Figure 1.6: ***Diagrammatic representation of the domain organisation of the four types of Hsp40s***. I: type I Hsp40; II: type II Hsp40; III: type III Hsp40; IV: type IV Hsp40. The subdomains shown are the J domain, the G/F region and the zinc finger region.

The G/F region is thought to be important in the regulation of the substrate-binding capabilities of Hsp70 possibly through stabilisation of the Hsp70-substrate complex optimisation of substrate selection or facilitating the transport of substrate from Hsp40 to Hsp70 (Genevaux *et al*., 2002; Han and Christen, 2003).

The zinc-binding domain could potentially play a role in stabilising Hsp40 tertiary structure as this domain is characterised by the availability of four cysteine-repeat sequences capable of co-ordinating binding of two zinc ions (Greene *et al*., 1998; Martinez-Yamout *et al*., 2000). Furthermore, the zinc-binding domain and the C-terminus could possibly serve as a requirement for substrate binding (Han and Christen, 2003).

The C-terminal domain is associated with substrate binding in types I and II Hsp40s, and is also crucial for the interaction of Hsp40 with the non-native polypeptides through hydrophobic interactions (Borges *et al*., 2005; Wu *et al*., 2005). It has been suggested that Hsp40 may bind the non-native polypeptides prior to transferring them to Hsp70 for recognition and binding (Li *et al*., 2009).

1.5. Protein quality control in the endoplasmic reticulum (ER)

The endoplasmic reticulum (ER) is a membrane-bound organelle within the cytoplasm of eukaryotic cells involved in protein folding, quality control and protein degradation (Ellgaard and Helenius, 2001; Sitia and Braakman, 2003). Secretory and membrane proteins undergo quality control in the ER that separate correctly folded proteins from unassembled and terminally misfolded proteins. Correctly folded proteins are transported to their final destination. Unassembled proteins are retained and refolded in the ER. Terminally misfolded proteins are subjected to degradation by the 26S proteasome in a process known as ER-associated degradation (ERAD) following retrotranslocation into the cytosol (Brodsky and McCracken, 1999; Plemper *et al*., 1999; Sommer and Wolf, 1997). The conditions leading to protein misfolding include genetic mutations, heat shock and oxidative stress. The accumulation of unfolded or misfolded proteins in the ER activates a signal transduction cascade referred to as the unfolded protein response (UPR) (Hoseki *et al*., 2010). The UPR induces the expression of ER-resident chaperone proteins such as BiP, PDI and ERAD

components involved in boosting the folding capacity of the ER and facilitate the removal of accumulating misfolded proteins (Ellgaard *et al*., 1999; Malhotra and Kaufman, 2007).

1.5.1. ER-associated degradation (ERAD)

The ERAD pathway involves degradation of terminally misfolded glycoprotein and non-glycosylated proteins (Figure 1.7). For ERAD of non-glycosylated proteins, ER-resident chaperone BiP and protein-disulfide isomerase (PDI) recognises misfolded proteins and recruits them to ERdj5. ERdj5, a disulfide reductase and essential for degradation of incorrectly folded proteins in the ER interact with BiP through the J-domain (Pathway 1). For ERAD of glycosylated proteins, misfolded glycoproteins are first recognized by calnexin (CNX) or calreticulin (CRT), transferred to ER degradation enhancing α-mannosidase-like protein (EDEM) and then to Endoplasmic Reticulum DnaJ protein 5 (ERdj5). ERdj5 interacts with EDEM and thus facilitates ERAD by cleaving disulphide bonds of misfolded glycoproteins and prevents oligomer formation (Pathway 2). In both ERAD pathways, ERdj5 is required in enhancing the degradation of terminally misfolded proteins (Ushioda *et al*., 2008).

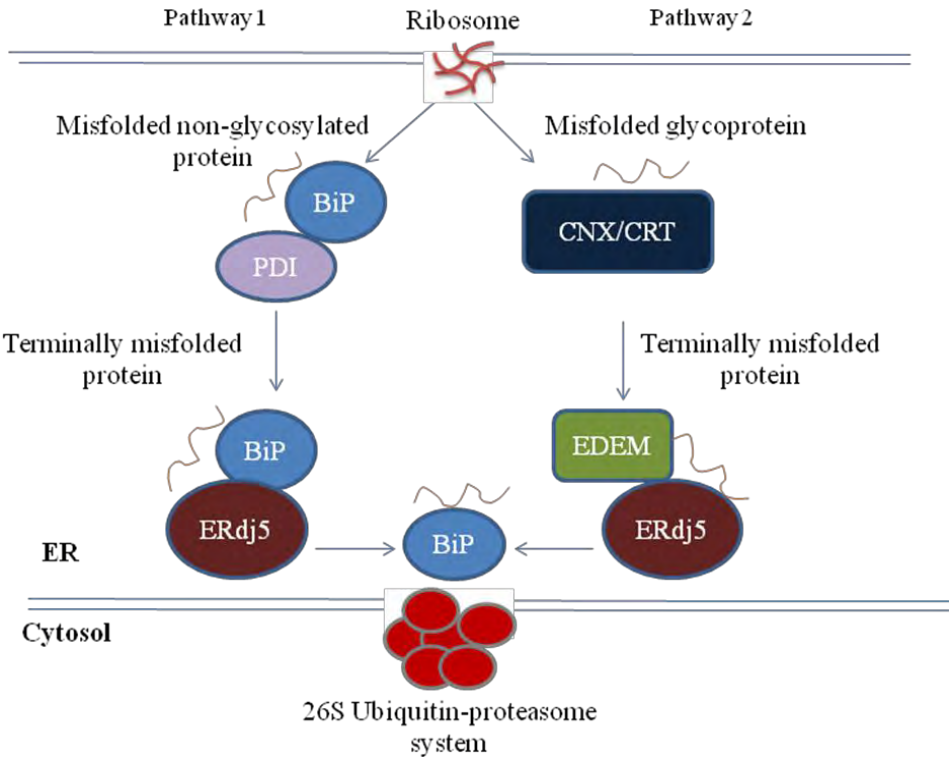

Figure 1.7: ERAD pathways for terminally misfolded glycoprotein and non-glycosylated proteins (Adapted from Ushioda *et al*., 2008). (1) : ERAD pathway for non-glycosylated protein; (2) : ERAD pathway for glycosylated protein.

1.5.2. ER-resident chaperone, BiP

Immunoglobulin binding protein, BiP, also termed glucose regulated protein 78kDa (GRP-78) is a member of the Hsp70 family, and the most abundant ER chaperone. BiP was initially termed immunoglobulin binding protein because of its role in the assembly of immunoglobulins (Haas and Wabl, 1983). BiP has an ATPase domain and a peptide-binding domain that undergo repetitive cycles of ATP hydrolysis and nucleotide exchange that promotes binding and release of the unfolded protein respectively (Minami *et al*., 1996). The ATPase cycle is regulated by Hsp40-type co-chaperones which stimulate ATPase hydrolysis and proteins involved in nucleotide exchange (Shen and Hendershot, 2005). In addition to its role in facilitating protein folding and assembly, BiP plays a role in identifying and targeting misfolded proteins for proteasomal degradation. Furthermore, BiP preserves the permeability barrier of the ER translocon during early stages of protein translocation (Hamman *et al*., 1998), serves as a sensor for ER stress (Bertolotti *et al*., 2000; Shen *et al*., 2002) and functions in the maintenance of ER calcium stores (Lievremont *et al*., 1997).

1.5.3. Protein-disulfide isomerase (PDI)

Protein-disulfide isomerase (PDI) is a 55 kDa protein in the ER which serves to assist secretory proteins in attaining the correct disulfide arrangement. PDI catalyses thiol-disulfide formation, isomerisation and reduction (Schwaller *et al*., 2003). PDI has two thioredoxin-like catalytic domains, one at the amino terminus and the other at the carboxyl terminus that usually contain a characteristic CXXC active-site motif (Edman *et al*., 1985; Ellgaard and Ruddock, 2005). Each active motif has two cysteines residues in the sequence which mediate catalytic activities (Schwaller *et al*., 2003). In addition to PDI, four yeast homologues has been identified namely, Mpd1p, Mpd2p, Eug1p and Eps1p (Sevier and Kaiser, 2002; Tu and Weissman, 2004). 19 PDI family proteins have been found in mammals including human ERdj5 (Cunnea *et al*., 2003; Hosoda *et al*., 2003).

1.5.4. ER-resident protein, ERdj5

Seven resident ER proteins with J domains (ERdj) have been identified in mammals (Table 1.1). ERdj5, also termed JPDI (J-domain containing PDI-like protein) is a member of the

PDI family which has been identified as an ER resident J-protein. In addition to having a J-domain, ERdj5 has four thioredoxin-like domains (Figure 1.8) that function as a co-chaperone for the ER resident Hsp70 chaperone, BiP (Cunnea *et al*., 2003; Hosoda *et al*., 2003). Several functions of ERdj5 have been reported. Ushioda *et al*. (2008) identified ERdj5 as an EDEM interacting protein and that it serves as a disulfide reductase that mediates the removal of incorrectly folded proteins. ERdj5 and ERdj4 have been reported by Dong *et al*. (2008) to participate in the ERAD of non glycosylated substrate. Homologue of human ERdj5 has been identified in *P. falciparum* Hsp40, Pfj2 (Botha *et al*., 2007).

Figure 1.8: ***Schematic representation of the domain structure of ERdj5***. J represents the J-domain. The four thioredoxin domains are labelled.

Table 1.1: Mammalian ERdj proteins

ERdj protein	**Molecular weight (kDa)**	**Yeast homologue**
ERdj1/Mtj1[a,b]	63	Sec63[a]
ERdj2/hSec63[c,d]	85	Sec63[b]
ERdj3/HEDJ[e,f,g]	43	Scj1[c]
ERdj4/Mdj1[h,i]	25	None
ERdj5/JPDI[j,k]	96	None
ERdj6/p58[IPK l]	58	None
ERdj7[m]	42	None

[a]Brightman *et al*. (1995); [b]Chevalier *et al*. (2000); [c]Skowronek *et al*. (1999); [d]Tyedmers *et al*. (2000); [e]Bies *et al*. (1999); [f]Lau *et al*. (2001); Yu *et al*. [g](2000); [h]Prols *et al*. (2001); [i]Shen *et al*. (2002); [j]Cunnea *et al*. (2003); [k]Hosoda *et al*. (2003); [l]Yan *et al*. (2002); [m]Zahedi *et al*. (2009).

1.6. *P. falciparum* heat shock proteins

The Hsp40s are a family of molecular co-chaperone that regulates the activity of Hsp70s. The Hsp40s are characterised by a highly conserved J-domain that promotes interaction with the Hsp70s (Genevaux, 2002). At least six PfHsp70s have been identified in *P. falciparum* (Peterson *et al*., 1988; Sargeant *et al*., 2006). The genome of *P. falciparum* codes for 43 Hsp40s which are classified into four types, namely type I, type II, type III and type IV (Botha *et al*., 2007).

1.6.1. P. falciparum Hsp70s

The *P. falciparum* genome encodes at least six PfHsp70s (Peterson *et al*., 1988; Sargeant *et al*., 2006) (Table 1.2). PfHsp70 has domains typical of Hsp70 as described in section 1.4.1. PfHsp70 are ubiquitous and expressed in the various stages of the *P. falciparum* life cycle (Sharma, 1992). High levels of PfHsp70s are particularly present in the liver of the human host during the asexual reproduction of the parasite (Kumar and Zheng 1992). An increase in temperature is known to cause a rise in the expression level of PfHsp70 which suggests that PfHsp70 may play an essential role in the survival of the parasite (Biswas and Sharma, 1994; Joshi *et al*., 1992).

Table 1.2: *P. falciparum* Hsp70s

Protein	Chromosome	kDa	Cellular localisation
PfHsp70-x	7	73.2	Cytoplasm[c]
PfHsp70-y	13	108.2	ER[c]
PfHsp70-z	7	100	Cytoplasm[c]
PfHsp70-1[a]	8	73.9	Nucleus and cytoplasm
PfHsp70-2[a,b]	9	72.4	ER[d]
PfHsp70-3[a]	11	73.3	Mitochondrion[c,e]

[a]Sharma (1992); [b]Nyalwidhe and Lingelbach (2006); [c]Sargeant *et al*. (2006); [d]Kumar *et al*. (1991); [e]Šlapeta and Keithly (2004).

Amongst the six PfHsp70s, PfHsp70-1 has been well studied. PfHsp70-1 has generated much research attention in terms of its chaperone properties for possessing ATPase activity and for the ability to suppress protein aggregation (Matambo *et al*., 2004; Ramya *et al*., 2006; Shonhai *et al*., 2008). PfHsp70-1 primarily localises in the cytosol and in the nucleus (Kappes *et al*., 1993). The localisation of PfHsp70-1 in the nucleus is enhanced in response to heat stress (Kappes *et al*., 1993).

PfHsp70-1 is approximately 74 kDa in molecular mass and has a C-terminal EEVD motif. This EEVD motif binds to co-chaperone, for example, Hop, to facilitate protein interaction (Demand *et al*., 1998). PfHsp70-1 shares a high amino acid sequence identity to another PfHsp70, namely, PfHsp70-x. PfHsp70-x is approximately 74 kDa in molecular mass and has a C-terminal EEVN motif. PfHsp70-x could be an alternate cytosolic PfHsp70, however, information regarding the role of PfHsp70-x is minimal. Due to the fact that PfHsp70-1 shares a high amino acid sequence identity and both possesses a highly conserved bipartite nuclear localisation signals (Robbins *et al*., 1991) suggests that PfHsp70-x may move to the nucleus (Shonhai *et al*., 2007).

According to a report by Nyalwidhe and Lingelbach (2006), PfHsp70-1is present in the parasitophorous vacuole and has also been detected in the Maurer's clefts (Vincensini *et al*., 2005). This suggests that the protein could possibly be exported to the erythrocyte (Shonhai *et al*., 2007). PfHsp70-1 has been experimentally shown to have a high basal ATPase activity and ATP-dependent chaperone activity *in vitro* (Matambo *et al*., 2004; Ramya *et al*., 2006). *In vivo* studies of PfHsp70-1 shows that the protein is capable of reversing the thermosensitivity of an *E. coli* DnaK mutant strain (Shonhai *et al*., 2005). In addition, PfHsp70-1 has a functional linker region and mutations in this region of the protein result in loss of functionality *in vivo* (Shonhai *et al*., 2005). According to Shonhai *et al*. (2005) there is a possible inter domain interaction using chimeric protein from the ATPase domain of *E. coli* DnaK and the peptide-binding domain of PfHsp70-1in *E. coli DnaK756* cells.

The PfHsp70 possesses a translation initiation factor known as eIF-2α. The phosphorylation of eIF-2α inhibits protein synthesis (Surolia and Padmanaban, 1991). The PfHsp70 suppresses eIF-2α phosphorylation through the activity of a heme-regulated kinase hence facilitates protein synthesis (Ramya *et al*., 2007). In addition, Ramya *et al*. (2007) suggested that antimalarial, 15-deoxyspergulain (DSG), inhibit protein synthesis. Furthermore, DSG is

capable of modulating PfHsp70-1 activity through possible interaction with the EEVD motif of the protein. The close proximity of the EEVD motif to the peptide-binding domain may inhibit protein folding through substrate-binding interference by PfHsp70-1 (Shonhai *et al*., 2007). In a recent study by Cockburn *et al*. (2011) PfHsp70-1 is shown to be inhibited by small molecule modulators, namely, malonganenone A-C, lapachol and bromo-ß-lapachona in malate dehydrogenase based aggregation suppression assays. Growth inhibition assays is also performed using *P. falciparum* 3D7-infected erythrocytes to show that all of the compounds with the exception of malonganenone are able to inhibit the growth of PfHsp70-1. A co-chaperone of Hsp70, *P. falciparum* heat shock protein 70 interacting protein (Hip) is capable of modulating the PfHsp70-1 and PfHsp70-3 chaperone function *in vitro* (Ramya *et al*., 2006).

1.6.2. P. falciparum Hsp40s

1.6.2.1. Type I PfHsp40s

The type I PfHsp40s, characterised by the presence of J-domain, G/F region, cysteine-repeat and C-terminal region consists of two PfHsp40s (Cheetham and Caplan, 1998). These include PFD0462w (Pfj1, PfDnaJA) and PF14_0359 which are proposed to exhibit house-keeping properties within the parasite because the export element, PEXEL/HT motif, is absent (Watanabe, 1997; Botha *et al*., 2007).

The mRNA and protein level of Pfj1 increases upon heat shock (Watanabe, 1997; Nicoll *et al*., 2007). *In vivo* complementation studies have shown that the replacement of the J-domain of a thermosensitive *E. coli* strain (OD259) with the J-domain from Pfj1 reverses the thermosensitivity of these proteins (Nicoll *et al*., 2007). Furthermore, Pfj1 interacts with the origin of replication in the apicoplast genome, therefore, the protein has been proposed to be associated in the replication of a *P. falciparum* apicoplast DNA (Kumar *et al*., 2010). Pfj1 has also been shown to stimulate the protein refolding activity of PfHsp70-1 *in vitro* (Misra and Ramachandran, 2009).

PF14_0359 co-localises in the parasite cytoplasm with PfHsp70-1 and assists in suppressing protein aggregation *in vitro* (Botha *et al*., 2011). The observation that the PF14_0359 stimulates the rate of ATP hydrolysis in the parasite and human Hsp70, and that these

ATPase activities are inhibited by small molecule modulator was first elucidated by Botha *et al*. (2011).

1.6.2.2. Type II PfHsp40s

The type II PfHsp40s differs from type I in that the cysteine-repeat region is absent. In this category, nine PfHsp40s have been identified (Table 1.3). Three of these PfHsp40s including PFA0660w, PFB0090c and PFE0055c bears the export motif (Bhattacharjee *et al*., 2008; Külzer *et al*., 2010). None of the PfHsp70s exhibit an export element and no clear relationship between the type II PfHsp40 and PfHsp70 have been defined. This has prompted the assumption that the exported type II PfHsp40s interact with human Hsp70 (Banumathy *et al*., 2002). The exported co-chaperones might be involved in the translocation of proteins across the parasite vacuole membrane while some of the non-exported co-chaperones might play a role in the cytoprotection of the parasite during cell stress (Nyalwidhe and Lingelbach, 2006; Rug and Maier, 2011). PFA0660w and PFE0055c have been reported to localise in the erythrocyte cytoplasm (Bhattacharjee *et al*., 2008; Külzer *et al*., 2010). PFE0055c partially co-localises with the Maurer's cleft marker skeleton-binding protein 1 (SBP1) (Bhattacharjee *et al*., 2008). In a recent study, PFA0660w and PFE0055c are shown to associate with mobile dot-like structures in the erythrocyte cytoplasm (Külzer *et al*., 2010). The co-localisation of the two proteins with the known Maurer's cleft markers did not occur and the dot-like structures appeared smaller than the Maurer's clefts. Therefore, it is suggested that PFA0660w and PFE0055c localises in an unknown organelle which is referred to as the J-dots.

The mRNA expression level of PFL0565w (Pfj4) is shown to increase upon heat shock (Watanabe, 1997). Pfj4 has a functional J-domain (Nicoll *et al*., 2007). Co-localisation and immunoprecipitation studies of Pfj4 with PfHsp70-1 have been reported (Pesce *et al*., 2008). LaCount *et al*. (2005) has reported possible interaction between Pfj4 and the *P. falciparum* gonial cell neoplasm protein 20 (PFGCN20) but this interaction has not been experimentally validated. PFGCN20 potentially plays a role as an ATP-binding subunit of an ABC transporter. The interaction between these proteins suggests possible involvement in protein transfer across membranes.

PF11_0099 (Pfj2) has a C-terminal ER retention signal, DDEL, and exhibits similarities with human ER-resident protein ERdj5 (Botha *et al*., 2007). According to a previous report by Ushioda *et al*. (2008), ERdj5 serve as a reductase in facilitating protein quality control through cleaving of disulfide bonds of misfolded proteins. The destabilisation of Pfj2 in *P. falciparum* may affect the parasite survival which suggests the protein could serve as a potential drug target.

Table 1.3: *P. falciparum* type II Hsp40s

Locus[a]	**Chromosome**	**kDa**
MAL13P1.277	13	24.3
PFA0660w	1	47
PFB0090c	2	48.3
PFB0595w	2	37.4
PFE0055c	5	46.4
PFF1415c	6	44.7
PFL0565w	12	28
PF11_0099	11	62.4
PF14_0137	14	45.2

[a]Bahl *et al*. (2003)

1.6.2.3. Type III PfHsp40s

The largest and most diverse group of Hsp40s in *P. falciparum* are the type III Hsp40s. 20 type III Hsp40s are encoded in the *P. falciparum* genome. They are characterised by the presence of a J-domain and are thought to be more specialised in their interactions with Hsp70 (Kelly, 1998; Young *et al*., 2004). The functions and locations of these proteins are still unknown but four, that is, PF10_0378 (Pfj3), PF11_0513, PFB0920w and PFL0055c are predicted to contain a PEXEL/HT motif and can thus be exported into the host cell. The

mRNA expression level of Pfj3 has been reported to significantly increase upon heat shock (Watanabe, 1997).

1.6.2.4. Type IV PfHsp40s

P. falciparum genome encodes 12 type IV Hsp40s, ten of which are predicted to contain the PEXEL/HT motif. PfHsp40 type IV contains a J-domain with a variation in the normally conserved HPD motif (Botha *et al*., 2007). Variation in the HPD motif stops interaction between Hsp40 and Hsp70. These proteins are unique to the parasite in that there are no human homologues. Of the ten proteins predicted to have the PEXEL motif, four are members of the ring-infected erythrocyte surface antigen (RESA) while the remaining six are members of the mature erythrocyte surface antigen (MESA). RESA and MESA interacts with erythrocyte membrane skeleton (Da Silva *et al*., 1994; Foley *et al*., 1991; Coppel *et al*., 1988). The presence of the RESA protein encoded in the four type IV PfHsp40s imparts resistance to heat shock, thus protecting the parasite from heat-induced damage during febrile episodes (Silva *et al*., 2005).

1.6.3. *P. falciparum* Hsp40, Pfj2

Pfj2 has been identified as a type II Hsp40 consisting of a J-domain with conserved HPD motif, G/F region and a thioredoxin-like domain (Figure 1.9) (Botha *et al*., 2007). Bioinformatic analysis has revealed that Pfj2 is 62.4 kDa in molecular size with 540 amino acids residues. Pfj2 is thought to possess a putative ER signal sequence and a putative PEXEL motif represented by RQLAK (Botha *et al*., 2007). The analysis also revealed the presence of an ER retension motif represented by DDEL in the amino acid sequence of Pfj2.

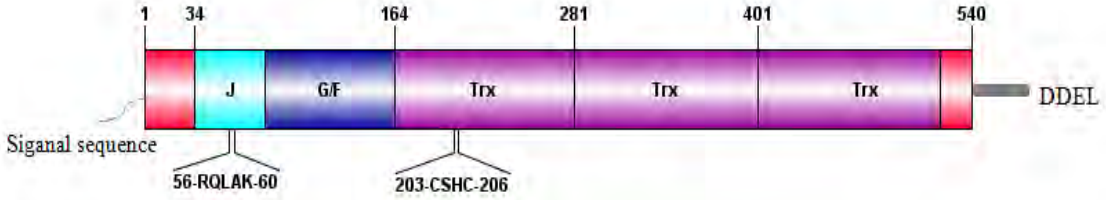

Figure 1.9: Schematic representation of the domain structures of Pfj2. J represents the J-domain. The G/F region represents the glycine/phenylalanine region. The thioredoxin, CSHC, domains are labelled. The position of the putative ER signal sequence is indicated. The position of the putative PEXEL motif, RQLAK, is labelled. The ER retension motif, DDEL, is labelled.

Studies have shown that the mRNA expression levels of Pfj2 decreases upon exposure to heat shock (Watanabe, 1997). Localisation studies of Pfj2 within the infected erythrocyte or parasite is yet to be proven experimentally.

Pfj2 has been identified as a *P. falciparum* Hsp40 chaperone that may potentially be involved in protein quality control in the ER, but has not been well studied and documented in the literature. Pfj2 chaperone is particularly interesting as it is potentially homologous to the human ER Hsp40, ERdj5 due to the domain similarity. ERdj5 has been shown to assist protein quality control by cleaving disulfide bonds of misfolded proteins in the ER as a result of it reductase activity (Ushioda *et al*., 2008). Pfj2 chaperone might well act in the same way to facilitate quality control of protein in *P. falciparum* thereby promoting survival of the parasite. The question therefore remains whether Pfj2 chaperone helps in the quality control of proteins within the parasite which can only be answered by characterising the Pfj2.

1.7. KNOWLEDGE GAP

P. falciparum encodes chaperone proteins including Pfj2. This protein has not been well characterised and little information regarding its biochemistry is available. Pfj2 evokes interest as it shows a degree of homology to the human ERdj5. Given that ERdj5 assists protein quality control in the ER, it is possible that Pfj2 performs a similar function in *P. falciparum* thereby promoting parasite survival in the cell. Given that many anti-malarial drugs are now becoming less effective, biochemical characterisation of Pfj2 could provide more information on its potential as a drug target for the control of an important and devastating human disease.

1.8. RESEARCH OBJECTIVES

1.8.1. Hypothesis

Pfj2, a Hsp40 chaperone is potentially homologous to human ER Hsp40, ERdj5, a resident protein of the endoplasmic reticulum (ER) that promotes protein quality control by facilitating the degradation of misfolded proteins and may perform a similar function.

1.8.2. Broad objective

The overall aim of this study is to express and purify His_6-Pfj2 in a bacterial system, and investigate the ability of the protein to stimulate the chaperone activity of the mammalian ER Hsp70, BiP using ATPase assays.

1.8.3. Specific objectives

- To perform a bioinformatics analysis of Pfj2 to compare domain similarities and identities with typical type II Hsp40s
- To clone the codon-optimised Pfj2 coding sequence into a prokaryotic pQE30 expression vector to enable over-production of a His_6-Pfj2
- To express His_6-Pfj2 and His_6-BiP in *E. coli* M15[*pREP4*] cells to determine protein production
- To purify recombinant His_6-Pfj2 and His_6-BiP in *E. coli* M15[*pREP4*] cells for use in ATPase assays
- To investigate whether His_6-Pfj2 stimulates the ATPase activity of mammalian His_6-BiP.

Chapter 2

Methodology

2.1. Introduction

This chapter describes the methodology used to obtain purified His_6-Pfj2 for use in ATPase assays. The experimental procedures included cloning of a codon-optimised, truncated gene sequence into the pQE30 vector followed by bacterial expression and purification of the protein under denaturing conditions using nickel affinity chromatography. Finally, ATPase assays were employed to determine the ability of His_6-Pfj2 to stimulate the chaperone activity of mammalian His_6-BiP. Prior to cloning, a bioinformatic analysis of the Pfj2 protein sequence was conducted to determine the degree of similarities and identities with other type II Hsp40 proteins namely, human ERdj5, *S. cerevisiae* Sis1, human Hsj1a and human DnaJB4. An analysis of the Pfj2 domains was also performed to identify the putative ER targeting and retention signals.

2.2. Bioinformatic analysis:

2.2.1. Sequence retrieval and alignment

Protein and nucleotide sequences for Pfj2 (Locus: PF11_0099) and PfBiP (Locus: PFI0875) were retrieved from PlasmoDB (http://PlasmoDB.org) (Bahl *et al*., 2003). Human ERdj5 (Accession: AAN73271.1), *Saccharomyces cerevisiae* Sis1 (Accession: CAA95866.1), human Hsj1a (Accession: AAA09034.1), human DnaJB4 (Accession: NP_008965.2), hamster GRP-78/BiP (Accession: P07823.1) and *S. cerevisiae* BiP (Accession: EDN63302.1) protein sequences were downloaded from the NCBI website (http://www.ncbi.nlm.nih.gov). The amino acid sequence of *Medicago sativa* MsHsp70-1 (EMBL-Bank CDS: AAV98051) was retrieved from the EMBL-EBI website (http://www.ebi.ac.uk). BioEdit v7.0.9 software was used to generate sequence alignments based on the ClustalW Multiple alignment tool (Thompson *et al*., 1994). ApE 2.0.39 software was used to generate the amino acid translation and alignment of the database and codon-optimised nucleotide sequences of Pfj2.

2.2.2. Codon-optimisation of the Pfj2 coding region

Domain analysis of Pfj2 to identify ER targeting and retention signals was performed using Phobius (Käll *et al*., 2007). The ER signal sequence was not included in the sequence on which to base the synthesis of Pfj2 coding region. Thus, to facilitate recombinant protein expression of Pfj2 in *Escherichia coli*, the Pfj2 coding region (31-510 amino acids) was codon-optimised. The codon-optimised Pfj2 nucleotide sequence was synthesised by GenScript (USA) and supplied as a pUC57-Pfj2 construct. To facilitate cloning of the sequence into pQE30, recognition sites for *Bam*HI and *Kpn*I were incorporated into the 5' and 3' ends of the nucleotide sequence respectively.

2.3. Cloning of Pfj2 into pQE30 expression vector

2.3.1. Materials

Ampicillin was purchased from Roche (USA). *Bam*HI, *Kpn*I, Lambda DNA, *Pst*1, T4 DNA ligase, dNTPs, *Pfu* DNA polymerase and *Dpn*I were obtained from Promega (USA). Agarose was purchased from Lonza (USA). pQE30 forward (5'-ggagaaattaactatgagagg-3') and reverse (5'-gttctgaggtcattactgg-3') primers were obtained from Qiagen (Germany). pQE30 was purchased from Qiagen (USA). *E. coli* JM109 cells [*endA*1 *glnV*44 *thi-1 relA*1 *gyrA*96 *recA*1 *mcrB*$^{+}$ Δ(*lac-proAB*) *e*14- [F' *traD*36 *proAB*$^{+}$ *lacI*^{q} *lacZ*ΔM15] *hsdR*17(r_K^- m_K^+)] were purchased from Promega (USA).

2.3.2. Preparation of E. coli competent cells

Yeast tryptone (YT) broth (1.6% tryptone, 1% yeast extract, 0.5% NaCl) and YT agar (YT supplemented with 1.5% bacteriological agar) containing 100 μg/ml of ampicillin were autoclaved and used as growth media. A colony of *E. coli* JM109 cells was used to inoculate 5 ml of YT broth. The culture was grown overnight in a shaking 37°C incubator and the following day diluted 1/200 into 50 ml YT broth and grown to mid-log phase (A_{600}=0.3-0.6). The cells were transferred into 250 ml centrifuge tubes and harvested by centrifugation at 5000x*g* for 5 minutes at 4°C. The pelleted cells were resuspended in 50 ml of ice-cold 0.1 M $MgCl_2$ and incubated on ice for 20 minutes. Following centrifugation at 5000x*g* for 5 minutes

at 4°C, the cells were resuspended in 25 ml of ice-cold 0.1 M $CaCl_2$ and placed on ice for 1-2 hours. The centrifugation step was repeated. Cells were resuspended in 5 ml of ice-cold 0.1 M $CaCl_2$ containing 10% glycerol and stored at -80°C in 100 µl aliquots for future use.

2.3.3. Transformation of E. coli JM109 cells

Competent *E. coli* JM109 cells (100 µl) were mixed with 100 ng plasmid DNA and incubated on ice for 30 minutes. Thereafter, the mixture was heat-shocked for 2 minutes at 42°C, cold-shocked on ice for 2 minutes and incubated for 1 hour with 900 µl YT broth in a 37°C shaking incubator. Cells were plated onto YT agar plate containing ampicillin (100 µg/ml) and incubated at 37°C overnight. A single colony was inoculated into 5 ml YT broth with 100 µg/ml ampicillin and grown at 37°C for 12 hours. The transformed culture was stored at -80°C in aliquots of YT broth containing 15% glycerol.

2.3.4. Plasmid DNA extraction and restriction digestion

Plasmid DNA was extracted using the QIAprep® Spin Miniprep Kit (Qiagen, USA) according to the manufacturer's instructions and eluted in 30 µl TE buffer (10 mM Tris-Cl, 1 mM EDTA, pH 8). Plasmid DNA was digested with *Bam*HI and *Kpn*I in a total reaction volume of 20 µl. The reaction was incubated at 37°C for 2 hours. An aliquot (3 µl) of gel-loading buffer (0.25% bromophenol blue, 10% SDS, 30% glycerol) was added and the digest was analysed by agarose gel electrophoresis (section 2.3.5).

2.3.5. Agarose gel electrophoresis

All samples were analysed by 0.8% agarose gel electrophoresis in TBE buffer (90 mM Tris, pH 8.3, 90 mM boric acid, 2 mM EDTA,) containing 0.5 µg/ml ethidium bromide. A DNA ladder of λ DNA digested with *Pst*I served as molecular marker. Samples were run at 100 V for approximately 1 hour. The DNA bands were visualised and pictures acquired using a ChemiDoc™ EQ (BioRad, USA). The DNA band of interest was gel-purified using the Zymoclean™ Gel DNA Recovery Kit according to the manufacturer's instructions.

2.3.6. Ligation and screening of the codon-optimised Pfj2 into pQE30

The gel-purified DNA was ligated into the pQE30 vector digested with *Bam*HI and *Kpn*I to generate pQE30-Pfj2. The ligation reaction which included 100 ng vector DNA, 17 ng insert DNA, 10 x ligation buffer and 0.1-1 units of T4 DNA ligase was assembled to a final volume of 10 µl, and incubated at 4°C overnight. An empty vector control reaction was prepared which comprised the above-mentioned reagents with the exception of insert DNA. The ligation was transformed into competent *E. coli* JM109 cells, and plasmid DNA extracted as described in sections 2.3.3 and 2.3.4. The successful cloning of pQE30-Pfj2 was confirmed by restriction analysis using *Bam*HI and *Kpn*I followed by agarose gel electrophoresis. Plasmids with 1549 bp inserts were sequenced by preparing a total reaction volume of 20 µl which consisted of 300 ng of plasmid DNA, 3.2 pmol of pQE30 primers, 5x BigDye buffer and 4 µl BigDye Terminator V3.1 (Applied Biosystems, USA). The PCR amplification parameters were 94°C for 3 minutes, followed by 30 cycles at 94°C for 30 seconds, 55°C for 30 seconds, 72°C for 2 minutes, and a final extension at 72°C for 5 minutes. The amplification product was cleaned using the Zymo Research DNA Clean and Concentrator-5™ Kit (USA) according to the manufacturer's instruction. The product was eluted with 10 µl of double distilled water and placed in a vacuum drier for 10 minutes. DNA sequencing was performed based on the chain-termination method with the ABI Genetic Analyser 3100 (Applied Biosystems, USA).

2.3.7. Site-directed mutagenesis

2.3.7.1. Primer design

The primers generated for the purpose of deletion mutagenesis of pQE30-Pfj2 were designed using GeneRunner™ (Hastings Software, USA) and synthesised by Inqaba Biotec (South Africa). Primers were designed to amplify a 1549 bp sequence of Pfj2. The primer sequences are shown in Table 2.1.

Table 2.1: Primers used for site-directed mutagenesis

Name of primer	Sequence	Tm (°C)	GC (%)
For-MpQE30-Pfj2	5' - CCATCACCATCACATCCGATCCAATG - 3'	76	50
Rev-MpQE30-Pfj2	5' - CATTGGATCGGATGTGATGGTGATGG - 3'	76	50

Reactions of 50 µl containing 100 ng pQE30-Pfj2, 5 µl of 10x reaction buffer, 5% DMSO, 25 mM $MgCl_2$, 10 mM dNTPs, 125 ng For-MpQE30-Pfj2, 125 ng Rev-MpQE30-Pfj2, and 2.5 U *Pfu* DNA polymerase were prepared. The amplification was performed in a GeneAmp PCR 9700 thermocycler (Applied Biosystems, USA) according to the cycling parameters in Table 2.2.

Table 2.2: Cycling parameters

Number of cycles	Temperature (°C)	Time (seconds)
1	95	30
18	95	30
	52	60
	68	30
1	68	420

*2.3.7.2. Dpn*I *treatment and agarose gel electrophoresis*

The reaction mixture was cooled to 37°C and 10 µl of the mutagenesis product was kept for agarose gel electrophoresis analysis prior to *Dpn*I treatment to remove parental plasmid. *Dpn*I (10 U) was added to the reaction, centrifuged at 500x *g* for 1 minute and incubated at 37°C overnight. Samples were analysed by 0.8% agarose gel electrophoresis as presented in Table 2.3. An aliquot of 100 ng of the *Dpn*I treated mutagenesis product was transformed

into competent *E. coli* JM109 cells as described in section 2.3.3. Plasmid DNA was extracted as described in section 2.3.4 and sequenced for verification.

Table 2.3: Samples analysed on a 0.8% agarose gel

Sample	Volume (µl)
*Pst*I-digested λ DNA size marker	3
Undigested pQE30-Pfj2, parental plasmid as a control	10
*Dpn*I treated mutagenesis amplification product, pQE30-Pfj2	10
pQE30-Pfj2 restricted with *Bam*HI as a control	10
pQE30-Pfj2 restricted with *Kpn*I as a control	10

2.4. Bacterial expression of recombinant proteins

2.4.1.Materials

Mouse anti-His primary antibody was obtained from GE Healthcare (UK). Anti-mouse IgG POD-labeled secondary antibody was purchased from Roche (USA). PageRuler^{TM} Plus Prestained Protein Ladder was purchased from Fermentas (USA). The pQE10-BiP construct was a kind gift from Prof. Richard Zimmermann (Universität des Saarlandes, Germany). *E. coli* M15[*pREP4*] cells [*lac*, *ara*, *gal*, *mtl*, *recA*$^{+}$, *uvr*$^{+}$, *Str*^{R}, (*pREP4*: *Kan*^{R}, *lacI*)] were purchased from Qiagen (USA).

2.4.2. Expression of His_6-Pfj2 and mammalian His_6-BiP in E. coli M15[pREP4] cells

Preparation of competent *E. coli* M15[*pREP4*] cells and transformation with pQE30-Pfj2 were performed as described in sections 2.3.2 and 2.3.3, in the presence of ampicillin (100 μg/ml) and kanamycin (50 μg/ml) for selection purposes.

A single colony of *E. coli* M15[*pREP4*] cells transformed with the pQE30-Pfj2 was inoculated into 25 ml YT broth and the culture was grown in a shaking 37°C incubator overnight. The overnight culture was diluted 1/50 into 250 ml of YT broth and grown at 37°C until A_{600} was approximately 0.6. A pre-induction sample (1 ml) was collected. The remaining culture was induced with 1 mM IPTG and samples were collected every hour for 5 hours and again after 12 hours. The samples were centrifuged at 13000x*g* for 1 minute and the pellets resuspended in a volume of PBS (137 mM NaCl, 2.7 mM KCl, 10 mM Na_2HPO_4, 2 mM KH_2PO_4 pH 7.4) equal to A_{600}/0.5*100 μl. Samples were treated with SDS-PAGE sample buffer (0.5 M Tris, pH 6.8, 10% glycerol, 10% SDS, 5% 2-mercaptoethanol, 1% bromophenol blue) and boiled at 100°C for 5 minutes. Proteins were analysed by SDS-PAGE and Western immunoblotting using a mouse monoclonal anti-His IgG primary antibody and anti-mouse IgG POD-labeled secondary antibody.

2.4.2.1. Sodium dodecyl sulfate polyacrylamide gel electrophoresis (SDS-PAGE)

Proteins were analysed by 12% SDS-PAGE at 150 V for approximately 1 hour in 1x SDS-PAGE running buffer (25 mM Tris, 192 mM glycine, 0.1% SDS). The protein bands were visualised by staining with Coomassie Brilliant Blue (0.2% Coomassie G-250, 40% methanol, 7% glacial acetic acid). The stain was removed after several washes with destain solution (40% methanol, 7% glacial acetic acid). PageRuler™ Plus Prestained Protein Ladder was used as molecular marker.

2.4.2.2. Western immunoblotting

Proteins resolved by SDS-PAGE were transferred onto nitrocellulose membrane (Trans-Blot Transfer medium, BioRad, USA) in transfer buffer (25 mM Tris, 192 mM glycine, 20% methanol) for 1 hour at 100 V with continuous stirring and cooling. To verify transfer, the

membrane was stained with Ponceau S (0.5% Ponceau S in 1% glacial acetic acid) and washed with distilled MilliQ water. The membrane was blocked in TBS-T (50 mM Tris, pH 7.5, 150 mM NaCl, 0.2% Tween-20) containing 5% non-fat milk powder overnight at 4°C. The membrane was incubated with mouse anti-His primary antibody diluted 1:5000 in blocking solution for 1 hour with shaking at room temperature, followed by 4x15 minutes washes with TBS-T. The membrane was subsequently incubated with anti-mouse IgG POD-labeled secondary antibody, diluted 1:6000 in blocking solution for 1 hour with shaking. Proteins were detected using the Roche BM Chemiluminescence Western Blotting Kit and visualized using a Chemidoc™ EQ (BioRad, USA).

2.5. Solubility studies

His_6-Pfj2 was expressed in *E. coli* M15[*pREP4*] cells as described in section 2.4.2. Following an overnight induction with 1 mM IPTG, the 250 ml cell culture was harvested by centrifugation at 6000x*g* for 20 minutes at 4°C. The pellet was resuspended in 2.5 ml cold lysis buffer (10 mM Tris, pH7.5, 300 mM NaCl, 50 mM imidazole, 1 mM PMSF, 0.1 mg/ml lysozyme) and frozen at -80°C overnight in 1 ml aliquots. The cell lysate was rapidly thawed and sonicated five times for 30 seconds at 4°C. The cell lysate was centrifuged at 16000x*g* for 30 minutes at 4°C. The supernatant (soluble fraction) and the pellet (insoluble fraction) were resuspended in 1 ml of PBS, treated with 5x SDS-PAGE sample buffer and boiled for 5 minutes at 100°C. The two fractions were analysed by SDS-PAGE (section 2.4.2.1) and Western immunoblotting (section 2.4.2.2).

2.6. Purification of His_6-Pfj2 and mammalian His_6-BiP

2.6.1. Materials

Urea, Imidazole, PMSF and lysozyme were purchased from Sigma-Aldrich (Germany). HisTrap affinity columns and Chelating Sepharose Fast Flow were purchased from GE Healthcare (Sweden). Snakeskin™ dialysis tubing was obtained from Thermo Scientific (USA).

2.6.2. Urea denaturing purification of His_6-Pfj2 from E. coli M15[pREP4] cells

An overnight culture of *E. coli* M15[*pREP4*] cells harbouring His_6-Pfj2 was harvested by centrifugation at 6000x*g* for 20 minutes at 4°C. The pellet was resuspended in cold denaturing lysis buffer (8 M Urea, 100 mM Tris, pH 8, 300 mM NaCl, 10 mM imidazole, 1 mM fresh PMSF) and frozen overnight at -20°C in 1 ml aliquots. The cells were rapidly thawed and sonicated five times for 30 seconds at 4°C. The cell lysate was centrifuged at 16000x*g* for 30 minutes at 4°C. The supernatant was loaded onto a Ni^{2+}-charged HisTrap column. The column was washed with cold wash buffer A (4 M Urea, 100 mM Tris, pH 8, 300 mM NaCl, 50 mM imidazole), then with buffer B (2 M Urea, 100 mM Tris, pH 8, 300 mM NaCl, 50 mM imidazole), and finally with buffer C (100 mM Tris, pH 8, 300 mM NaCl, 50 mM imidazole) to remove unbound protein. The bound proteins were eluted in cold elution buffer (100 mM Tris, pH 8, 300 mM NaCl, 1 M imidazole) and dialysed using dialysis tubing in dialysis buffer (50 mM Tris, pH 8, 200 mM NaCl), treated with 5 x SDS-PAGE sample buffer and boiled for 5 minutes. Purified protein with loaded amount of 0.954 mg/L was separated by SDS-PAGE and Western immunoblotting as described in sections 2.4.2.1 and 2.4.2.2. Protein concentration was measured using a Thermo Scientific nanodrop spectrophotometer (USA). Three independent His_6-Pfj2 purification experiments were performed for future use in ATPase assays.

2.6.3. Preparation of Ni^{2+}-chelating sepharose beads

An aliquot (250 µl) of sepharose beads was centrifuged at 500x*g* for 5 minutes. The beads were resuspended in 5x volume (1250 µl) of distilled MilliQ water and again centrifuged at 500x*g* for 5 minutes. An equal volume of 0.1 M $NiSO_4$ was added to the beads and the sample was agitated for 15 minutes, followed by centrifugation at 500x*g* for 5 minutes. The beads were washed in 1250 µl of distilled MilliQ water in three consecutive washing steps with centrifugation at 500x*g* for 5 minutes between each step. The beads were resuspended in 250 µl of lysis buffer.

2.6.3.1. Native purification of mammalian His_6-BiP

E. coli M15[*pREP4*] cells, expressing mammalian His_6-BiP were harvested by centrifugation at 6000x*g* for 20 minutes at 4°C. The pellet was resuspended in cold native lysis buffer (10 mM Tris, pH 7.5, 300 mM NaCl, 40 mM imidazole, 1 mM fresh PMSF, 0.1 mg/ml lysozyme) and frozen overnight at -80°C in 1 ml aliquots. The cells were rapidly thawed and sonicated five times for 30 seconds at 4°C. The cell lysate was centrifuged at 16000x*g* for 30 minutes at 4°C. The supernatant was added to 500 µl of 50% (v/v) Ni^{2+}-chelating sepharose beads prepared as described in section 2.6.3, for binding at 4°C for 4 hours with gentle agitation. The beads were centrifuged at 1500x*g* for 2 minutes to remove the unbound protein fraction and an aliquot (80 µl) of unbound protein was prepared for SDS-PAGE and Western analysis. Thereafter, the beads were washed three times in cold wash buffer (10 mM Tris, pH 7.5, 300 mM NaCl, 40 mM imidazole) and centrifuged at 1500x*g* for 2 minutes. The bound protein was eluted in cold elution buffer (10 mM Tris, pH 7.5, 300 mM NaCl, 100 mM imidazole) and dialysed with dialysis tube in dialysis buffer (10 mM Tris, pH7, 200 mM NaCl). Purified protein with loaded amount of 10.252 mg/L was separated by 12% SDS-PAGE and detected by Western immunoblotting using mouse anti-His primary antibody and anti-mouse IgG POD-labeled secondary antibody. Protein concentration was determined with a Thermo Scientific nanodrop spectrophotometer (USA). Three independent His_6-BiP purification experiments were performed for future use in ATPase assays.

2.7. ATPase assays of His_6-Pfj2 and mammalian His_6-BiP

2.7.1. The phosphate standard curve

Phosphate standard reactions were prepared from serial dilutions of 50 mM KH_2PO_4 with concentrations ranging from 0 to 6 nmol/µl. The reactions were added to 1x ATPase-buffered solution (100 mM Hepes, 100 mM $MgCl_2$, 1 M KCl, 100 mM DTT) and 10% SDS before incubation at 37°C for 3 hours. The absorbance was read at 850 nm. Excel 2007 software was used to analyse the result.

2.7.2. ATPase assays of His_6-Pfj2 and mammalian His_6-BiP using ammonium molybdate and ascorbic acid

His_6-Pfj2 and mammalian His_6-BiP were purified as described in sections 2.6.2 and 2.6.3.1. Reactions of 1 ml (10 mM Hepes, 10 mM $MgCl_2$, 20 mM KCl, 0.5 mM DTT, 0.4 µM His_6-BiP, 0.4 µM His_6-Pfj2) were prepared and pre-incubated at 37°C for 5 minutes. Thereafter, 60 µl of ATP was added to start the reactions. The reactions remained at 37°C and 50 µl samples were collected in microtitre plate wells containing 50 µl of 10% SDS at 0, 15, 30, 60, 120 and 180 minute intervals. Subsequently, 50 µl of 1% (w/v) ammonium molybdate in 1 M HCl, 50 µl of 6% (w/v) ascorbic acid in phosphate free water and 125 µl of 2% (w/v) sodium citrate and 2% (v/v) acetic acid also in phosphate free water were added for colour development. The samples were incubated at 37°C for 3 hours and the plate was read at 850 nm with a BioTek microtitre plate reader (USA). MsHsp70-1 (alfalfa Hsp70-1) and His_6-Hsj1a (kindly donated by Ingrid Cockburn) were readily available in our laboratory and were included as controls. Three independent ATPase assays were performed with triplicate measurement for each time point using a fresh batch of purified protein.

Chapter 3

Results

3.1. Introduction

This chapter describes results obtained from the cloning of pQE30-Pfj2, the expression and purification of His_6-Pfj2, and the effect of His_6-Pfj2 on the ATPase activity of mammalian His_6-BiP. The recombinant plasmid was generated by inserting the codon-optimised Pfj2 sequence into a prokaryotic expression vector pQE30. A *Bam*HI restriction endonuclease recognition site was engineered at the 5' end of Pfj2 coding sequence and *Kpn*I at the 3' end of the sequence. In order to facilitate production of His_6-Pfj2, codon-optimised Pfj2 was synthesised for optimal expression in *E. coli*. His_6-Pfj2 was expressed in *E. coli* M15[*pREP4*] cells and purified under denaturing conditions using nickel affinity chromatography. Finally, ATPase assays were conducted to determine whether His_6-Pfj2 can act as a co-chaperone by stimulating the activity of mammalian His_6-BiP. Alfalfa Hsp70-1 and human His_6-Hsj1a were used as controls. This chapter also presents a bioinformatic analysis of Pfj2. Firstly, a multiple sequence alignment of Pfj2 and other type II Hsp40s namely, *Saccharomyces cerevisiae* Sis1, human Hsj1a and DnaJB4 was carried out to identify conserved regions typical of type II Hsp40s such as J-domain and G/F rich region. Secondly, a pairwise sequence alignment of Pfj2 with human ERdj5 was generated in order to compare domain similarities between the two proteins. Thirdly, the Pfj2 sequence was analysed to locate the putative ER signal sequence. The alignment between database obtained Pfj2 and codon-optimised Pfj2 nucleotide sequences was also performed. Finally, a multiple sequence alignment of PfBiP, hamster GRP-78/BiP, *Medicago sativa* MsHsp70-1 and *S. cerevisiae* BiP was generated to determine conserved N- and C-terminal residues essential for functional interactions and substrate binding. The methodology employed in each experiment was described in the previous chapter. This chapter present the results obtained.

3.2. Bioinformatic analysis of Pfj2

3.2.1. Sequence alignment of Pfj2 with typical type II Hsp40s

The amino acid sequence of Pfj2 was retrieved from the PlasmoDB database. Other type II Hsp40s namely, human ERdj5, *S. cerevisiae* Sis1, human Hsj1a and human DnaJB4 were retrieved from the NCBI database. A multiple sequence alignment was generated using ClustalW to compare domain similarities. The results are shown in Figure 3.1.

The multiple sequence alignment shows the presence of a J-domain with conserved HPD motifs and G/F region typical of type II Hsp40s in the N-terminus of each amino acid sequence. The J-domains are highlighted in grey with HPD motifs highlighted in red. The G/F rich regions are highlighted in turquoise. The size of Pfj2 is predicted to be 62.3 kDa using BioEdit (Hall, 1999) and the number of amino acid residues is 540. Human Hsj1a is the smallest in protein size, 37.8 kDa, and has the smallest number of amino acid, 277. *S. cerevisiae* Sis1 and human DnaJB4 have very similar protein sizes of 37.5 kDa and 37.8 kDa respectively, and the number of amino acid is also similar, 352 and 337 respectively. ERdj5 has the biggest protein size of 91.1 kDa and amino acid of 793. Even though the proteins all have different number of amino acids, the percentage identity and similarity presented refers to the highlighted J-domain and the G/F region. The sequence identity and similarity of the J-domain and G/F region of Pfj2 with other type II Hsp40s and the predicted protein sizes are presented in Table 3.1.

Table 3.1: Comparison of the J-domain and G/F region of type II Hsp40s sequence identity, similarity, size of proteins and number of amino acid residues with Pfj2

Type II Hsp40s	% Identity	% Similarity	Size (kDa)	Number of amino acid residues
ERdj5	21	31	91.1	793
Sis1	27	40	37.5	352
Hsj1a	32	42	30.6	277
DnaJB4	30	45	37.8	337

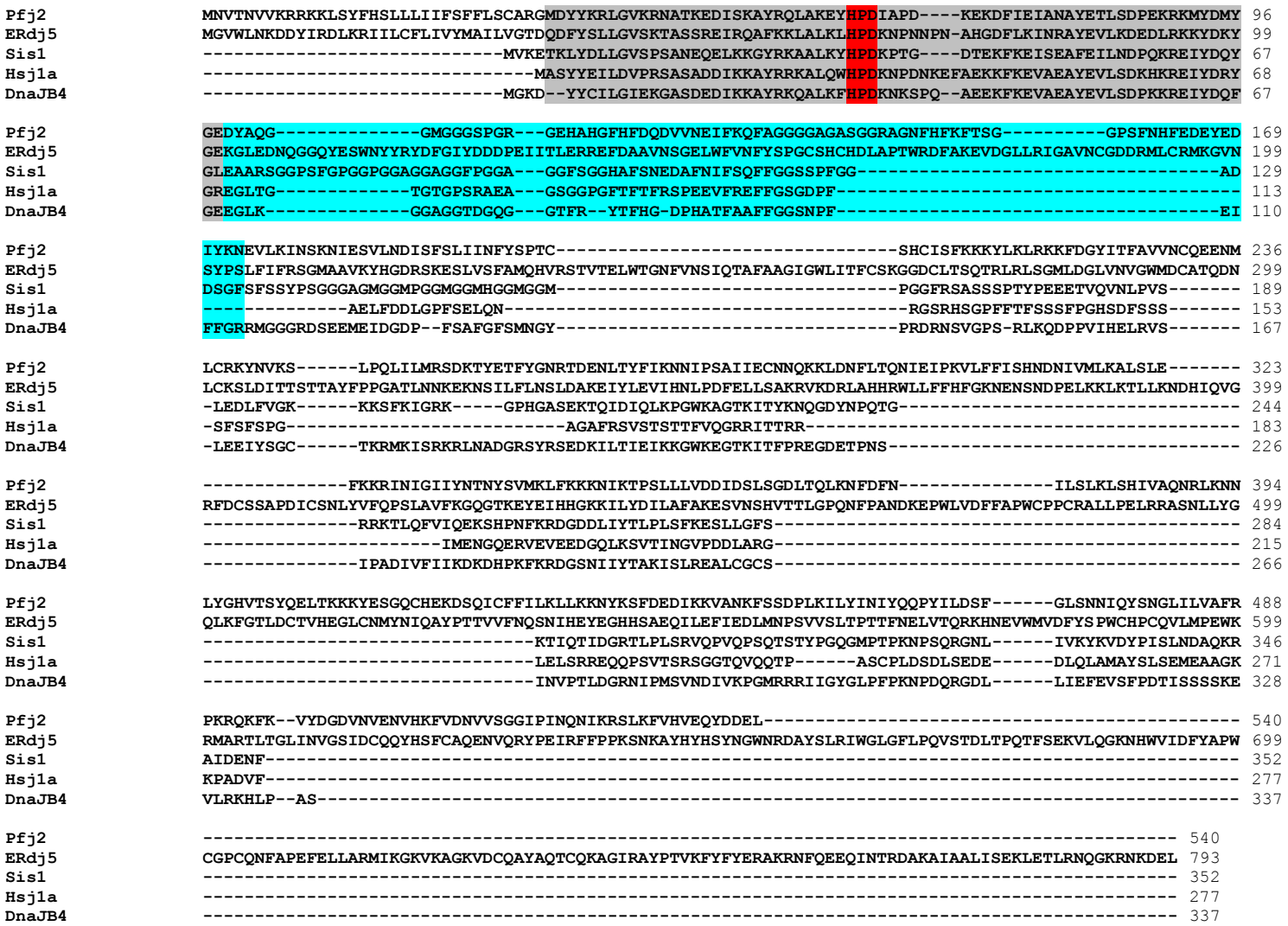

Figure 3.1: **Multiple sequence alignment of the amino acid sequence of Pfj2 with typical type II Hsp40s**. The J-domains are highlighted in grey with conserved HPD motifs highlighted in red. The G/F regions are highlighted in turquoise. Pfj2 (locus: PF11_ _0099), ERdj5 (accession: AAN73271.1), Sis1 (accession: CAA95866.1), Hsj1a (accession: AAA09034.1) and DnaJB4 (accession: NP_008965.2).

3.2.2. Sequence alignment of Pfj2 with human ERdj5

The amino acid sequence of Pfj2 was obtained from the PlasmoDB database and human ERdj5 was retrieved from the NCBI database. Pairwise sequence alignment was generated using ClustalW to identify domain similarities and identities. The results are shown in Figure 3.2.

The percentage identity and similarity of Pfj2 and ERdj5 were calculated as 14% and 26% respectively. Although the proteins are not highly conserved and are of different sizes, each amino acid sequence contains a J domain and conserved HPD motif in the N-terminal region. The J-domains are highlighted in grey and HPD motifs are highlighted in red. A G/F region is identified in both sequences at the N-terminus and is highlighted in turquoise. Furthermore, CXYC-variant motif signifying thioredoxin-like domains are present in both sequences and are highlighted in yellow. ER-retention motifs are highlighted in green and are represented by DDEL in Pfj2 and KDEL in ERdj5 at the C-terminus of the protein. This analysis also showed the presence of a putative PEXEL motif represented by RQLAK and highlighted violet in the amino acid sequence of Pfj2. As expected, a PEXEL motif was absent in the amino acid sequence of ERdj5. Putative ER signal sequences are highlighted in pink in the N-terminal regions of Pfj2 and ERdj5. The predicted protein sizes and number of amino acid residues of Pfj2 and ERdj5 are presented in Table 3.1 in section 3.2.1.

Figure 3.2: **Pairwise alignment of the amino acid sequence of Pfj2 and ERdj5**. The putative Pfj2 ER signal sequence is highlighted in pink. The J-domains are highlighted in grey with HDP motifs highlighted in red. Putative Pfj2 PEXEL motif is highlighted in violet. The G/F rich regions are highlighted in turquoise and thioredoxin-like domains in yellow. The ER retention motifs for Pfj2 and ERdj5 are highlighted in green respectively. Pfj2 (locus: PF11_ _0099) and ERdj5 (accession: AAN73271.1).

3.2.3. Signal prediction of Pfj2

The putative ER signal sequence of Pfj2 was identified using Phobius (Käll *et al*., 2007) (Refer to section 2.2.2). The Phobius server is used for the prediction of signal peptides from the amino acid sequence of a protein. The results are shown in Figure 3.3.

The predicted signal sequence of Pfj2 is represented by the red line in the N-terminal region of the amino acid sequence. The blue and green lines represent the non cytoplasmic and cytoplasmic regions respectively. A predicted transmembrane domain is not evident in the analysis.

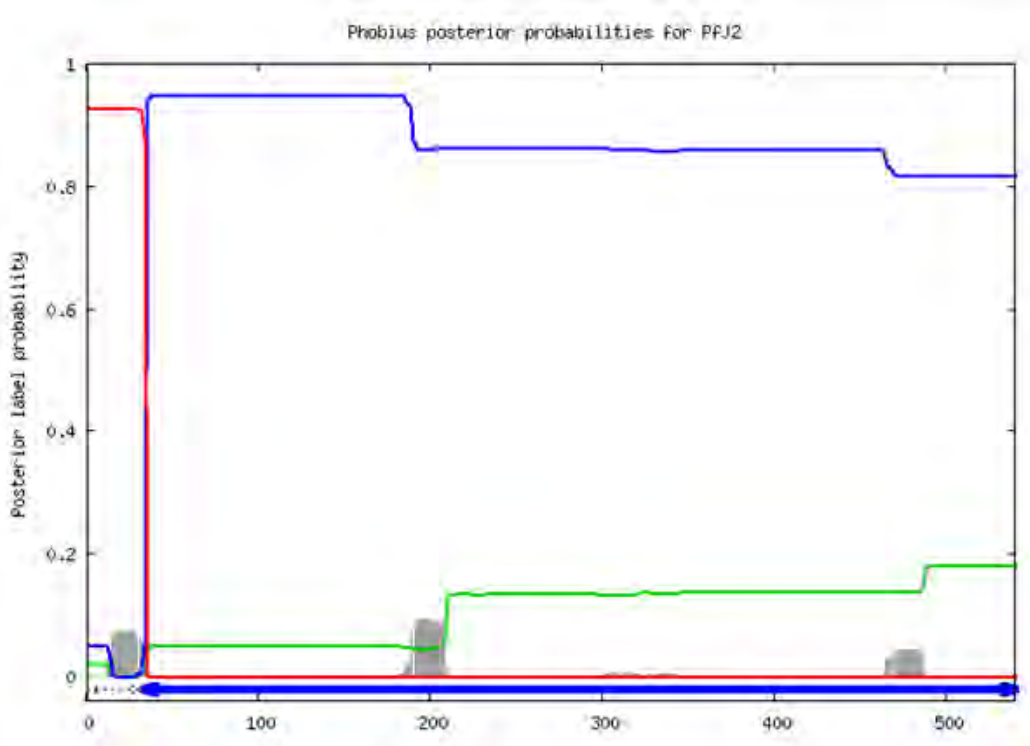

Figure 3.3: **Prediction of a putative signal sequence of Pfj2**. Red: Predicted signal peptide; Blue: Non cytoplasmic domain; Green: Cytoplasmic domain.

3.2.4. Sequence alignment of Hsp70s

The amino acid sequence of PfBiP was retrieved from PlasmoDB. Hamster GRP-78 and *S. cerevisiae* BiP (Sis1BiP) were obtained from NCBI. *Medicago sativa* Hsp70 (MsHsp70-1) was obtained from EMBL-EBI. A multiple sequence alignment was generated using ClustalW to determine conserved residues in the N- and C-terminal domains that are essential for functional interactions and substrate binding. The results are shown in Figure 3.4.

Multiple sequence alignment showed highly conserved amino acid residues in the N-terminal domain of the Hsp70s. These include phosphate binding sites highlighted in turquoise, connecting regions highlighted in red and adenosine regions highlighted in grey. The C-terminal consists of ß-subdomain highlighted in green that forms a hydrophobic substrate compartment which accommodates peptide substrate (Mayer *et al*., 1998). Highlighted in pink is the α-helical subdomain essential for substrate binding (Mayer *et al*., 1998). The size of PfBiP is predicted to be 72.3 kDa using BioEdit (Hall, 1999) and the number of amino acid residues is 652. The hamster GRP-78, Sis1BiP and MsHsp70-1 have very similar protein sizes of 72.3 kDa, 74.4 kDa and 70.9 kDa respectively. The number of amino acid of these proteins is also similar and is 654, 682 and 649 respectively. The overall sequence identity and similarity of PfBiP and other Hsp70s and the predicted protein sizes are presented in Table 3.2.

Table 3.2: Comparison of Hsp70s sequence identity, similarity, size of proteins and number of amino acid residues with PfBiP

Hsp70s	% Identity	% Similarity	Size (kDa)	Number of amino acid residue
GRP-78	64	78	72.3	654
Sis1BiP	73	57	74.4	682
MsHsp70-1	72	55	70.9	649

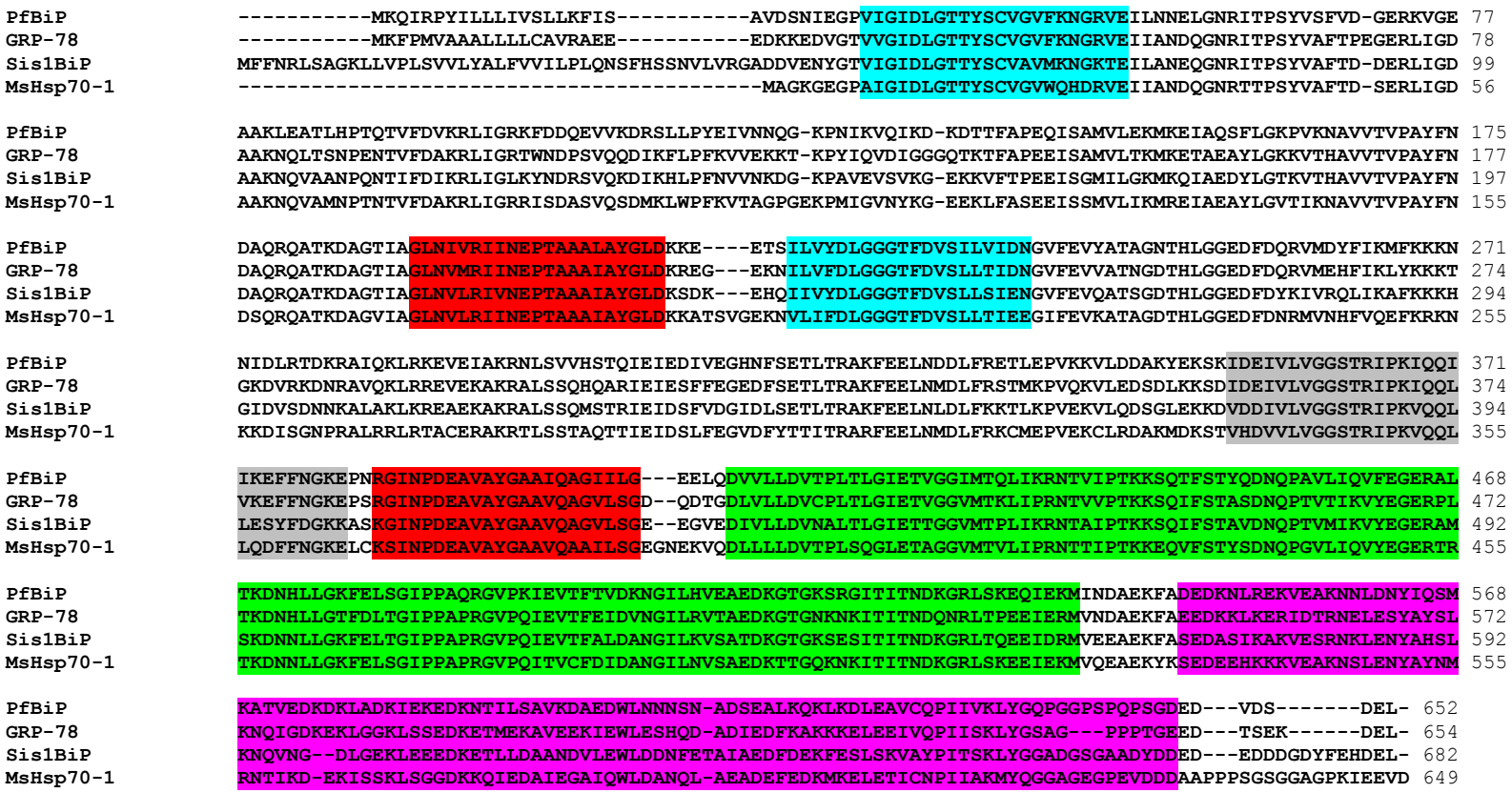

Figure 3.4: **Multiple sequence alignment of various Hsp70s**. Turquoise highlighted regions represent phosphate binding sites. The connecting regions are shaded in red. Adenosine phosphate binding region are highlighted in grey. Highlighted in green is the ß-subdomain and in pink is the α-helical subdomain. PfBiP (Locus: PFI0875), GRP-78 (Accession: P07823.1), Sis1BiP (Accession: EDN63302.1) and MsHsp70-1 (EMBL-Bank CDS: AAV98051).

3.3. Codon optimisation of Pfj2

Codon optimisation is a technique used to increase protein expression levels by increasing the translational efficiency of the gene of interest. This technique involves alteration of rare codons in the gene of interest to those used more frequently by the host. pUC57-Pfj2 which contains the full-length codon-optimised Pfj2 coding sequence in pUC57 was obtained from GenScript. The nucleotide sequence of Pfj2 obtained from PlasmoDB (Locus: PF11_0099) and codon-optimised Pfj2 was translated into amino acid using ApE 2.0.39. The results are shown in Figure 3.5.

Nucleotide sequences are arranged in codons and corresponding 1-letter amino acid codes are presented below each codon. The nucleotide sequences are numbered. Although the nucleotide sequences of the database obtained Pfj2 and codon-optimised Pfj2 are different (highlighted in yellow), both nucleotide sequences encode the same protein.

```
                1                                                          60
Optimised       ATG GAT TAT TAC AAA CGT CTG GGC GTG AAA CGC AAT GCG ACC AAA GAA GAT ATT TCT AAA
Database        ATG GAT TAT TAC AAA AGA CTG GGC GTT AAA CGG AAC GCC ACA AAA GAA GAT ATT TCA AAA
                 M   D   Y   Y   K   R   L   G   V   K   R   N   A   T   K   E   D   I   S   K

               61                                                         120
Optimised       GCC TAC CGC CAG CTG GCA AAA GAA TAT CAT CCG GAT ATC GCC CCG GAT AAA GAA AAA GAT
Database        GCT TAT AGG CAG CTA GCT AAA GAA TAT CAT CCA GAT ATA GCG CCC GAC AAA GAA AAA GAT
                 A   Y   R   Q   L   A   K   E   Y   H   P   D   I   A   P   D   K   E   K   D

              121                                                         180
Optimised       TTC ATC GAA ATC GCG AAC GCC TAC GAA ACG CTG AGC GAT CCG GAA AAA CGT AAA ATG TAC
Database        TTT ATA GAA ATT GCA AAC GCC TAT GAA ACG TTA TCA GAT CCT GAG AAA AGA AAA ATG TAT
                 F   I   E   I   A   N   A   Y   E   T   L   S   D   P   E   K   R   K   M   Y

              181                                                         240
Optimised       GAT ATG TAC GGT GAA GAT TAT GCG CAG GGC GGT ATG GGC GGT GGC TCT CCG GGT CGC GGC
Database        GAT ATG TAT GGT GAG GAC TAT GCC CAA GGA GGT ATG GGA GGA GGA AGT CCC GGG AGA GGG
                 D   M   Y   G   E   D   Y   A   Q   G   G   M   G   G   G   S   P   G   R   G
```

	241																			300
Optimised	GAA	CAT	GCA	CAC	GGC	TTT	CAC	TTC	GAT	CAG	GAT	GTG	GTT	AAT	GAA	ATC	TTC	AAA	CAG	TTC
Database	GAA	CAT	GCA	CAT	GGT	TTT	CAT	TTT	GAT	CAA	GAT	GTA	GTA	AAT	GAA	ATA	TTT	AAA	CAA	TTT
	E	H	A	H	G	F	H	F	D	Q	D	V	V	N	E	I	F	K	Q	F

	301																			360
Optimised	GCG	GGT	GGC	GGT	GGC	GCA	GGT	GCC	AGC	GGT	GGC	CGT	GCG	GGT	AAC	TTT	CAT	TTC	AAA	TTT
Database	GCA	GGA	GGT	GGT	GGT	GCG	GGT	GCG	AGT	GGT	GGT	AGA	GCG	GGG	AAT	TTT	CAT	TTT	AAA	TTT
	A	G	G	G	G	A	G	A	S	G	G	R	A	G	N	F	H	F	K	F

	361																			420
Optimised	ACC	AGC	GGT	GGC	CCG	TCT	TTC	AAC	CAC	TTC	GAA	GAT	GAA	TAC	GAA	GAT	ATT	TAC	AAA	AAC
Database	ACA	TCT	GGT	GGT	CCT	AGT	TTT	AAT	CAT	TTT	GAA	GAT	GAA	TAT	GAA	GAT	ATA	TAT	AAA	AAT
	T	S	G	G	P	S	F	N	H	F	E	D	E	Y	E	D	I	Y	K	N

	421																			480
Optimised	GAA	GTG	CTG	AAA	ATC	AAC	AGC	AAA	AAC	ATC	GAA	TCT	GTT	CTG	AAC	GAT	ATC	AGT	TTC	AGC
Database	GAA	GTT	TTA	AAA	ATA	AAT	TCT	AAG	AAT	ATT	GAA	TCT	GTT	TTA	AAT	GAC	ATA	TCA	TTT	TCT
	E	V	L	K	I	N	S	K	N	I	E	S	V	L	N	D	I	S	F	S

	481																			540
Optimised	CTG	ATC	ATC	AAC	TTC	TAT	AGT	CCG	ACC	TGC	AGC	CAT	TGT	ATC	TCT	TTC	AAG	AAA	AAA	TAC
Database	TTA	ATA	ATA	AAT	TTT	TAT	TCA	CCT	ACA	TGT	TCT	CAT	TGT	ATA	TCT	TTT	AAA	AAG	AAA	TAT
	L	I	I	N	F	Y	S	P	T	C	S	H	C	I	S	F	K	K	K	Y

	541																			600
Optimised	CTG	AAA	CTG	CGT	AAA	AAA	TTC	GAT	GGT	TAC	ATC	ACG	TTC	GCA	GTG	GTT	AAC	TGC	CAG	GAA
Database	TTA	AAA	TTA	CGT	AAG	AAA	TTT	GAT	GGA	TAT	ATA	ACA	TTT	GCT	GTT	GTA	AAT	TGT	CAA	GAG
	L	K	L	R	K	K	F	D	G	Y	I	T	F	A	V	V	N	C	Q	E

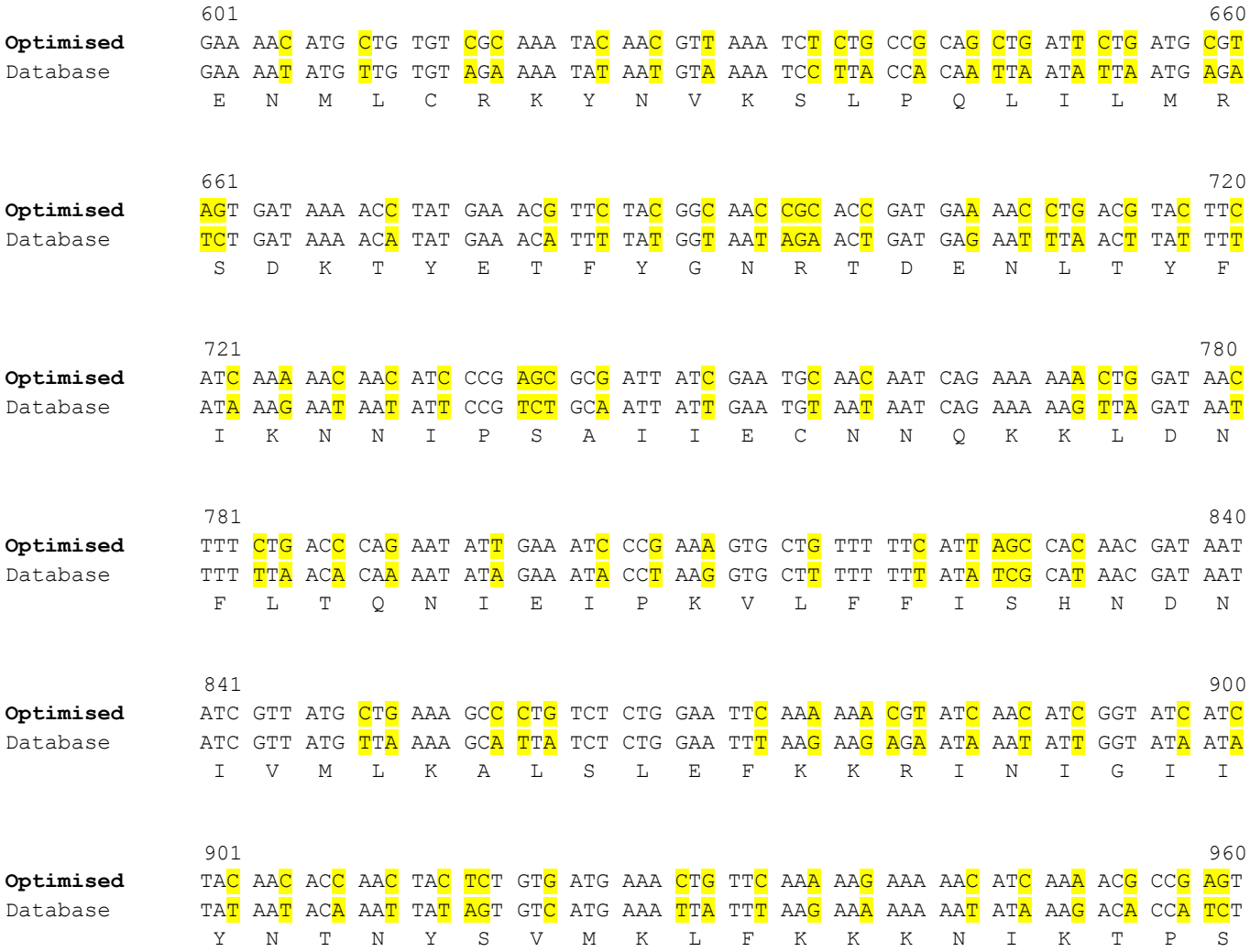
601 660
Optimised GAA AAC ATG CTG TGT CGC AAA TAC AAC GTT AAA TCT CTG CCG CAG CTG ATT CTG ATG CGT
Database GAA AAT ATG TTG TGT AGA AAA TAT AAT GTA AAA TCC TTA CCA CAA TTA ATA TTA ATG AGA
E N M L C R K Y N V K S L P Q L I L M R
661 720
Optimised AGT GAT AAA ACC TAT GAA ACG TTC TAC GGC AAC CGC ACC GAT GAA AAC CTG ACG TAC TTC
Database TCT GAT AAA ACA TAT GAA ACA TTT TAT GGT AAT AGA ACT GAT GAG AAT TTA ACT TAT TTT
S D K T Y E T F Y G N R T D E N L T Y F
721 780
Optimised ATC AAA AAC AAC ATC CCG AGC GCG ATT ATC GAA TGC AAC AAT CAG AAA AAA CTG GAT AAC
Database ATA AAG AAT AAT ATT CCG TCT GCA ATT ATT GAA TGT AAT AAT CAG AAA AAG TTA GAT AAT
I K N N I P S A I I E C N N Q K K L D N
781 840
Optimised TTT CTG ACC CAG AAT ATT GAA ATC CCG AAA GTG CTG TTT TTC ATT AGC CAC AAC GAT AAT
Database TTT TTA ACA CAA AAT ATA GAA ATA CCT AAG GTG CTT TTT TTT ATA TCG CAT AAC GAT AAT
F L T Q N I E I P K V L F F I S H N D N
841 900
Optimised ATC GTT ATG CTG AAA GCC CTG TCT CTG GAA TTC AAA AAA CGT ATC AAC ATC GGT ATC ATC
Database ATC GTT ATG TTA AAA GCA TTA TCT CTG GAA TTT AAG AAG AGA ATA AAT ATT GGT ATA ATA
I V M L K A L S L E F K K R I N I G I I
901 960
Optimised TAC AAC ACC AAC TAC TCT GTG ATG AAA CTG TTC AAA AAG AAA AAC ATC AAA ACG CCG AGT
Database TAT AAT ACA AAT TAT AGT GTC ATG AAA TTA TTT AAG AAA AAA AAT ATA AAG ACA CCA TCT
Y N T N Y S V M K L F K K K N I K T P S

```
               961                                                                        1020
Optimised      CTG CTG CTG GTT GAT GAT ATC GAT TCT CTG AGT GGC GAT CTG ACC CAG CTG AAA AAC TTC
Database       TTA TTA CTT GTC GAT GAT ATT GAT AGT TTA TCA GGG GAT TTA ACA CAA TTA AAA AAT TTC
                L   L   L   V   D   D   I   D   S   L   S   G   D   L   T   Q   L   K   N   F

               1021                                                                       1080
Optimised      GAT TTC AAC ATC CTG AGT CTG AAA CTG AGC CAT ATC GTG GCG CAG AAC CGC CTG AAA AAC
Database       GAT TTT AAT ATT TTG TCA TTA AAA TTA AGT CAC ATT GTT GCA CAA AAT AGA TTA AAA AAT
                D   F   N   I   L   S   L   K   L   S   H   I   V   A   Q   N   R   L   K   N

               1081                                                                       1140
Optimised      AAT CTG TAC GGT CAC GTT ACC AGT TAT CAG GAA CTG ACC AAG AAA AAA TAC GAA AGT GGC
Database       AAT TTA TAT GGA CAT GTA ACA TCT TAC CAA GAA TTA ACC AAA AAA AAA TAT GAA TCG GGA
                N   L   Y   G   H   V   T   S   Y   Q   E   L   T   K   K   K   Y   E   S   G

               1141                                                                       1200
Optimised      CAG TGC CAT GAA AAA GAT AGC CAG ATT TGC TTT TTC ATC CTG AAA CTG CTG AAG AAA AAC
Database       CAA TGT CAT GAG AAG GAT TCA CAA ATA TGT TTC TTT ATT TTA AAA TTA TTA AAA AAA AAT
                Q   C   H   E   K   D   S   Q   I   C   F   F   I   L   K   L   L   K   K   N

               1201                                                                       1260
Optimised      TAT AAA AGC TTC GAT GAA GAT ATC AAA AAA GTG GCA AAC AAA TTC AGC TCT GAT CCG CTG
Database       TAT AAA TCA TTT GAT GAA GAT ATT AAA AAG GTA GCA AAC AAA TTC TCA AGT GAC CCC TTA
                Y   K   S   F   D   E   D   I   K   K   V   A   N   K   F   S   S   D   P   L

               1261                                                                       1320
Optimised      AAA ATT CTG TAT ATT AAC ATC TAC CAG CAG CCG TAT ATC CTG GAT TCT TTT GGT CTG AGT
Database       AAA ATT TTA TAT ATT AAT ATA TAT CAA CAA CCA TAT ATA TTA GAT TCT TTT GGA CTA TCG
                K   I   L   Y   I   N   I   Y   Q   Q   P   Y   I   L   D   S   F   G   L   S
```

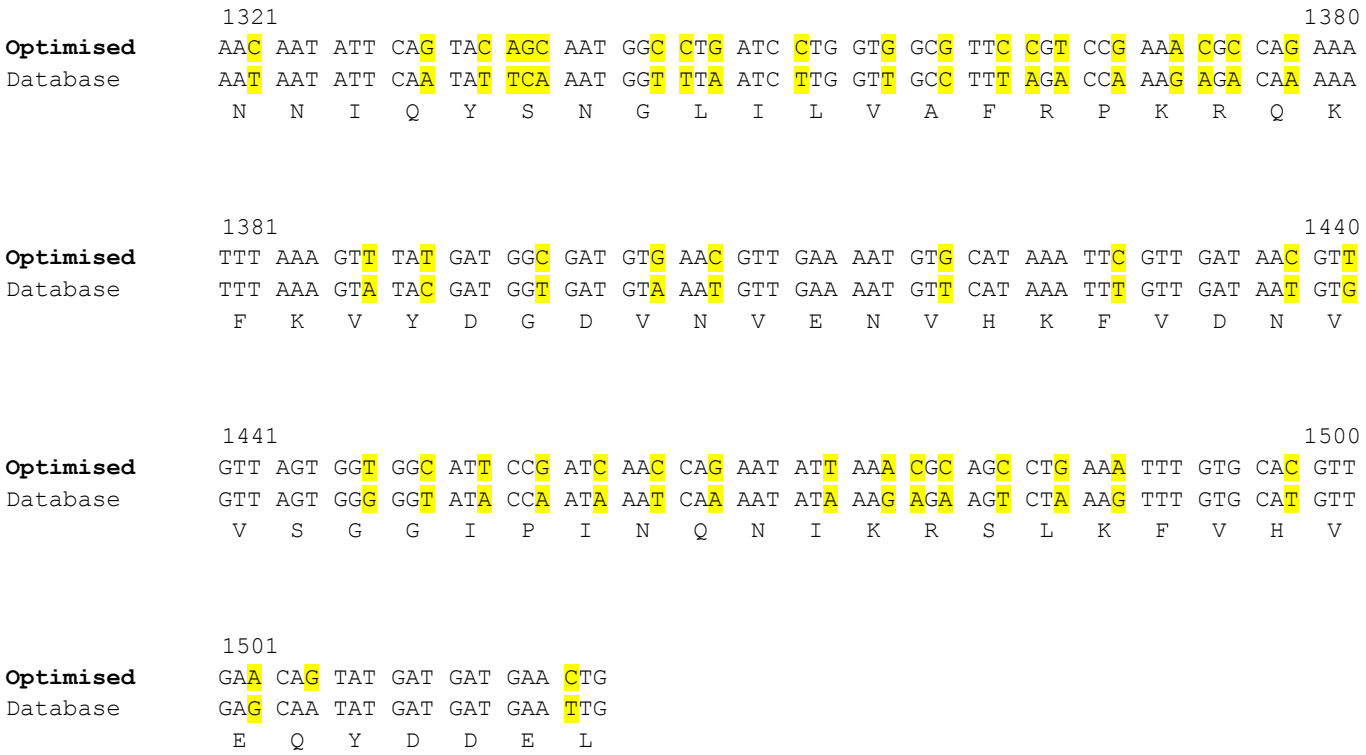

Figure 3.5. **The nucleotide sequence and predicted amino acid sequence alignment of the database obtained Pfj2 and codon-optimised Pfj2**.

Different nucleotides are highlighted in yellow.

3.4. Cloning of Pfj2

3.4.1. Confirmation of pUC57-Pfj2

The codon-optimised Pfj2 was cloned into pUC57 by GenScript and supplied as a pUC57-Pfj2. The pUC57-Pfj2 had essential features including *lacZ*, rep (pMB1) and the ampicillin resistance gene (Amp^R). A schematic diagram of pUC57-Pfj2 which is 4228 bp in size is shown in Figure 3.6A.

pUC57-Pfj2 was restricted with *Bam*HI and *Kpn*I and the digest was analysed by agarose gel electrophoresis. The results are shown in Figure 3.6B. Undigested pUC57-Pfj2 is present in lane 1. Lanes 2 and 3 contain linearised pUC57-Pfj2 restricted with *Bam*HI and *Kpn*I respectively. Three prominent bands were present in lane 4 which contains partially digested pUC57-Pfj2 restricted with *Bam*HI and *Kpn*I. The top band represents linearised pUC57-Pfj2 restricted once at 4228 bp, the middle band shows linearised pUC57 at 2683 bp and the lower band shows linearised Pfj2 coding sequence at 1545 bp.

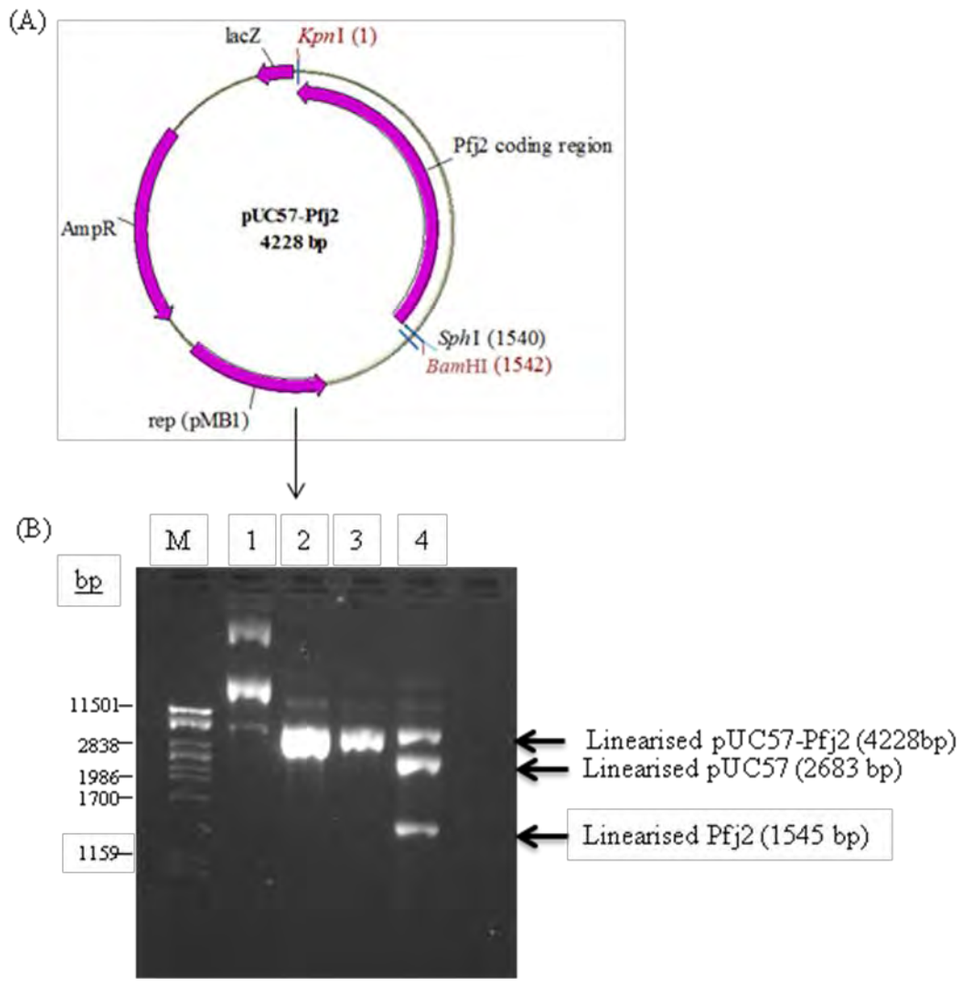

***Figure 3.6:* Restriction of pUC57-Pfj2. (A)** Plasmid map of pUC57-Pfj2. **(B)** Lane M: λ *Pst*I molecular marker; Lane 1: Undigested pUC57-Pfj2; Lane 2: pUC57-Pfj2 restricted with *Bam*HI; Lane 3: pUC57-Pfj2 restricted with *Kpn*I; Lane 4: pUC57-Pfj2 restricted with *Bam*HI and *Kpn*I.

3.4.2. Ligation of Pfj2 into pQE30 and verification of pQE30-Pfj2

The 1545 bp band representing the codon-optimsed Pfj2 sequence was excised from the gel and purified before ligation into pQE30. The Pfj2 coding region was ligated downstream of the His_6-tag sequence. Important features of the 3443 bp pQE30 vector include the IPTG-inducible T5 promoter which facilitates high level expression of His_6-tagged proteins through recognition by RNA polymerase in *E. coli*. The vector encodes *lac* operator sequences (*lac* O) that allows for efficient repression of T5 promoter. A his_6 sequence facilitates purification of recombinant protein by nickel affinity chromatography. A ß-lactamase gene encoding ampicillin resistance (Amp^R) is present to enable specific gene selection. The pQE30 vector has multiple cloning sites (MSC) which contains restriction sites that are commonly used in molecular cloning (Figure 3.7A) (QIAexpress® The Complete System for 6xHis Technology). A schematic diagram of pQE30-Pfj2 is shown in Figure 3.7A.

The integrity of pQE30-Pfj2 was confirmed by digestion with *Bam*HI and *Kpn*I followed by agarose gel electrophoresis. The results are shown in Figure 3.7C. Lane 1 contains undigested pQE30-Pfj2. Lane 2 is linearised pQE30 restricted with *Bam*HI at 3443 bp. Lane 3 contains pQE30-Pfj2 restricted with *Bam*HI and *Kpn*I. The double restriction resulted in linearised pQE30 at 3443 bp and the Pfj2 coding sequence at 1545 bp.

(A)

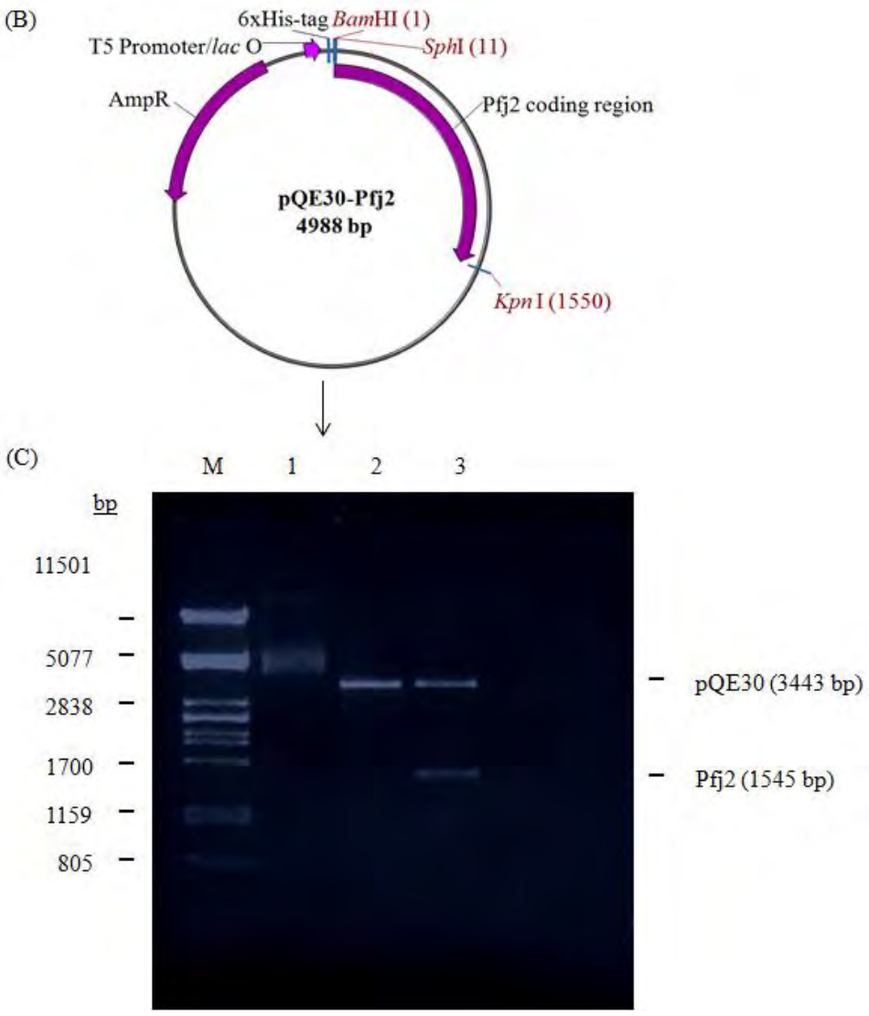

Figure 3.7: **Confirmation of pQE30-Pfj2**. **(A)** Multiple cloning site of pQE30. **(B)** Plasmid map of pQE30-Pfj2. **(C)** Lane M: λ *Pst*I molecular marker; Lane 1: Undigested pQE30-Pfj2; Lane 2: pQE30 restricted with *Bam*HI; Lane 3: pQE30-Pfj2 restricted with *Bam*HI and *Kpn*I.

3.4.3. Sequencing of pQE30-Pfj2

To further verify pQE30-Pfj2, the plasmid was subjected to DNA sequencing as described in section 2.3.6. Approximately 400 bps of readable sequence was obtained using forward and reverse primers, therefore, the entire sequence was not obtained. Furthermore, the frame-shift mutation detected hereafter may have interfered with protein folding and function. The results are shown in Figure 3.8.

Figure 3.8 shows the position of a start codon, ATG, highlighted in turquoise at the 5'end of the nucleotide sequence. Located downstream of the ATG, is the His_6-tag sequence highlighted in yellow. GCA, highlighted in teal represents the first codon of the Pfj2 coding sequence. The ER signal sequence has been deleted from the Pfj2 coding sequence, therefore, the gene sequence is incomplete with a start codon of GCA instead of ATG. The three dashes (_ _ _) represent the missing internal region of the nucleotide sequence. The stop codon, TAA, is indicated in green upstream of the *Kpn*I restriction site, highlighted in pink at the 3'end of the nucleotide sequence. DNA sequencing of pQE30-Pfj2 showed the presence of two *Bam*HI sites downstream of the His_6-tag highlighted in grey and red respectively. This result was unexpected because only one *Bam*HI restriction site was engineered in the 5' end of the nucleotide sequence. This additional *Bam*HI site generated a frame-shift in the codon-optimised Pfj2 coding sequence resulting in an incorrect open reading frame.

5'TAGAAATCATAAAAAATTTATTTGCTTTGTGAGCGGATAACAATTATAATAGATTCAATTG
TGAGCGGATAACAATTTCACACAGAATTCATTAAAGAGGAGAAATTAACTATGAGAGGATC
GCATCACCATCACCATCACGGATCCGATCCAATGGATCCGCATGCGCACGTGGTATGGATTA
TTACAAACGTCTGGGCGTGAAACGCAATGCGACCAAAGAAGATATTTCTAAAGCCTACCGC
CAGCTGGCAAAAGAATATCATCCGGATATCGCCCCGGGATAAAGAAAAAGATTTCATCGAA
ATCGCGAACGCCTACGAAACGCTGAGCGATCCGGAAAAACGTAAAATGTACGATATGTACG
GTGAAGATTATGCGCAGG_ _ _GTCACGTTACCAGTTATCAGGAACTGACCAAGAAAAAATA
CGAAAGTGGCCAGTGCCATGAAAAAGATAGCCAGATTTGCTTTTTCATCCTGAAACTGCTGA
AGAAAAACTATAAAAGCTTCGATGAAGATATCAAAAAAGTGGCAAACAAATTCAGCTCTGA
TCCGCTGAAAATTCTGTATATTAACATCTACCAGCAGCCGTATATCCTGGATTCTTTTGGTCT
GAGTAACAATATTCAGTACAGCAATGGCCTGATCCTGGTGGCGTTCCGTCCGAAACGCCAGA
AATTTAAAGTTTATGATGGCGATGTGAACGTTGAAAATGTGCATAAATTCGTTGATAACGTT
GTTAGTGGTGGCATTCCGATCAACCAGAATATTAAACGCAGCCTGAAATTTGTGCACGTTGA
ACAGTATGATGATGAACTGTAAGGTACCCCGGGTCGACCTGCAGCC'3

Figure 3.8: **Nucleotide sequence of pQE30-Pfj2**. Turquoise: Start codon, ATG; Yellow: His_6-tag; Grey: *Bam*HI; Red: *Bam*HI; Teal: first codon of the codon-optimised Pfj2 coding sequence, GCA; Green; Stop codon, TAA; Pink: *Kpn*I.

3.4.4. Site-directed mutagenesis

To eliminate the first *Bam*HI site downstream of the His_6-tag, pQE30-Pfj2 was subjected to site directed mutagenesis. Site-directed mutagenesis was performed by whole plasmid amplification using complementary forward and reverse primers (Refer to Table 2.1, section 2.3.7.1). The primers were designed to amplify the 4988 bp sequence of pQE30-Pfj2. Following amplification, the product was treated with *Dpn*I to remove parental plasmid and analysed by 0.8% agarose gel electrophoresis. The results are shown in Figure 3.9.

Lane 1 contains the parental plasmid, undigested pQE30-Pfj2. Lane 2 contains the mutagenesis amplification product, pQE30-Pfj2, treated with *Dpn*I. The resolved undigested pQE30-Pfj2 bands in lane 1 serves as a control to determine whether *Dpn*I is able to cleave the template DNA of the mutagenic amplified product in lane 2. There is no band in the mutated amplified product in lane 2 corresponding to the undigested pQE30-Pfj2 band observed in lane 1. This suggests that the *Dpn*I has successfully cleaved the template DNA of the mutagenic amplified product. However, if the DNA bands observed in lane 2 corresponds with the undigested pQE30-Pfj2 in lane 1, the *Dpn*I would have not been effective in cleaving the template pQE30-Pfj2 of the amplified product. Lanes 3 and 4 represents linearised pQE30-Pfj2 controls restricted with *Bam*HI and *Kpn*I respectively resolved at the expected size of 4988 bp to indicate where the mutagenic amplification product should resolve.

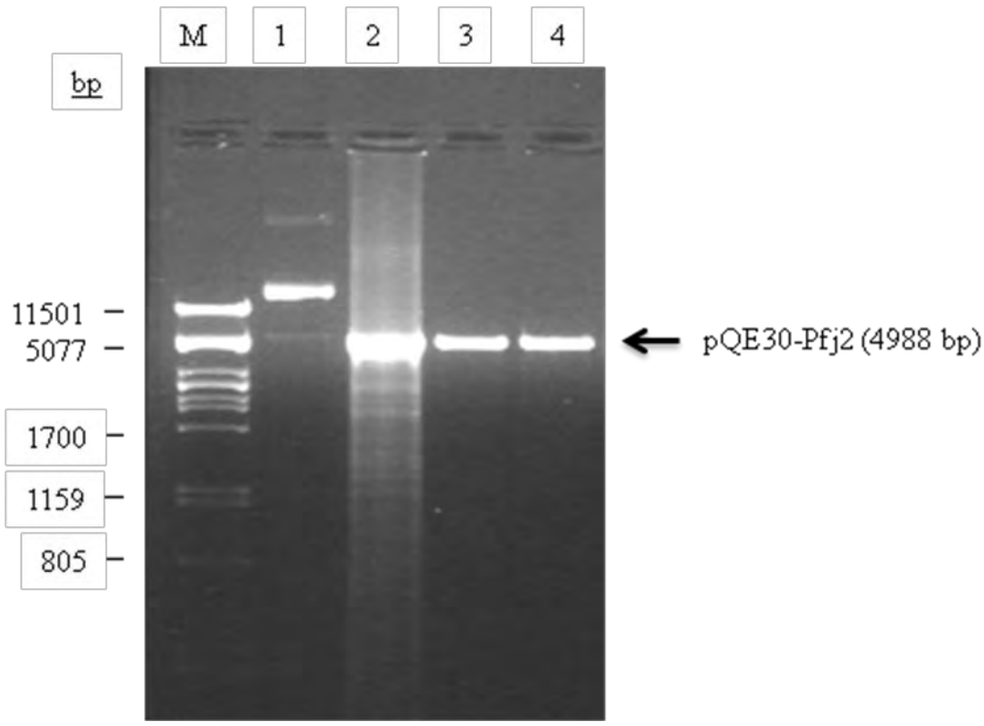

Figure 3.9: **Site-directed mutagenesis on pQE30-Pfj2.** Lane M: λ *Pst*I molecular marker; Lane 1: Undigested pQE30-Pfj2; Lane 2: *Dpn*I treated mutagenesis amplification product, pQE30-Pfj2; Lane 3: pQE30-Pfj2 restricted with *Bam*HI; Lane 4: pQE30-Pfj2 restricted with *Kpn*I.

3.4.5. Verification of pQE30-Pfj2 following site-directed mutagenesis

To confirm that site-directed mutagenesis was successful, DNA sequencing was performed using pQE30 forward and reverse primers as described in section 3.3.3. The results are shown in Figure 3.10.

DNA sequencing showed that the first *Bam*HI site downstream of the His_6-tag was successfully mutated by deletion mutagenesis, thereby, correcting the frame-shift mutation. Two nucleotides, GG, were deleted from the first *Bam*HI site leaving ATCC highlighted in grey. The mutagenesis eliminated the frame-shift in the coding sequence of His_6-Pfj2 and corrected the open reading frame. The second *Bam*HI site highlighted in red is downstream of the His_6-tag (yellow). The start codon, ATG, is positioned at the 5' end of the nucleotide sequence and is highlighted in turquoise. GCA, highlighted in teal, represents the first codon of the codon-optimised Pfj2 coding sequence.

5'CCTCGAGAAATCATAAAAAATTTATTTGCTTTGTGAGCGGTCCACAATTATAATAGATTCA
ATTGTGAGCGGATAACAATTTCACACAGAATTCATTAAAGAGGAGAAATTAACTATGAGAG
GATCGCATCACCATCACCATCACATCCGATCCAATGGATCCGCATGCGCACGTGGTATGGAT
TATTACAAACGTCTGGGCGTGAAACGCAATGCGACCAAAGAAGATATTTCTAAAGCCTACC
GCCAGCTGGCAAAAGAATATCATCCGGATATCGCCCCGGATAAAGAAAAAGATTTCATCGA
AATCGCGAACGCCTACGAAACGCTGAGCGATCCGGAAAAACGTAAAATGTACGATATGTAC
GGTGAAGATTATGCGCAGGGCGGTATGGGCGG_ _ _GGTCACGTTACCAGTTATCAGGAAC
TGACCAAGAAAAAATACGAAAGTGGCCAGTGCCATGAAAAAGATAGCCAGATTTGCTTTTT
CATCCTGAAACTGCTGAAGAAAAACTATAAAAGCTTCGATGAAGATATCAAAAAAGTGGCA
AACAAATTCAGCTCTGATCCGCTGAAAATTCTGTATATTAACATCTACCAGCAGCCGTATAT
CCTGGATTCTTTTGGTCTGAGTAACAATATTCAGTACAGCAATGGCCTGATCCTGGTGGCGTT
CCGTCCGAAACGCCAGAAATTTAAAGTTTATGATGGCGATGTGAACGTTGAAAATGTGCATA
AATTCGTTGATAACGTTGTTAGTGGTGGCATTCCGATCAACCAGAATATTAAACGCAGCCTG
AAATTTGTGCACGTTGAACAGTATGATGATGAACTGTAAGGTACCCCGGGTCGACCTGCAGC
C'3

Figure 3.10: **Nucleotide sequence of pQE30-Pfj2 following site-directed mutagenesis**. Turquoise: Start codon, ATG; Yellow: His_6-tag; Grey: Mutated site; Red: *Bam*HI; Teal: first codon of the codon-optimised Pfj2 coding sequence: Green; Stop codon, TAA; Pink: *Kpn*I.

3.5. Expression of His_6-Pfj2 and His_6-BiP in *E. coli* M15[*pREP4*] cells

3.5.1. Heterologous expression of His_6-Pfj2

pQE30-Pfj2 was transformed into *E. coli* M15[*pREP4*] cells and His_6-Pfj2 expression in *E. coli* M15[*pREP4*] cells induced with 1 mM IPTG at 37°C. Expression was assessed every hour for 5 hours and at 12 hours post-induction. The proteins were analysed by 12% SDS-PAGE and Western immunoblotting. The results are shown in Figure 3.11.

A band corresponding to the expected mobility of His_6-Pfj2 at approximately 62 kDa can be seen in lanes 2-7 in Figure 3.11A. Apparent on the gel is a protein band that is increasing in intensity over time with maximal intensity at 12 hours post-induction (lane 7). The band is absent in the un-induced sample (lane 1). Lane 8 contains the 41 kDa His_6-PFA (plasmid generously donated by Mr Michael O. Daniyan) used to approximate the size of His_6-Pfj2. To confirm the presence of His_6-Pfj2, Western immunoblotting using anti-His_6 antibodies was performed (Figure 3.11B). Prominent bands representing His_6-Pfj2 of increasing intensity were observed (lanes 2-7). A band was detected for His_6-PFA (lane 8).

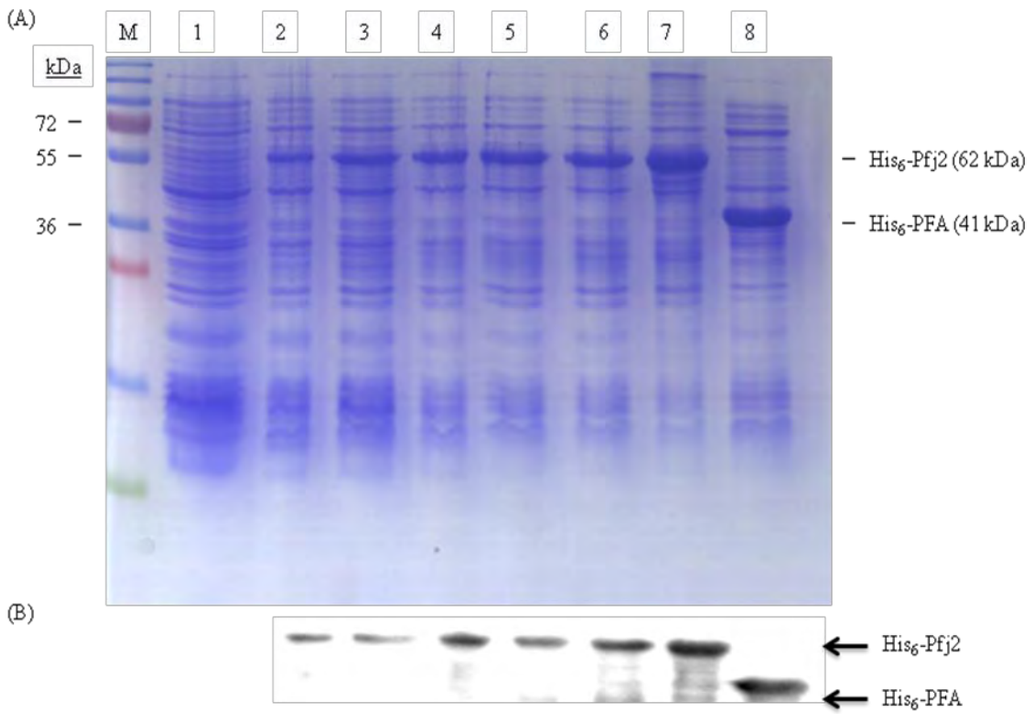

***Figure 3.11:* Expression of His_6-Pfj2 in *E. coli* M15[*pREP4*] cells. (A)** Lane M: PageRuler™ Plus Prestained Protein Ladder; Lane 1: un-induced His_6-Pfj2; Lane 2: His_6-Pfj2 harvested 1 hour post-induction; Lane 3: His_6-Pfj2 harvested 2 hours post-induction; Lane 4: His_6-Pfj2 harvested 3 hours post-induction; Lane 5: His_6-Pfj2 harvested 4 hours post-induction; Lane 6: His_6-Pfj2 harvested 5 hours post-induction; Lane 7: His_6-Pfj2 harvested 12 hours post-induction; Lane 8: total protein of *E. coli* M15[*pREP4*] cells expressing His_6-PFA. **(B)** Western immunoblotting confirming induced His_6-Pfj2 and His_6-PFA expression using mouse anti-His_6 antibodies (1/5000 dilution) and anti-mouse IgG POD-labeled antibodies (1/6000 dilution).

3.5.2. Heterologous expression of His_6-BiP

His_6-BiP expression in *E. coli* M15[*pREP4*] cells was induced with 1 mM IPTG at 37°C. The expression of His_6-BiP was assessed every hour for 5 hours and 12 hours post-induction. The proteins were analysed by 12% SDS-PAGE and Western immunoblotting. The results are shown in Figure 3.12.

A band corresponding to the expected mobility of His_6-BiP at approximately 78 kDa is observed in lanes 2-7 in Figure 3.12A. Maximal protein intensity can be seen in the sample induced four hours post-induction in lane 5. No corresponding protein band is observed in the un-induced sample in lane 1. His_6-Pfj2 was used to estimate the approximate size of His_6-BiP. The presence of His_6-BiP and His_6-Pfj2 was confirmed by Western immunoblotting using anti-His_6 antibodies (Figure 3.12B). Prominent bands representing His_6-BiP of decreasing intensity at 5 and 12 hours were observed (lanes 6-7). A band was detected for His_6-Pfj2 (lane 8).

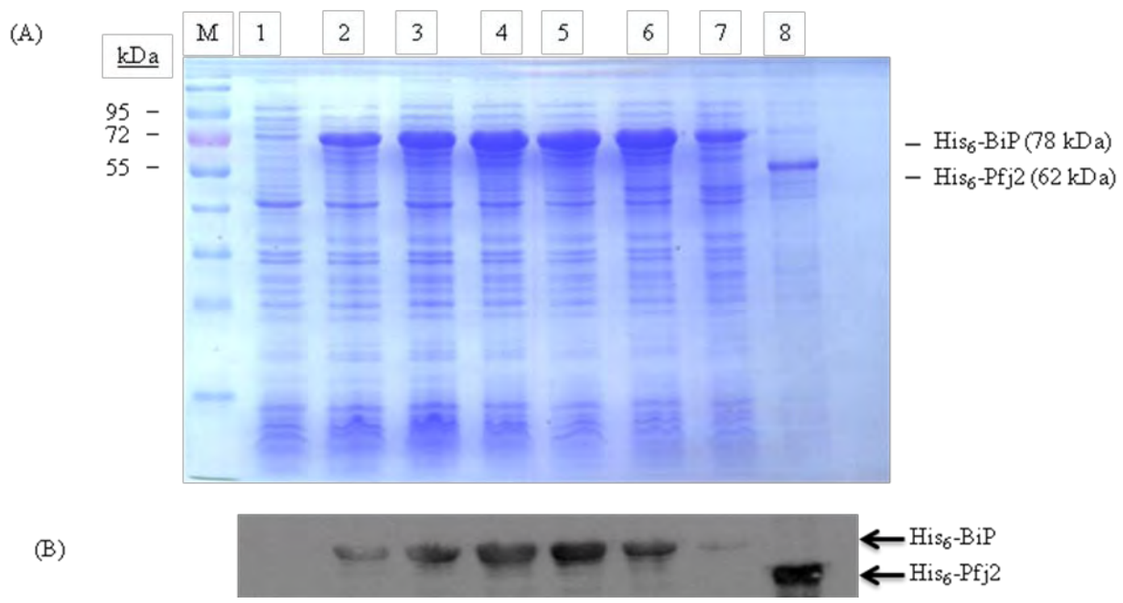

Figure 3.12: **Expression of mammalian His_6-BiP in *E. coli* M15[pREP4] cells.** **(A)** Lane M: PageRuler™ Prestained protein ladder; Lane 1: Un-induced His_6-BiP; Lane 2: His_6-BiP harvested 1 hour post-induction; Lane 3: His_6-BiP harvested 2 hours post-induction; Lane 4: His_6-BiP harvested 3 hours post-induction; Lane 5: His_6-BiP harvested 4 hours post-induction; Lane 6: His_6-BiP harvested 5 hours post-induction; Lane 7: His_6-BiP harvested 12 hours post-induction; Lane 8: total protein of *E. coli* M15[*pREP4*] cells expressing His_6-Pfj2. **(B)** Western immunoblotting for verification of His_6-BiP and His_6-Pfj2 expression using mouse anti-His_6 primary antibody (1/5000 dilution) and anti-mouse IgG POD-labeled secondary antibody (1/6000 dilution).

3.6. Solubility studies

3.6.1. Solubility studies of His_6-Pfj2 in E. coli M15[pREP4] cells at 37°C

In order to determine whether native or denaturing conditions would be used for purification of His_6-Pfj2, it was necessary to determine its solubility in *E. coli* M15[*pREP4*] cells. Protein expression was induced and cells harvested 12 hours post induction and separated into supernatant (S) and pellet (P) fractions by centrifugation. The samples were analysed by 12% SDS-PAGE and Western immunoblotting. The results are shown in Figure 3.13.

No corresponding protein band was observed in the un-induced sample in lane 1 as expected. Distinct protein bands corresponding to the expected mobility of His_6-Pfj2 can be seen in the total protein (TP) and pellet fraction in lanes 2 and 4 respectively. No corresponding band was evident in lane 3 which contains the supernatant fraction. His_6-PFA in lane 5 is 41 kDa in size and was used to estimate the size of His_6-Pfj2. To detect His_6-Pfj2 and His_6-PFA, Western immunoblotting using anti-His_6 antibodies was carried out (Figure 3.13B). Prominent bands were observed for His_6-Pfj2 in the total protein, pellet fraction and His_6-PFA.

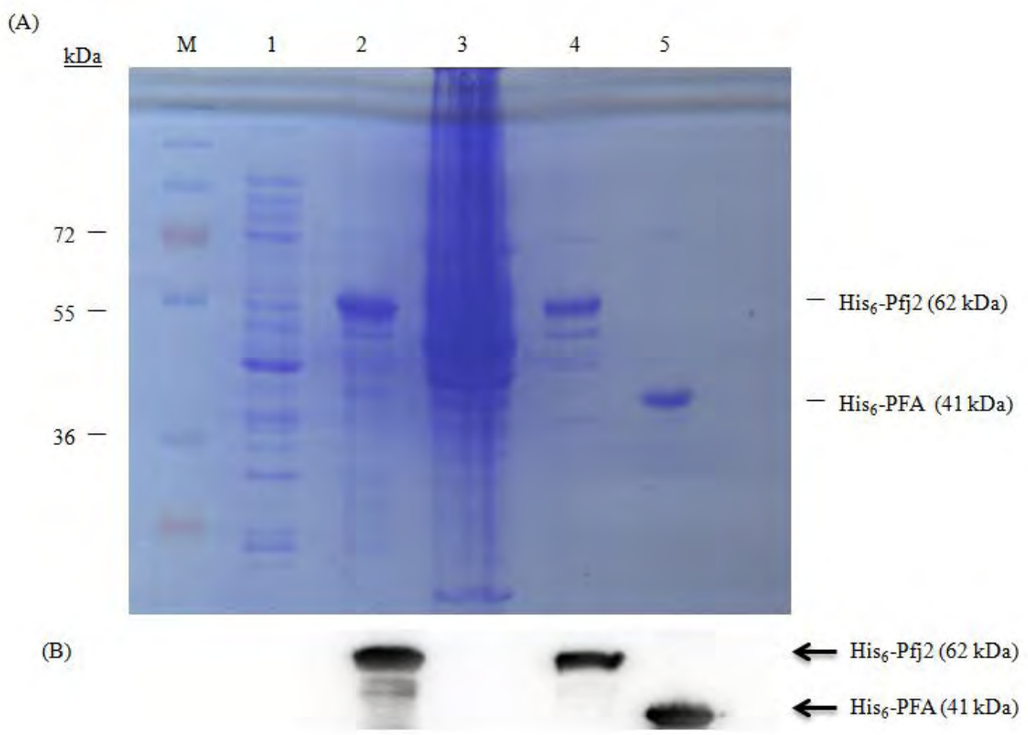

Figure 3.13: **Solubility analysis of His_6-Pfj2 in *E. coli* M15[*pREP4*] cells at 37°C. (A)** Lane M: PageRuler™ Plus Prestained Protein Ladder; Lane U: total cell extract from uninduced sample; Lane 1: total cell extract from 12 hour un-induced sample; Lane 2: total protein from 12 hour induced sample; Lane 3: supernatant fraction from 12 hour induced sample; Lane 4: pellet fraction from 12 hour induced sample; Lane 5: total cell extract of *E. coli* M15[*pREP4*] cells expressing His_6-PFA. **(B)** Western immunoblotting for verification of the detected His_6-Pfj2 and His_6-PFA using mouse anti-His_6 antibodies (1/5000 dilution) and anti-mouse IgG POD-labeled antibodies (1/6000 dilution).

3.6.2. Solubility studies of His_6-Pfj2 in E. coli M15[pREP4] cells at 20°C

In an attempt to improve solubility, an induction experiment was performed in *E. coli* M15[*pREP4*] cells at 20°C with 0.4 mM IPTG. Cells were harvested at A_{600} of 0.4 and 0.6. The harvested cells were separated into supernatant and pellet fractions and samples analysed by 12% SDS-PAGE and Western immunoblotting. The results are shown in Figure 3.14.

His_6-Pfj2 was not observed in the supernatant fraction (lanes 1 and 2). Distinct protein bands can be seen in the induced pellet fraction at A_{600} of 0.4 and 0.6 in lanes 3 and 4. The presence of His_6-Pfj2 was confirmed by Western immunoblotting using anti-His_6 antibodies. Prominent bands representing His_6-Pfj2 were detected in the pellet fraction at A_{600} of 0.4 and 0.6, and not in supernatant fractions.

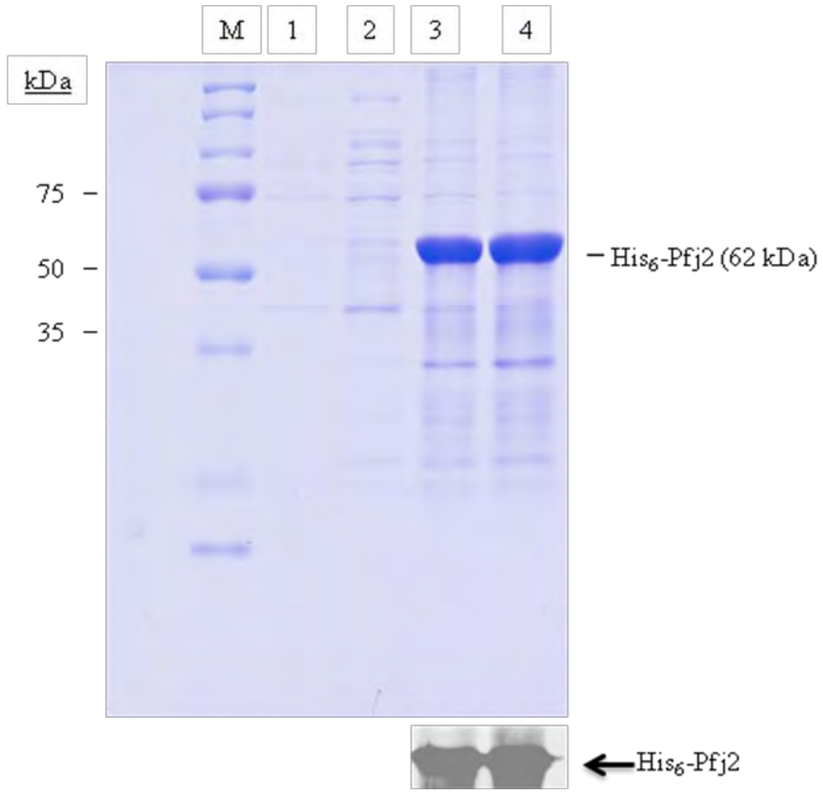

***Figure 3.14*: <u>Solubility analysis of His_6-Pfj2 in *E. coli* M15[*pREP4*] cells at 20°C</u>**. **(A)** Lane M: Precision Plus Protein™ Dual Color Standards; Lane 1: supernatant induced at 0.4; Lane 2: supernatant induced at 0.6; Lane 3: pellet induced at 0.4; Lane 4: pellet induced at 0.6. **(B)** His_6-Pfj2 detection by Western immunoblotting using mouse anti-His_6 primary antibody (1/5000 dilution) and ECL anti-mouse IgG HRP-conjugated secondary antibody (1/5000 dilution).

3.7. Purification of His_6-Pfj2 and His_6-BiP

3.7.1. Denaturing purification of His_6-Pfj2 from E. coli M15[pREP4] cells

Because His_6-Pfj2 was found to be present in the insoluble fraction, native purification was not possible. His_6-Pfj2 was purified under denaturing conditions in 8 M urea using Ni-chelating affinity column. Sequential washes and elutions under native conditions were then performed to refold His_6-Pfj2. The progress of the purification was analysed by 12% SDS-PAGE. The results are shown in Figure 3.15.

Several protein bands including His_6-Pfj2 were present in the total protein fraction after sonication in lane 1. Wash steps with 50 mM imidazole were carried out, and are represented in lanes 2 and 3 in which protein bands were absent. Following washing, the protein was eluted with 1 M imidazole. Lanes 4-9 contain samples of the eluted protein. As can be seen from Figure 3.15, the majority of the protein corresponding to the expected mobility of His_6-Pfj2 was eluted in the third elution in lane 6. Faint protein bands corresponding to the expected mobility of His_6-Pfj2 are present in elutions 2 and 4 (lanes 5 and 7). Several bands were also present below the expected mobility of His_6-Pfj2 in elutions 2-4 (lanes 5-7). No proteins bands were evident in elutions 1, 5 and 6 (lanes 4, 8, and 9).

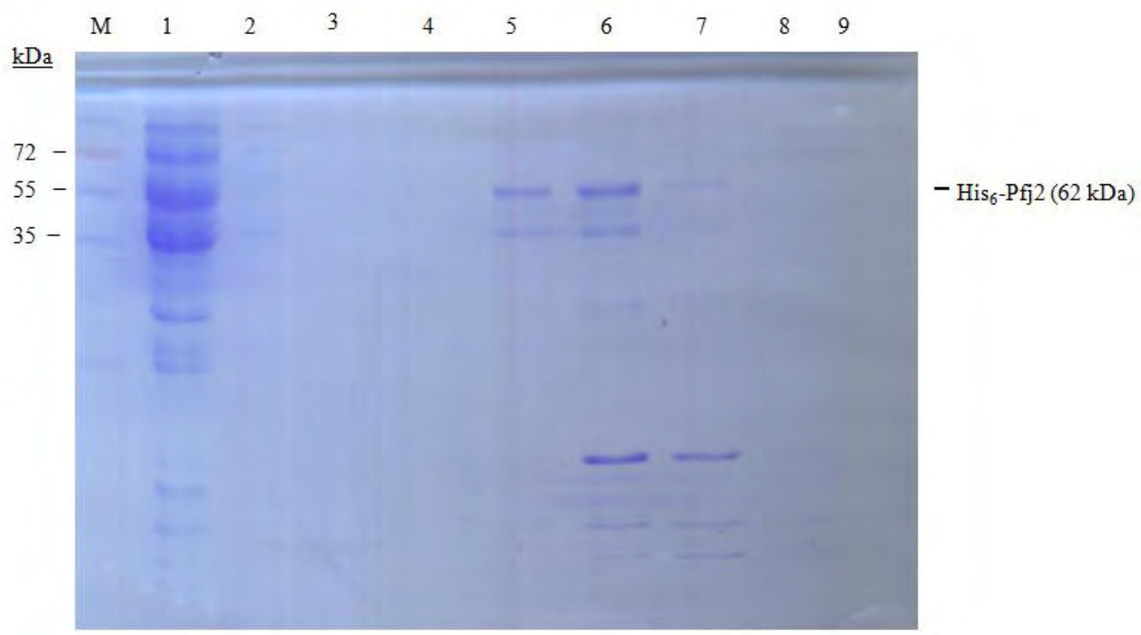

Figure 3.15: **Urea denaturing purification of His_6-Pfj2 from *E. coli* M15[*pREP4*] cells using nickel affinity chromatography**. Lane M: PageRuler™ Prestained protein ladder; Lane 1: total protein in 8M urea; Lane 2: wash step with 50 mM imidazole in 4M urea; Lane 3: wash step with 50 mM imidazole without urea; Lanes 4-9: elutions with 1 M imidazole.

Following elution, protein fractions in elutions 2 and 3 which contained purified His_6-Pfj2 were chosen for dialysis. Purified His_6-Pfj2 was dialysed and analysed by 12% SDS-PAGE and Western immunoblotting. The results are shown in Figure 3.16.

Panel A which contains 2.5 µg of loaded protein shows a faint band representing His_6-Pfj2. The protein was detected by Western immunoblotting using anti-His_6 antibodies (Panel B). The purification experiment was performed in triplicate for future ATPase assays yielding 0.714 mg/L, 0.954 mg/L and 0.816 mg/L of protein.

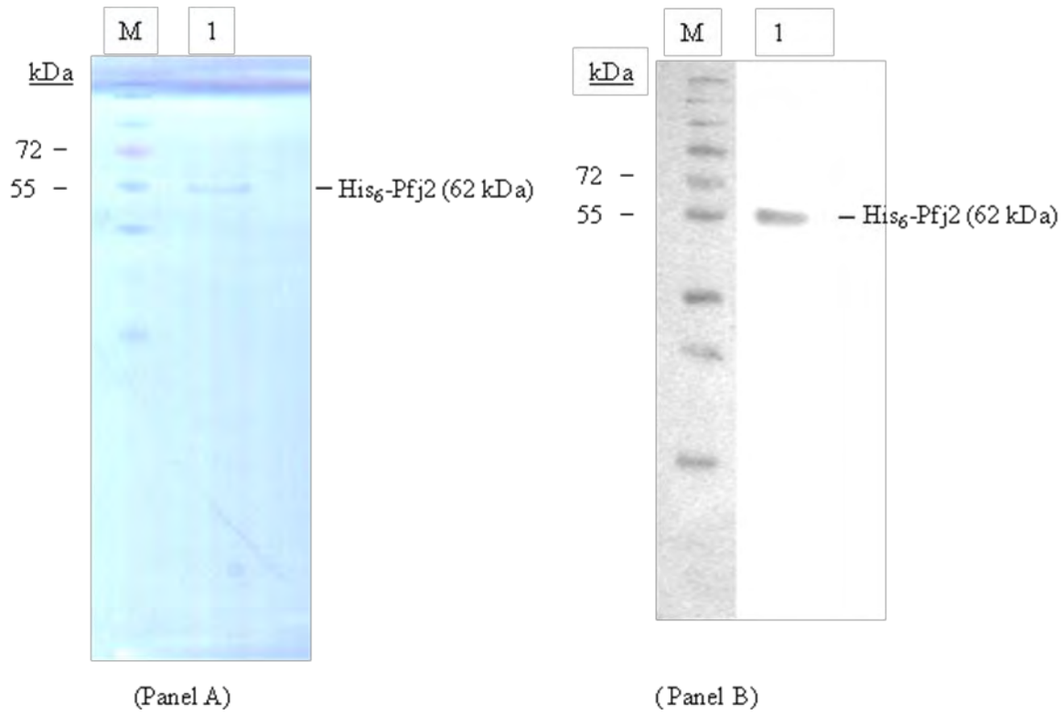

Figure 3.16: **Dialysed His_6-Pfj2**. Panel (A) Lane M: PageRuler™ Plus Prestained Protein Ladder; Lane 1: His_6-Pfj2. Panel (B) His_6-Pfj2 was detected by Western immunoblotting using mouse anti-His_6 antibodies (1/5000) and anti-mouse IgG POD-labeled antibodies (1/6000).

3.7.2. Native purification of His_6-BiP from E. coli M15[pREP4] cells

Batch purification of His_6-BiP in *E. coli* M15[*pREP4*] cells was carried out under native conditions using nickel affinity chromatography. The progress of the purification was analysed by 12% SDS-PAGE and Western immunoblotting. The results are shown in Figure 3.17.

Several protein bands including His_6-BiP were present in the total protein after sonication in lane 1. Protein bands were evident in lane 2, representing the flow through which contain the unbound protein. Wash steps with 40 mM imidazole were carried out, and unbound protein fractions are present in lanes 3-5. Following washing, the protein was eluted with 100 mM imidazole. Lanes 6-8 contain samples of eluted protein. As can be seen from Figure 3.17, the majority of the protein corresponding to the expected mobility of His_6-BiP was eluted in the first elution in lane 6. Significant amounts of protein were eluted in lanes 7 and 8. Lane 9 contains the bead fraction in which a prominent protein band is evident. To confirm the presence of His_6-BiP, Western immunoblotting using anti-His_6 antibodies was performed (Figure 3.17B). Prominent bands representing His_6-BiP were observed (lanes 1-9).

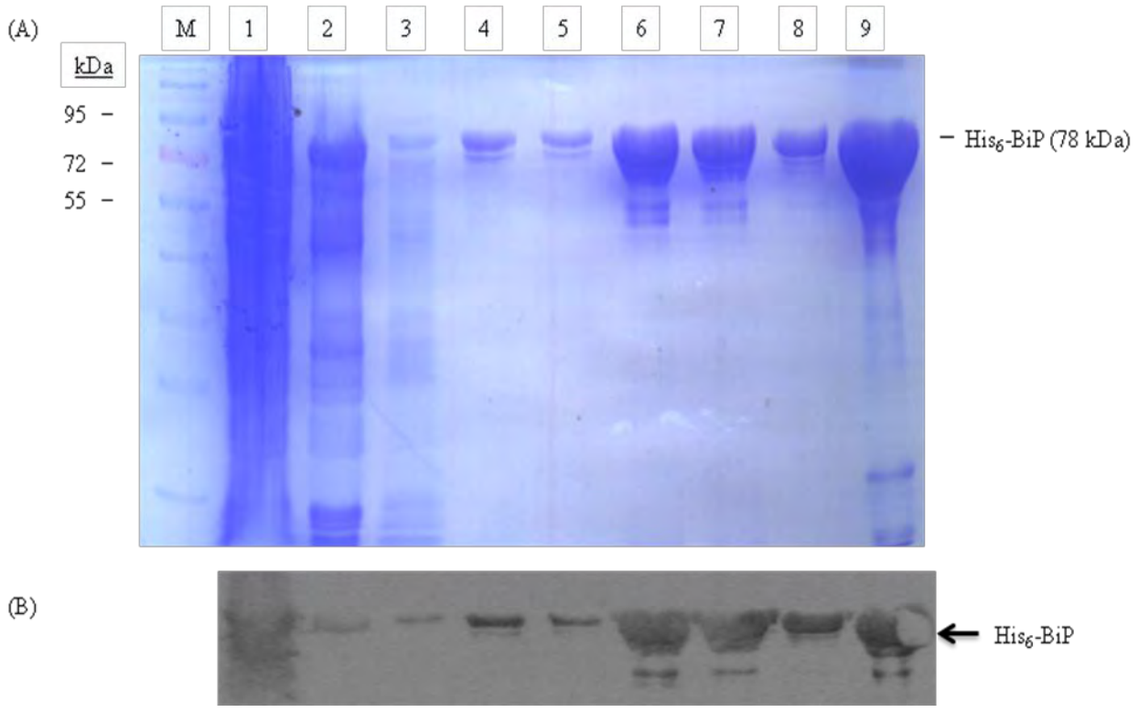

Figure 3.17: **Native purification of His_6-BiP from *E. coli* M15[*pREP4*] cells by nickel affinity chromatography. (A)** SDS-PAGE analysis illustrating Lane M: PageRuler™ Prestained protein ladder; Lane 1: total protein; Lane 2: unbound protein fraction; Lanes 3-5: wash steps with 40 mM imidazole; Lanes 6-8: elutions with 100 mM imidazole; Lane 9: eluted nickel-charged bead fraction. **(B)** His_6-BiP was detected by Western immunoblotting using mouse anti-His_6 antibodies (1/5000) and anti-mouse IgG POD-labeled antibodies (1/6000).

Following elution the protein was dialysed to remove excess salt and analysed by 12% SDS-PAGE and Western immunoblotting. The results are shown in Figure 3.18.

Panel A which contains 3.7 µg of loaded protein shows a prominent band representing His_6-BiP. However, it is evident from the amount of protein observed on the gels in figures 3.16 and 3.18 that the calculated amount of 3.7 µg for His_6-BiP is underestimated. The presence of His_6-BiP was confirmed by Western immunoblotting using anti-His_6 antibodies. The purification experiment was performed in triplicate for subsequent ATPase assays yielding 7.392 mg/L, 8.008 mg/L and 10.252 mg/L of protein.

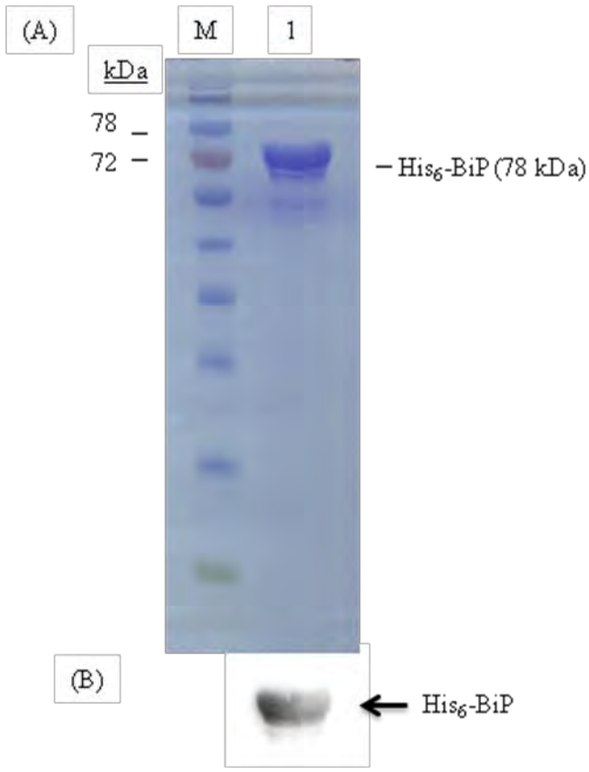

Figure 3.18: **Dialysed His_6-BiP**. **(A)** Lane M: PageRuler™ Plus Prestained Protein Ladder; Lane 1: His_6-BiP. **(B)** His_6-BiP was detected by Western immunoblotting using mouse anti-His_6 antibodies (1/5000) and anti-mouse IgG POD-labeled antibodies (1/6000).

3.8. ATPase assays of His_6-Pfj2 and mammalian His_6-BiP

To investigate whether His_6-Pfj2 was capable of stimulating the chaperone activity of mammalian His_6-BiP, ATPase assays were performed. The release of inorganic phosphate was spectrophotomerically quantified using ammonium molybdate and ascorbic acid at 850 nm. Alfalfa Hsp70-1 and human His_6-Hsj1a were used as controls. ATPase activity was expressed as nmolPi/min/mg.

3.8.1. Phosphate standard curve

Prior to ATPase assay, a phosphate standard curve was generated to extrapolate the concentration of phosphate released (Figure 3.19). The linear regression equation was $y = 0.0544x + 0.0293$ and the correlation coefficient was $R^2 = 0.9994$.

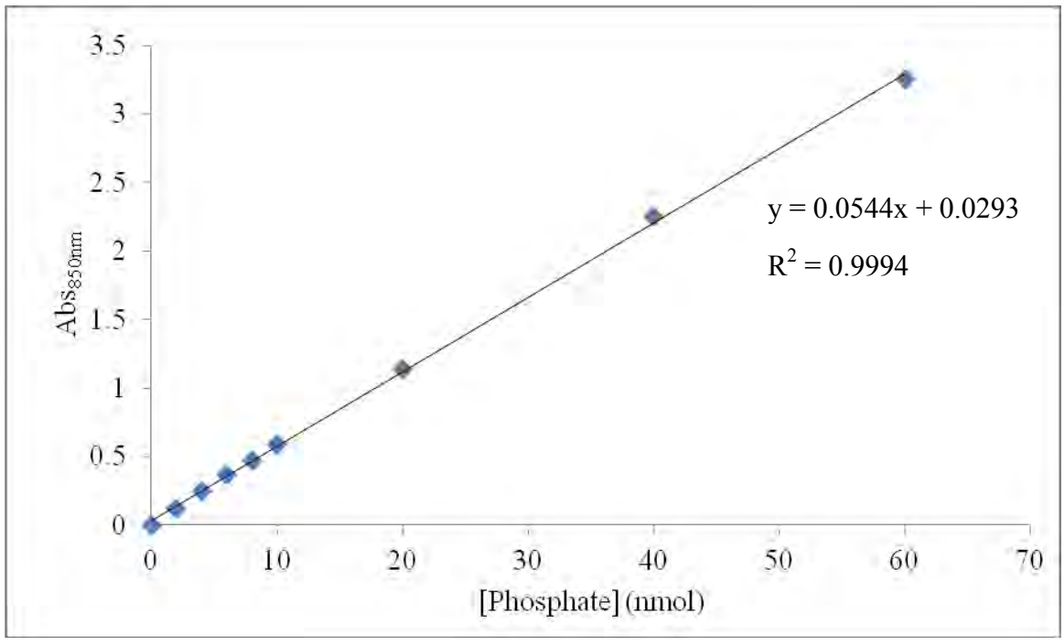

Figure 3.19: **Phosphate standard curve**. The phosphate concentrations used were 0-60 nmol at 37°C. The absorbance was read at 850 nm.

3.8.2. ATPase activity

The ATPase activity of His_6-BiP was determined alone and in the presence of His_6-Pfj2 and His_6-Hsj1a. The ATPase activity of alfalfa Hsp70-1 was determined alone as positive control.

The result of phosphate released over time (Figure 3.20) shows a high rate of phosphate released for alfalfa Hsp70-1 (1). His_6-BiP in the presence of His_6-Hsj1a (2) shows an increase in the rate of phosphate released when compared with His_6-BiP alone (4). However, no increase was observed with His_6-BiP in the presence of His_6-Pfj2 (3). No intrinsic phosphate release activities were observed with His_6-Pfj2 (5) and His_6-Hsj1a (6).

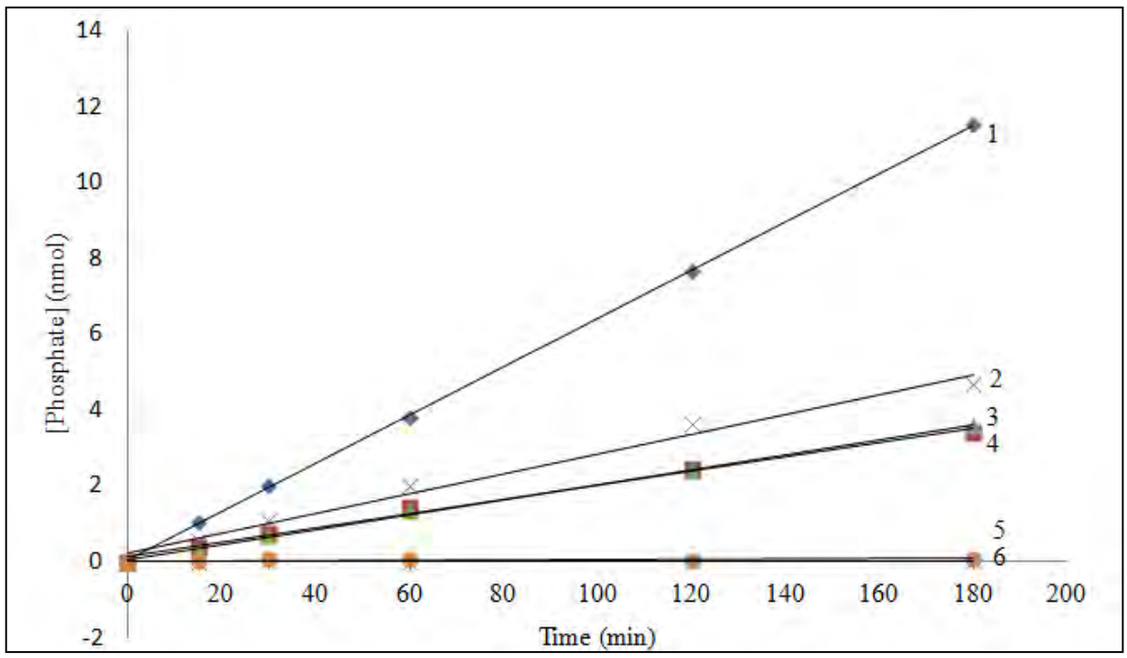

Figure 3.20: **Phosphate released over time**. 1: Alfalfa Hsp70-1(0.05 µM); 2: His_6-BiP and His_6-Hsj1a each with a concentration of 0.4 µM; 3: His_6-BiP and His_6-Pfj2 each with a concentration of 0.4 µM; 4: His_6-BiP (0.04 µM); 5: His_6-Pfj2 (0.04 µM); 6: His_6-Hsj1a (0.04 µM). The phosphate versus time graph was generated through linear regression from the combination of data obtained from three independent ATPase assays using freshly purified proteins for each assay.

Table 3.3: Phosphate released over time

Protein	**Linear regression equation**	**Coefficient of correlation**
Alfalfa Hsp70-1	y = 0.0638x + 0.0401	R^2 = 0.9999
His_6-BiP	y = 0.0188x + 0.1384	R^2 = 0.9929
His_6-BiP and His_6-Pfj2	y = 0.0196x + 0.0664	R^2 = 0.9981
His_6-BiP and His_6-Hsj1a	y = 0.0262x + 0.2287	R^2 = 0.9871
His_6-Hsj1a	y = 0.0001x – 0.0011	R^2 = 0.2392
His_6-Pfj2	y = 0.0003x + 0.0261	R^2 = 0.5001

The ability of His_6-Pfj2 and His_6-Hsj1a to stimulate the ATPase activity of His_6-BiP is described Figure 3.21. As indicated with the asterisk (*), a significant stimulation of His_6-BiP ATPase activity was observed in the presence of His_6-Hsj1a when compared with His_6-BiP alone, and no stimulation was observed in the presence of His_6-Pfj2. As expected, His_6-Pfj2 and His_6-Hsj1a alone shows no intrinsic ATPase activity. Alfalfa Hsp70-1 has a high intrinsic ATPase activity as expected. The estimated values of the specific ATPase activity are presented in Table 3.4.

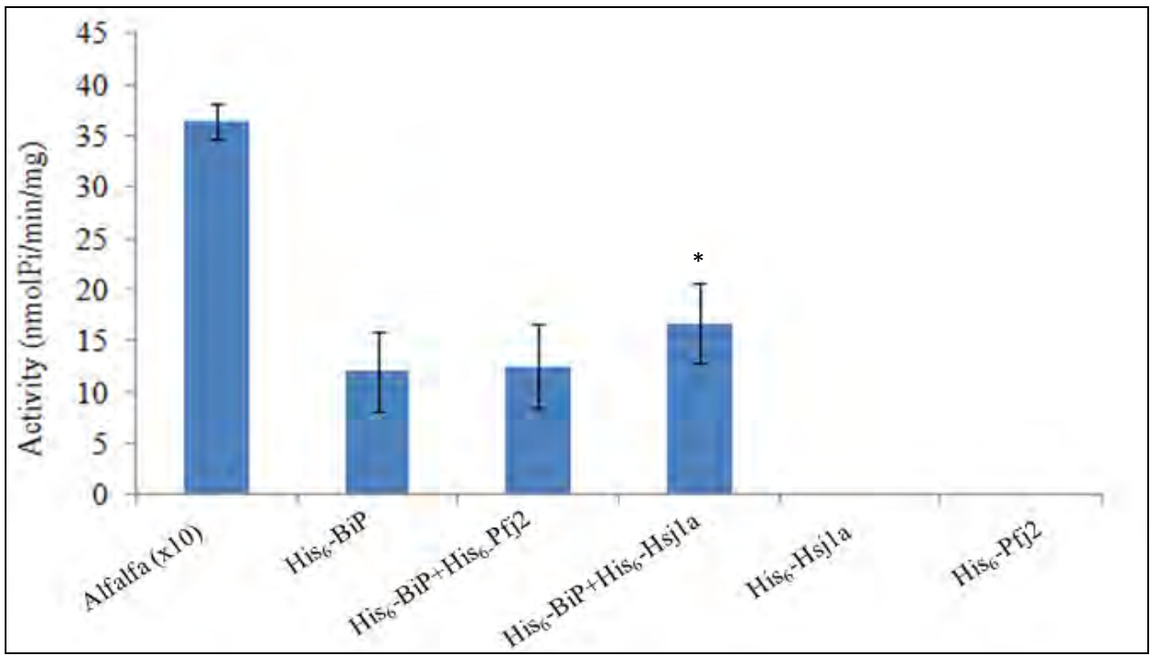

Figure 3.21: **ATPase assay**. **A**lfalfa Hsp70-1 (0.05 μM; value shown on graph is $1/10^{th}$ of the original value); His_6-BiP (0.4 μM); His_6-BiP and His_6-Pfj2 each with a concentration of 0.4 μM; His_6-BiP and His_6-Hsj1a each with a concentration of 0.4 μM; His_6-Hsj1a (0.4μM); His_6-Pfj2 (0.4μM). The ATPase assay graph was generated from the combination of data obtained from three independent ATPase assays using freshly purified proteins for each experiment. * represents significant stimulation.

Table 3.4: ATPase activity of proteins

Protein	**ATPase activity (nmolPi/min/mg)**
Alfalfa Hsp70-1	364.36 ± 16.67
His_6-BiP	12.07 ± 3.92
His_6-BiP and His_6-Pfj2	12.59 ± 4.06
His_6-BiP and His_6-Hsj1a	16.77 ± 3.84 *
His_6-Hsj1a	_
His_6-Pfj2	_

*Student's T-Test showed significant stimulation ($p<0.05$) of ATPase activity of mammalian His_6-BiP in the presence of His_6-Hsj1a when compared with His_6-BiP alone.

Chapter 4

Discussion and Conclusions

4.1. Overall discussion

Many cases of human mortalities are reported annually as a result of malaria. *P. falciparum* is a protozoan parasite that causes a severe form of malaria, and nearly all malaria deaths result from infection by this species of parasite (World Health Organisation, 2012). The *P. falciparum* genome encodes at least 43 Hsp40s including a type II Hsp40, Pfj2. Pfj2 is particularly interesting as it is potentially homologous to the human ER Hsp40, ERdj5, which has been shown to facilitate protein quality control in the ER by promoting the degradation of misfolded proteins (Ushioda *et al*., 2008). Pfj2 could potentially perform the same function in *P. falciparum* thereby promoting the parasite's survival. Biochemical characterisation could provide some insights pertaining the function of Pfj2 *in vivo* and its potential as a drug target, given that *P. falciparum* has developed resistance to many of the available anti-malarial drugs thus requiring that new drugs and drug targets be identified. Therefore, the overall aim of this study was to express and purify His_6-Pfj2 in a bacterial system, and investigate the ability of the protein to stimulate the activity of the mammalian Hsp70, His_6-BiP.

Pfj2 has been identified as a *P. falciparum* Hsp40 chaperone that may facilitate protein quality control in the ER, but has not been well studied or documented in the literature. ER proteins are involved in oxidative protein folding by acting as catalysts and folding assistants. They may also act as oxidases or reductases by catalysing disulfide bond formation of newly synthesised polypeptides in the ER or as isomerases to correct non-native disulfide bonds and as chaperone or co-chaperones to prevent protein aggregation and facilitate folding of nascent proteins. ER proteins consist of members of the Hsp70 family of proteins including BiP. (Haas and Wabl, 1983). Cofactors of BiP belonging to the Hsp40 class of proteins include ERdj1–7 (Otero *et al*., 2010).

Studies have identified several ER J-proteins termed ERdj1/Mtj1 (Brightman *et al*., 1995; Chevalier *et al*., 2000), ERdj2/hSec63 (Skowronek *et al*., 1999; Tyedmers *et al*., 2000), ERdj3/HEDJ (Bies *et al*.,1999; Lau *et al*., 2001; Yu *et al*., 2000), ERdj4/Mdj1 (Prols *et al*., 2001; Shen *et al*., 2002), and ERdj5/JPDI that has both a J-domain and oxidoreductase activity (Cunnea *et al*., 2003, Hosoda *et al*., 2003), ERdj6/$p58^{IPK}$(Yan *et al*., 2002) and ERdj7(Zahedi *et al*., 2009). ERdj5 was cloned from human (Cunnea *et al*., 2003) and has an N-terminal J-domain followed by four thioredoxin-like sequences with a -CXYC- variant motif -CSHC-, -CPPC-, -CHPC- and CGPC-. In addition, ERdj5 has a C-terminal -KDEL ER retention sequence (Cunnea *et al*., 2003, Hosada *et al*., 2003). ERdj5 has been shown to assist protein quality control by cleaving disulfide bonds of misfolded proteins in the ER as a result of it reductase activity and interacts through its J-domain in an ATP-dependent manner with BiP, an ER-resident member of the Hsp70 chaperone family involved in ER-associated degradation and protein translocation (Ushioda *et al*., 2008).

Interestingly Pfj2 chaperone is potentially homologous to the human ER Hsp40, ERdj5 in terms of sequence homology (Botha *et al*., 2007). The most intriguing feature underlining the similarity between ERdj5 and Pfj2 is the presence of J-domain and thioredoxin-like domain on the same

polypeptide backbone. These features are essential to catalyse the disulfide bond formation and isomerisation in the ER as well as the reduction of disulfide bonds in the ER lumen prior to dislocation of proteins destined for degradation (Tortorella *et al*., 1998, Fagioli *et al*., 2001). Since many membrane and secretory proteins possess disulfide bonds that are essential to achieve their native state Pfj2, like ERdj5 and other PDI related proteins in the ER , having these unique features may function as a catalyst in the oxidation and isomerisation of disulfides on nascent polypeptides undergoing folding in the oxidising environment of the ER (Noiva, 1999). These proteins may also be involved in the dislocation of short-lived proteins targeted for proteasomal degradation (Tsai *et al*., 2002). However, an important question to be addressed in this study was to determine whether Pfj2 acts as a thioredoxin, a PDI-like protein or as a DnaJ partner for a corresponding parasite Hsp70 BiP.

In *P. falciparum*, several proteins have been annotated as PDI-like or putative PDI in the PlasmoDB database (http://www.plasmoDB.org) (Bahl *et al*., 2003). Among these are MAL8P1.17, (PfPDI), PFI0950w, PF14_0694 and PF11_0352 and Pfj2 which possesses a putative N-terminal signal-peptide, a putative C-terminal ER-retention sequence, a putative PEXEL motif and a putative thioredoxin motif according to a Prosite analysis (http://www.expasy.ch/prosite). Notably, Pfj2 has a putative thioredoxin motif, indicating that it might possess oxidoreductase activity and therefore could serve as potential target for developing a new anti-malarial strategies anchored on impaired folding of exported parasite proteins. The analysis of the amino acid sequence of Pfj2 showed the presence of a J-domain with conserved HPD motif and G/F region but low sequence similarity and identity when aligned with other type II Hsp40s. Botha *et al.* (2007) observed that Pfj2 appears to be distinctly different from the other PEXEL/HT containing type II Hsp40 proteins due to the overlap of the proposed PEXEL/HT motif with helix II of the J-domain. This is contrary to what is seen in other type II Hsp40 proteins where the PEXEL/HT motifs precede the J-domain. This observation, coupled with the presence of thioredoxin motif, may explain the low level of sequence similarity and identity between these proteins. The presence of a J-domain and putative thioredoxin motif in the amino acid sequence of Pfj2 and the fact that they are both ER resident proteins may indicate a degree of functional relationship between ERdj5 and Pfj2.

In this study, the ability of His_6-Pfj2 to stimulate the ATPase activity of Hsp70 was investigated. Multiple alignment of the amino acid sequence of PfBiP, hamster GRP-78/BiP, MsHsp70-1 and *S. cerevisiae* BiP showed that these proteins are highly conserved at the amino acid level. The proteins also exhibited similarities in terms of protein sizes and the number of amino acid residues. The results of this analysis and the availability of hamster GRP-78/BiP accounts for its use in this study.

The codon optimised coding sequence of Pfj2 was synthesised for use in this study. The native Pfj2 coding sequence was codon-optimised and cloned into pUC57 cloning vector by GenScript. pUC57-Pfj2 was engineered to include *Bam*HI and *Kpn*I restriction sites at the 5' end and 3' end

of the sequence to facilitate cloning into pQE30. An initial attempt at expressing the native sequence was unsuccessful (data not shown). The presence of rare codons which are not recognised by the *E. coli* translational machinery accounted for the need for codon optimisation. Codon optimisation helps to improve codon usage and therefore maximise protein expression in the organism of choice, in this case *E. coli* (Burgess-Brown *et al*., 2008).

The availability of bacterial expression systems, ease of growth and high level of protein expression within a short period of time made this the system of choice for the expression and purification of His_6-Pfj2 (QIAexpress® The Complete System for 6xHis Technology). However, bacterial expression systems have inherent disadvantages. These include protein aggregation and formation of inclusion body resulting in protein insolubility (Thomas and Baneyx, 1996). These problems can be overcome by reducing IPTG concentration, temperature and time of expression (Hannig and Makrides, 1998). The expression vector, pQE30, has been designed for high-level expression of His_6-tagged proteins in *E. coli* based on the T5 promoter transcription–translation system (Bujard *et al*., 1987; Stüber *et al*., 1990). *E. coli* M15[*pREP4*] cells generate high levels of lac repressor protein by *pREP4* to ensure tight control at the transcriptional level (QIAexpress® The Complete System for 6xHis Technology).

The cloning of pQE30-Pfj2 was initiated by double restriction digest of pUC57-Pfj2 and the vector pQE30 with *Bam*HI and *Kpn*I followed by ligation. Following sequencing analysis an additional *Bam*HI site was detected downstream of the His_6-tag resulting in a frame-shift mutation necessitating the use of site directed mutagenesis. There are several approaches to mutagenesis including site-directed mutagenesis, random mutagenesis and *in vitro* saturation. Site-directed mutagenesis is typically performed using the PCR. Using this technique, nucleotide substitutions, additions and deletions can be made in the sequence (Kadowaki *et al*., 1989). Primer extension (Ho *et al*., 1989), inverse PCR (Ochman *et al*., 1988) and cassette mutagenesis which require synthetic oligonucleotides for amplification can also be performed (Zoller, 1991). Random mutagenesis can be introduced by chemical mutagenesis, error prone PCR (enzymatic mutagenesis), PCR with degenerate primers, UV irradiation, mutator strains, nucleotide analogues, or DNA recombination (Kuchner and Arnold, 1997). However, advances in oligonucleotide synthesis, identification and construction of new commercial polymerases have made oligonucleotide PCR based mutagenesis a method of choice for this study. Following site-directed mutagenesis, pQE30-Pfj2 was confirmed by restriction digest and DNA sequencing.

The expression and solubility studies were done as an initial step towards formulating the best approach for the purification of His_6-Pfj2. Following IPTG induction at 37°C in *E. coli* M15[*pREP4*] cells, SDS-PAGE and Western immunoblotting, maximal protein expression was observed at 12 hours post-induction. The results also showed that His_6-Pfj2 was largely detected in the insoluble or pellet fraction. Solubility of the protein is not only important for ease of purification, but also for maintaining the protein in a folded state, which is necessary for

biological activity. However, various attempts at improving the solubility of His_6-Pfj2 including expression at lower temperature (20°C) and lower IPTG concentration (0.4 μM) did not yield soluble proteins. Furthermore, Pfj2 resides in the ER, an organelle which is lacking in the prokaryotic *E. coli* expression system used in this study. The ER plays an important role in protein synthesis and modification. The ER compartment facilitates the folding of newly synthesised polypeptides and plays a role in the assembly of multimeric proteins (Vitale *et al.,* 1993). Proteins are retained in the ER until the correct conformation is attained. Ridder *et al*. (1995) also reported that proteins which form insoluble inclusion bodies in *E. coli* are often soluble when expressed in yeast. Therefore, another approach to improve His_6-Pfj2 solubility may involve expression in a eukaryotic system, for example, yeast or mammalian cells. Such systems may facilitate the folding of Pfj2 and prevent its aggregation when over-expressed. However, these expression systems are often complicated and expensive (Tolia and Joshua-Tor, 2006).

A unique feature of the ER resident proteins include a thioredoxin-like domain which may serve as a catalyst in the oxidation and isomerisation of disulfides bonds during the Pfj2 folding process in the oxidising environment of the ER (Noiva, 1999). Determination of Pfj2 secondary structure will help to provide insight into its folded state and suitability for use in biological assays. Fourier transform infrared spectroscopy (FTIR) constitutes one of the commonly used experimental methods for estimating the secondary structure of polypeptides and proteins (Byler and Susi, 1986; Kong and Yu, 2007). The secondary structure is reflected by the amide I and amide II bands. Amide I absorbed around 1620 to 1690 cm^{-1} due to stretching vibrations of carbonyl (C=O) groups while amide II absorbed around 1480 to 1585 cm^{-1} due to bending vibrations of NH groups (Byler and Susi, 1986; Kong and Yu, 2007).

The insolubility of His_6-Pfj2 expressed in a bacterial system prompted the use of column purification under denaturing conditions using 8 M urea. The disadvantage of this approach is that protein may not fold into its correct tertiary structure and functional activity could be compromised as the native state is not always attained following full denaturing purification (Kathir *et al*., 2005). The use of strong denaturants and reducing agents for improving the solubility of protein aggregates was described by De Bernardez (1998) and Lilie *et al*. (1998) and successful purification under denaturing conditions while maintaining the functional activities of the proteins has also been reported (Matambo *et al*., 2004; Ramya *et al*., 2006; Samudzi *et al*., 2012). Purification of highly insoluble proteins by pH adjustment with and without a lower concentration of denaturant has been reported as an alternative approach to using strong denaturant at high concentration (Singh and Panda, 2005). However, the extreme pH used in this technique may prevent proper refolding and subsequently affect the biological functions of the protein.

Batch purification of His_6-BiP was carried out under native conditions as previously reported (Alder *et al*., 2005). Although His_6-BiP was highly soluble and yielded relatively pure protein, Western immunoblotting showed the presence of possible degradation or contamination products

which may explain the presence of faint bands below the prominent band of His_6-BiP in Figure 3.17. Furthermore, a high proportion of the protein remained bound to the nickel charged beads. Increasing the imidazole concentration may reduce the binding of protein to the beads, causing more protein to be eluted, thereby improving the protein yield. Moreover, the calculated amount of 3.7 µg for His_6-BiP appears low. This is possibly due to an error in the method used to estimate protein concentration. Protein concentration for His_6-BiP was determined using a nanodrop spectrophotometer. Another approach towards measuring protein concentration should have been performed. One such method includes Bradford Assay which could perhaps have provided a more accurate measurement.

Hsp40s interact with Hsp70 partners, including human BiP, to stimulate cycles of ATP hydrolysis and thus allowing Hsp70 proteins to bind and release substrates (Liberek *et al*., 1991, Szabo *et al*., 1994). Consistent with a previous report by Cheetham *et al*. (1994), His_6-Hsj1a significantly stimulates the ATPase activity of mammalian His_6-BiP. ERdj5 have been shown to bind BiP and stimulate its ATPase activity *in vitro*. (Ushioda *et al*., 2008). The results of the ATPase assays in this study revealed that, despite domain similarity with ERdj5, His_6-Pfj2 did not stimulate the ATPase activity of mammalian His_6-BiP in the system used. This indicates that His_6-Pfj2 may not be capable of functioning as a co-chaperone for mammalian His_6-BiP. A *P. falciparum* Hsp70, for example, PfBiP could be used to determine the chaperone ATPase activity of His_6-Pfj2. Since correct folding of His_6-Pfj2 is important for co-chaperone activity, possible misfolding of the protein may explain the lack of ATPase activity observed. One approach to addressing the problem of protein misfolding is the optimisation of the buffer conditions by the addition of agents that could promote protein solubility and enhance refolding (Bondos and Bicknell, 2002). These agents include kosmotropes, for example, magnesium sulfate ($MgSO_4$) and calcium sulfate ($CaSO_4$) that generally stabilise the native state of proteins by increasing the surface tension of the solvent (Cappel and Gilbert, 1988; Timasheff, 1998). In addition, the three independent ATPase assays that were performed with freshly purified proteins were carried out using the same protein concentration for each experiment. Several His_6-Pfj2 concentrations could be used in further ATPase studies to determine the required protein concentration needed to stimulate the ATPase activity of mammalian His_6-BiP. Furthermore, ERdj5 could be included as Hsp40 control since it has been shown to possess chaperone activity by stimulating human BiP (Ushioda *et al*., 2008).

4.2. Conclusions

The overall aim of this study was to express and purify codon-optimised His_6-Pfj2 in a bacterial system, and investigate the ability of the protein to stimulate the activity of mammalian His_6-BiP using ATPase assays. The codon-optimised coding sequence of Pfj2 was successfully inserted into the prokaryotic expression vector, pQE30 to facilitate overproduction of a histidine-tagged Pfj2. His_6-Pfj2 and His_6-BiP were successfully expressed in *E. coli* M15[*pREP4*] cells and purified using nickel affinity chromatography under denaturing and native conditions

respectively for use in ATPase assays. ATPase assays were performed and the results showed that His_6-Pfj2 did not stimulate the chaperone activity of mammalian His_6-BiP in this system suggesting that it may not act as a co-chaperone. However, optimisation of the assay is necessary to validate this observation. This study has created a platform for future molecular and cellular characterisation of Pfj2.

4.3. Future work

Further studies on Pfj2 can be performed. The solubility and purification of His_6-Pfj2 could be improved using several approaches. One such approach could be to express His_6-Pfj2 in several *E. coli* strains in order to find a strain of *E. coli* which produces the greatest amount of His_6-Pfj2. Following successful optimisation of the purification method, further *in vitro* characterisation to determine the specific interacting partners of Pfj2 could be investigated. This may include the extension of ATPase assays to other Hsp70s of human and *P. falciparum* origin, malate dehydrogenase (MDH) assay and Surface Plasmon Resonance (SPR). In addition, the ATPase assay of His_6-Pfj2 interaction with mammalian His_6-BiP could be validated by using a range of His_6-Pfj2 concentrations to determine the optimal protein concentration required to elicit the stimulation of the ATPase activity of mammalian His_6-BiP. Furthermore, a *P. falciparum* BiP (PfBiP) and ERdj5 could be included as controls used in future ATPase assays.

In vivo studies of His_6-Pfj2 could be performed. These include reductase assays which could be performed to test for the ability of His_6-Pfj2 to reduce disulfide bonds, thus promoting unfolding of proteins with disulfide bonds. This would be evidence that His_6-Pfj2 is involved with PfBiP and the translocon in retrograde transport and degradation of protein *in vivo*. The purified His_6-Pfj2 could be used to generate chicken antibodies (IgYs), which can be applied in various cell biological assays including immunofluorescence staining and analysis to determine the localisation of endogenous Pfj2 in *P. falciparum* infected erythrocytes using confocal microscopy. Finally, co-localisation studies could be performed to investigate possible interactions between Pfj2 and potential PfHsp70 partners using confocal microscopy and transmission electron microscopy, and confirmed by co-immunoprecipitation experiments using cell lysates expressing His_6-Pfj2.

REFERENCES

Aikawa,M., 1988. Human Cerebral Malaria. *The American Journal of Tropical Medicine and Hygiene*, **39**, 3-10.

Alder,N., Shen,Y., Brodsky,J., Hendershot,L., Johnson,A., 2005. The molecular mechanisms underlying BiP-mediated gating of the Sec61 translocon of the endoplasmic reticulum. *Journal of cell Biology*, **168**, 389-399.

Ansorge,I., Benting,J., Bhakdi,S., Lingelbach,K., 1996. Protein sorting in *Plasmodium falciparum*-infected red blood cells permeabilized with the pore-forming protein streptolysin O. *Biochemical Journal*, **315**, 307-314.

Bahl,A., Brunk,B., Crabtree,J., Fraunholz,M.J., Gajria,B., Grant,G.R, Ginsburg,H., Gupta,D., Kissinger,J.C., Labo,P., Li,L., Mailman,M.D., Milgram,A.J., Pearson,D.S., Roos,D.S., Schug,J., Stoeckert,C.J Jr., Whetzel,P., 2003. PlasmoDB: the *Plasmodium* genome resource. A database integrating experimental and computational data. *Nucleic Acids Research*, **31**, 212–215.

Banumathy,G., Singh,V., Tatu,U., 2002. Host chaperones are recruited in membrane-bound complexes by *Plasmodium falciparum*. *Journal of Biological Chemistry*, **277**, 3902-3912.

Baruch,D.I., Pasloske,B.L., Singh,H.B., Bi,X., Ma,X.C., Feldman,M., Taraschi,T.F., Howard,R.J., 1995. Cloning the *P. falciparum* gene encoding PfEMP1, a malarial variant antigen and adherence receptor on the surface of parasitized human erythrocytes. *Cell*, **82**, 77-87.

Beare,N.A., Taylor,T.E., Harding,S.P., Lewallen,S., Molyneux,ME., 2006. Malarial retinopathy: a newly established diagnostic sign in severe malaria. *American Journal of Tropical Medicine and Hygiene*, **75**, 790–797.

Behr,C., Sarthou, J.L., Rogier,C., Trape,J.F., Dat,M.H, Michel,J.C., Aribot,G., Dieye,A., Claverie,J.M., Druihle,P., 1992. Antibodies and reactive T cells against the malaria heat-shock protein Pf72/Hsp70-1 and derived peptides in individuals continuously exposed to *Plasmodium falciparum*. *The Journal of Immunology*, **149**, 3321-3330.

Bertolotti,A., Zhang,Y., Hendershot,L.M., Harding,H.P., Ron,D., 2000. Dynamic interaction of BiP and ER stress transducers in the unfolded-protein response. *Nature Cell Biology*, **2**, 326-332.

Bhattacharjee,S., van Ooij,C., Balu,B., Adams,J.H., and Haldar,K., 2008. Maurer's clefts of *Plasmodium falciparum* are secretory organelles that concentrate virulence protein reporters for delivery to the host erythrocyte. *Blood*, **111**, 2418–2426.

Bies,C., Blum,R., Dudek,J., Nastainczyk,W., Oberhauser,S., Jung,M., Zimmermann,R., 2004. Characterization of pancreatic ERdj3p, a homolog of yeast DnaJ-like protein Scj1p. *Biological Chemistry*, **385**, 389-395.

Bies,C., Guth,S., Janoschek,K., Nastainczyk,W., Volkmer,J., Zimmermann,R., 1999. A Scj1p homolog and folding catalysts present in dog pancreas microsomes. *Biological Chemistry*, **380**, 1175-1182.

Biswas,S., Sharma,Y.D., 1994. Enhanced expression of *P. falciparum* heat shock protein Pfhsp70-1 at higher temperatures and parasites survival. *FEMS Microbiology Letters*, **124**, 425-429.

Bondos,S.E., 2003. Bicknell A. Detection and prevention of protein aggregation before, during, and after purification. *Analytical Biochemistry*, **316**, 223–231.

Borges,J.C., Fischer,H., Craievich,A.F., Ramos,C.H.I., 2005. Low Resolution Structural Study of Two Human HSP40 Chaperones in Solution. *Journal of Biological Chemistry*, **280**, 13671-13681.

Borges,J.C., Ramos,C.H.I., 2005. Protein folding assisted by chaperones. *Protein and peptide letters,* **12**, 257–261.

Botha,M., Pesce,E.R., Blatch,G.L., 2007. The Hsp40 proteins of *Plasmodium falciparum* and other apicomplexa: Regulating chaperone power in the parasite and the host. *Cell Biology*, **39**, 1781-1803.

Botha,M., Chiang, A.N., Needham,P.G., Stephens,L.L., Hoppe,H.C., 2011. *Plasmodium falciparum* encodes a single cytosolic type I Hsp40 that functionally interacts with Hsp70 and is upregulated by heat shock. *Cell Stress Chaperones*, **16**, 389-401.

Brightman,S.E., Blatch,G.L., Zetter,B.R., 1995. Isolation of a mouse DNA encoding MTJ1, a new murine member of the DnaJ family of proteins. *Gene***, 153**, 249-254.

Brodsky,J.L., McCracken,A.A., 1999. ER protein quality control and proteasome-mediated protein degradation. *Seminars in Cell & Developmental Biology*, **10**, 507-513.

Bujard,H., Gentz,R., Lanzer,M., Stueber,D., Mueller,M., Ibrahimi,I., Haeuptle,M.T., Dobberstein,B., 1987. A T5 promoter-based transcription-translation system for the analysis of proteins *in vitro* and *in vivo*. *Methods in Enzymology*, **155**, 416–433.

Burgess-Brown,N.A., Sharma,S., Sobott,F., Loenarz,C., Oppermann,U., Gileadi,O., 2008. Codon optimization can improve expression of human genes in Escherichia coli: A multi-gene study. *Protein Expression and Purification*, **59**, 94-102.

Byler,D.M., Susi,H., 1986. Examination of the secondary structure of proteins by deconvolved FTIR spectra. *Biopolymers*, **25**, 469–487.

Cappel,R.E., Gilbert,H.F., 1993. Oxidative inactivation of 3-hydroxy-3-methylglutaryl-coenzyme A reductase and subunit cross-linking involve different dithiol/disulfide centers. *Journal of Biological Chemistry*, **268**, 342-348.

Celli A., 1933. A history of malaria in the Italian campagna from ancient times. *London*.

Chang,H.H., Falick,A.M., Carlton,P.M., Sedat,J.W., DeRisi,J.L., Marletta,M.A., 2008. N-terminal processing of proteins exported by malaria parasites. *Molecular and Biochemical Parasitology*, **160**, 107-115.

Cheetham,M.E., Caplan,A.J., 1998. Structure, function and evolution of DnaJ: conservation and adaptation of chaperone function. *Cell Stress & Chaperones*, **3**, 28-36.

Cheetham,M., Jackson,A., 1994. Regulation of 70-kDa Heat-Shock-Protein ATPase Activity and Substrate Binding by Human DnaJ-Like Proteins, HSJ1a and HSJ1b. *European Journal of Biochemistry*.**226**, 99-107.

Chevalier,M., Rhee,H., Elguindi,E.C., Blond,S.Y., 2000. Interaction of murine BiP/GRP78 with the DnaJ homologue MTJ1. *Journal of Biological Chemistry*, **275**, 19620-19627.

Coppel,R.L., Lustigman,S., Murray,L., Anders,R.F., 1988. MESA is a *Plasmodium falciparum* phosphoprotein associated with the erythrocyte membrane skeleton. *Molecular and Biochemical Parasitology*, **31**, 223-231.

Cox,F., 2010. History of the discovery of the malaria parasites and their vectors. *Parasites & Vectors*, **3**, 5.

Craig,A., Scherf,A., 2001. Molecules on the surface of the *Plasmodium falciparum* infected erythrocyte and their role in malaria pathogenesis and immune evasion. *Molecular and Biochemical Parasitology*, **115**, 129-143.

Cunnea,P.M., Miranda-Vizuete,A., Bertoli,G., Simmen,T., Damdimopoulos,A.E., Hermann,S., Leinonen,S., Huikko,M.P., Gustafsson,J., Sitia,R., Spyrou,G., 2003. ERdj5, an Endoplasmic Reticulum (ER)-resident Protein Containing DnaJ and Thioredoxin Domains, Is Expressed in Secretory Cells or following ER Stress. *Journal of Biological Chemistry*, **278**, 1059-1066.

Da Silva,E., Foley,M., Dluzewski,A.R., Murray,L.J., Anders,R.F., Tilley,L., 1994. The *Plasmodium falciparum* protein RESA interacts with the erythrocyte cytoskeleton and modifies erythrocyte thermal stability. *Molecular and Biochemical Parasitology*, **66**, 59-69.

De Bernardez Clark,E., 1998. Refolding of recombinant proteins. *Current Opinion in Biotechnology*, **9**, 157-163.

Demand,J., Lüders,J., Höhfeld,J., 1998. The Carboxy-Terminal Domain of Hsc70 Provides Binding Sites for a Distinct Set of Chaperone Cofactors. *Molecular Cell Biol*ogy **18**, 2023–2028.

Desai,M., ter Kuile,F.O., Nosten,F., McGready,R., Asamoa,K., Brabin,B., Newman,R.D., 2007. Epidemiology and burden of malaria in pregnancy. *Lancet Infectious Diseases*, **7**, 93-104.

Dudek,J., Greiner,M., Muller,A., Hendershot,LM., Kopsch,K., Nastainczyk,W., Zimmermann,R., 2005. ERj1p has a basic role in protein biogenesis at the endoplasmic reticulum. *Nature Structural & Molecular Biology*, **12**, 1008-1014.

Edman,J.C., Ellis,L., Blacher,R.W., Roth,R.A., Rutter,W.J., 1985. Sequence of protein disulphide isomerase and implications of its relationship to thioredoxin. *Nature*, **317**, 267-270.

Ellgaard,L., Ruddock,L.W., 2005. The human protein disulphide isomerase family: substrate interactions and functional properties. *EMBO Reports*, **6**, 28-32.

Ellgaard,L., Helenius,A., 2001. ER quality control: towards an understanding at the molecular level. *Current Opinion in Cell Biology*, **13**, 431-437.

Ellgaard,L., Molinari,M., Helenius,A., 1999. Setting the Standards: Quality Control in the Secretory Pathway. *Science*, **286**, 1882-1888.

Fagioli,C., Mezghrani,A., Sitia,R., 2001. Reduction of interchain disulfide bonds precedes the dislocation of Ig-μ chains from the endoplasmic reticulum to the cytosol for proteasomal degradation. *Journal of Biological Chemistry*, **276**, 40962-40967.

Feldman,D.E., Frydman,J., 2000. Protein folding in vivo: the importance of molecular chaperones. *Current Opinion in Structural Biology*, **10**, 26-33.

Fink,A.L., 1999. Chaperone-Mediated Protein Folding. *Physiological Reviews*, **79**, 425-449.

Flaherty,K.M., DeLuca-Flaherty,C., McKay,D.B., 1990. Three-dimensional structure of the ATPase fragment of a 70K heat-shock cognate protein. *Nature*, **346**, 623-628.

Foley,M., Tilley,L., Sawyer,W.H., Anders,R.F., 1991. The ring-infected erythrocyte surface antigen of *Plasmodium falciparum* associates with spectrin in the erythrocyte membrane. *Molecular and Biochemical Parasitology*, **46**, 137-147.

Gamo,F.J., Sanz,L.M., Vidal,J., de Cozar,C., Alvarez,E., Lavandera,J.L., Vanderwall,D.E., Green,D.V.S., Kumar,V., Hasan,S., Brown,J.R., Peishoff,C.E., Cardon,L.R., Garcia-Bustos,J.F., 2010. Thousands of chemical starting points for antimalarial lead identification. *Nature*, **465**, 305-310.

Genevaux,P., Schwager,F., Georgopoulos,C., Kelley,W.L., 2002. Scanning Mutagenesis Identifies Amino Acid Residues Essential for the in Vivo Activity of the *Escherichia coli* DnaJ (Hsp40) J-Domain. *Genetics*, **162**, 1045-1053.

Greene,M.K., Maskos,K., Landry,S.J., 1998. Role of the J-domain in the cooperation of Hsp40 with Hsp70. *Proceedings of the National Academy of Sciences*, **95**, 6108-6113.

Guerin,P.J., Olliaro,P., Nosten,F., Druilhe,P., Laxminarayan,R., Binka,F., Kilama,W.L., Ford,N., White,N.J., 2002. *The Lancet Infectious Disease*, **2**, 564-573.

Haas,I.G., Wabl,M., 1983. Immunoglobulin heavy chain binding protein. *Nature*, **306**, 387-389.

Hall,T.A., 1999. BioEdit: a user-friendly biological sequence alignment editor and analysis program for Windows 95/98/NT. *Nucleic Acids Symposium Series*, **41**, 95–98.

Hamman,B.D., Hendershot,L.M., Johnson,A.E., 1998. BiP Maintains the Permeability Barrier of the ER Membrane by Sealing the Lumenal End of the Translocon Pore before and Early in Translocation. *Cell*, **92**, 747-758.

Han,W., Christen,P., 2003. Mechanism of the Targeting Action of DnaJ in the DnaK Molecular Chaperone System. *Journal of Biological Chemistry*, **278**, 19038-19043.

Hannig,G., Makrides,S.C., 1998. Strategies for optimizing heterologous protein expression in *Escherichia coli*. *Trends in Biotechnology*, **16**, 54-60.

Hennessy,F., Nicoll,W.S., Zimmermann,R., Cheetham,M.E., Blatch,G.L., 2005. Not all J domains are created equal: Implications for the specificity of Hsp40-Hsp70 interactions. *Protein Science*, **14**, 1697-1709.

Hiller,N.L., Bhattacharjee,S., van Ooij,C., Liolios,K., Harrison,T., Lopez-Estraño,C., Haldar,K., 2004. A Host-Targeting Signal in Virulence Proteins Reveals a Secretome in Malarial Infection. *Science*, **306**, 1934-1937.

Ho,S.N., Hunt,H.D., Horton,R.M., Pullen,J.K., Pease,L.R., 1989. Site-directed mutagenesis by overlap extension using the polymerase chain reaction. *Gene*, **77**, 51-59.

Hoseki,J., Ushioda,R., Nagata,K., 2010. Mechanism and components of endoplasmic reticulum-associated degradation. *Journal of Biochemistry*, **147**, 19-25.

Hosoda,A., Kimata,Y., Tsuru,A., Kohno,K., 2003. JPDI, a Novel Endoplasmic Reticulum-resident Protein Containing Both a BiP-interacting J-domain and Thioredoxin-like Motifs. *Journal of Biological Chemistry*, **278**, 2669-2676.

http://www.ebi.ac.uk
(Access 1 December 2011)

http://www.expasy.ch/prosite
(Access 1 December 20011)

http://www.ncbi.nlm.nih.gov
(Access 1 December 2011)

Jacquerioz,FA., Croft,AM., 2009. Drugs for preventing malaria in travellers. *Cochrane Database of Systematic Reviews*, **4**, CD006491.

Joiner,K.A., 1991. Rhoptry lipids and parasitophorous vacuole formation: A slippery issue. *Parasitology Today*, **7**, 226-227.

Joshi,B., Biswas,S., Sharma,Y.D., 1992. Effects of heat-shock on *P. falciparum* viability, growth and expression of the heat-shock PfHsp70-1 gene. *FEBS Letters*, **312**, 91-94.

Kadowaki,H., Kadowaki,T., Wondisford,F.E., Taylor,S.I., 1989. Use of the polymerase chain reaction catalyzed by *Taq* DNA polymerase for site-specific mutagenesis. *Gene*, **76**, 161-166.

Käll,L., Krogh,A., Sonnhammer,E.L.L., 2005. An HMM posterior decoder for sequence feature prediction that includes homology information. *Bioinformatics*, **21**, 251–257.

Kappes,B., Suetterlin,B.W., Hofer-Warbinek,R., Humar,R., Franklin,R.M., 1993. Two major phosphoproteins of *Plasmodium falciparum* are heat shock proteins. *Molecular & Biochemical Parasitology*, **59**, 83-94.

Kathir,K.M., Kumar,T.K.S., Rajalingam,D., Yu,C., 2005. Time-dependent changes in the denatured state(s) influence the folding mechanism of an all β-sheet protein. *Journal of Biological Chemistry*, **280**, 29682-29688.

Kelly,W.L., 1998. The J-domain family and the recruitment of chaperone power. *Trends in Biological Sciences*, **23**, 222-227.

Kilejian,A., Jensen,J.B., 1977. A histidine-rich protein from *Plasmodium falciparum* and its interaction with membranes. *Bull World Health Organ*, **55**, 191-197.

Kong,J., Yu,S., 2007. Fourier Transform Infrared Spectroscopic Analysis of Protein Secondary Structures. *Acta Biochimica et Biophysica Sinica*, **39**, 549–559.

Kooij,T.W.A., Janse,C.J., Waters,A.P., 2006. *Plasmodium* post-genomics: better the bug you know? *Nature Reviews Microbiology*, **4**, 344-357.

Kuchner,O., Arnold,F.H., 1997. Directed evolution of enzyme catalysts. *Trends in Biotechnology*, **15**, 523–530.

Külzer,S., Rug,M., Brinkmann,K., Cannon,P., Cowman, A., Lingelbach,K., Blatch,G.L., Maier,A.G., Przyborski,J.M., 2010. Parasite-encoded Hsp40 proteins define novel mobile structures in the cytosol of the *P. falciparum*-infected erythrocyte. *Cellular Microbiology*, **12**, 1398–1420.

Kumar,A., Tanveer,A., Biswas,S, Ram,E.V., Gupta,A., Kumar,B., Habib,S., 2010. Nuclear-encoded DnaJ homologue of *Plasmodium falciparum* interacts with replication ori of the apicoplast genome. *Molecular Microbiology*, **75**, 942-956.

Kumar,N., Zhao,Y., Graves,P., Perez Folgar,J., Maloy,L., Zheng,H., 1990. Human immune response directed against *Plasmodium falciparum* heat shock-related proteins. *Infection and Immunity*, **58**, 1408–1414.

Kumar,N., Zheng,H., 1992. Nucleotide sequence of a *Plasmodium falciparum* stress protein with similarity to mammalian 78 kDa glucose-regulated protein. *Molecular & Biochemical Parasitology*, **56**, 353-356.

Kumar,N., Koski,G., Harada,M., Aikawa,M., Zheng,H., 1991. Induction and localization of *Plasmodium falciparum* stress proteins related to the heat shock protein 70 family. *Molecular & Biochemical Parasitology*, **48**, 47-58.

Kurisu,J., Honma,A., Miyajima,H., Kondo,S., Okumura,M., Imaizumi,K., 2003. MDG1/ERdj4, an ER-resident DnaJ family member, suppresses cell death induced by ER stress. *Genes Cells*, **8**, 189-202.

LaCount,D.J., Vignali,M., Chettier,R., Phansalkar,A., Bell,R., Hesselberth,J.R., Schoenfeld,L.W., Ota,I., Sahasrabudhe,S., Kurschner,C., Fields,S., Hughes,R.E., 2005. A protein interaction network of the malaria parasite *Plasmodium falciparum*. *Nature*, **438**, 103-107.

Lau,P.P., Villanueva,H., Kobayashi,K., Nakamuta,M., Chang,B. H., Chan,L., 2001. A DnaJ protein, apobec-1-binding protein-2, modulates apolipoprotein B mRNA editing. *Journal of Biological Chemistry*, **276**, 46445-46452.

Laufen,T., Mayer,M.P., Beisel,C., Klostermeier,D., Mogk,A., Reinstein,J., Bukau,B., 1999. Mechanism of regulation of Hsp70 chaperones by DnaJ cochaperones. *Proceedings of the National Academy of Sciences*, **96**, 5452-5457.

Laveran, A., 1881. Un nouveau parasite trouvé dans le sang de malades atteints de fièvre palustre. Origine parasitaire des accidents de l'impaludisme. *Bulletins et Mémoires de la Société Médicale des Hôpitaux de Paris*, **17**,158-164.

Li,J., Qian,X., Sha,B., 2009. Heat shock protein 40: structural studies and their functional implications. *Protein and Peptide Letters*, **16**, 606-612.

Liberek,K., Skowyra,D., Zylicz,M., Johnson,C., Georgopoulos,C., 1991. The *Escherichia coli* DnaK chaperone, the 70-kDa heat shock protein eukaryotic equivalent, changes conformation upon ATP hydrolysis, thus triggering its dissociation from a bound target protein. *Journal of Biological Chemistry*, **266**, 14491-14496.

Lievremont,J.P., Rizzuto,R., Hendershot,L., Meldolesi,J., 1997. BiP, a Major Chaperone Protein of the Endoplasmic Reticulum Lumen, Plays a Direct and Important Role in the Storage of the Rapidly Exchanging Pool of Ca^{2+}. *Journal of Biological Chemistry*, **272**, 30873-30879.

Lilie,H., Schwarz,E., Rudolph, R., 1998. Advances in refolding of proteins produced in *E. coli*. *Current Opinion in Biotechnology*, **9**, 497-501.

Malhotra,J.D., Kaufman,R.J., 2007. The endoplasmic reticulum and the unfolded protein response. *Seminars in Cell & Developmental Biology*, **18**, 716-731.

Marti,M., Good,R.T., Rug,M., Knuepfer,E., Cowman,A.F., 2004. Targeting Malaria Virulence and Remodeling Proteins to the Host Erythrocyte. *Science*, **306**, 1930-1933.

Martinez-Yamout,M., Legge,G.B., Zhang,O., Wright,P.E., Dyson,H.J., 2000. Solution Structure of the Cysteine-rich Domain of the *Escherichia coli* Chaperone Protein DnaJ. *Journal of Molecular Biology*, **300**, 805-818.

Matambo,T.S., Odunuga,O.O., Boshoff,A., Blatch,G.L., 2004. Overproduction, purification, and characterization of the *Plasmodium falciparum* heat shock protein 70. *Protein Expression and Purification*, **33**, 214-222.

Mayer,M., Bukau,B., 2005. Hsp70 chaperones: Cellular functions and molecular mechanism. *Cellular and Molecular Life Sciences*, **62**, 670-684.

Meyer,HA., Grau,H., Kraft,R., Kostka,S., Prehn,S., Kalies,K.U., Hartmann,E., 2000. Mammalian Sec61 is associated with Sec62 and Sec63. *Journal of Biological Chemistry*, **275**, 14550-14557.

Minami,Y., Hohfeld,J., Ohtsuka,K., Hartl,F.U., 1996. Regulation of the heat-shock protein 70 reaction cycle by the mammalian DnaJ homolog, Hsp40. *Journal of Biological Chemistry*, **271**, 19617-19624.

Misra,G., Ramachandran,R., 2009. Hsp70-1 from *Plasmodium falciparum*: protein stability, domain analysis and chaperone activity. *Biophysical Chemistry*, **142**, 55-64.

Modisakeng,K.W., Jiwaji,M., Pesce,E.R., Robert,J., Amemiya,C.T., Dorrington,R.A., Blatch,G.L., 2009. Isolation of a *Latimeria menadoensis heat shock protein 70* (*Lmhsp70*) that has all the features of an inducible gene and encodes a functional molecular chaperone. *Molecular Genetics and Genomics*, **282**, 185-196.

Newton,P., Proux,S., Green,M., Smithuis,F., Rozendaal,J., Prakongpan,S., Chotivanich,K., Mayxay,M., Looareesuwan,S., Farrar,J., Nosten,F., White,N.J., 2001. Fake artesunate in southeast Asia. *Lancet*, **357**, 1948-1950.

Nicoll,W.S., Botha,M., McNamara,C., Schlange,M., Pesce,E.R., Boshoff, A., Ludewig,M.H., Zimmermann,R., Cheetham,M.E., Chapple,J.P., Blatch, G.L., 2007. Cytosolic and ER J-domains of mammalian and parasitic origin can functionally interact with DnaK. *International Journal of Biochemistry and Cell Biology*, **39**, 1357-2725.

Noiva,R., 1999. Protein disulfide isomerase: the multifunctional redox chaperone of the endoplasmic reticulum. *Seminars in Cell & Developmental Biology*, **10**, 481–493.

Nyalwidhe,J., Lingelbach, K., 2006. Proteases and chaperones are the most abundant proteins in the parasitophorous vacuole of *Plasmodium falciparum*-infected erythrocytes. *Proteomics*, **6**, 1563–1573.

Ochman,H., Gerber,A.S., Hartl,D.L., 1988. Genetic applications of an inverse Polymerase Chain Reaction. *Genetics*, **120**, 321-623.

Otero,J.H., Lizák,B., Hendershot,L.M., 2010. Life and death of a BiP substrate. *Seminars in Cell & Developmental Biology*, **21**, 472-478.

Pellecchia,M., Szyperski,T., Wall,D., Georgopoulos,C., Wüthrich,K., 1996. NMR Structure of the J-domain and the Gly/Phe-rich Region of the *Escherichia coli* DnaJ Chaperone. *Journal of Molecular Biology*, **260**, 236-250.

Pesce,E.R., Acharya,P., Tatu,U., Nicoll,W.S., Shonhai,A., Hoppe,H.C, Blatch,G.L., 2008. The *Plasmodium falciparum* heat shock protein 40, Pfj4, associates with heat shock protein 70 and shows similar heat induction and localisation patterns. *International Journal of Biochemistry & Cell Biology*, **40**, 2914-2926.

Peterson,M.G., Crewther,P.E., Thompson,J.K., Corcoran,L.M., Coppel,R.L., Brown,G.V., Anders,R.F., Kemp,D.J., 1988. A second antigenic heat shock protein of *Plasmodium falciparum*, *DNA*, **7**, 71-78.

Plemper,R.K., Bordallo,J., Deak,P.M., Taxis,C., Hitt,R., Wolf,D.H., 1999. Genetic interactions of Hrd3p and Der3p/Hrd1p with Sec61p suggest a retro-translocation complex mediating protein transport for ER degradation. *Journal of Cell Science*, **112**, 4123-4134.

Pologe,L.G., Pavlovec,A., Shio,H., Ravetch,J., 1987. Primary structure and subcellular localization of the knob-ssociated histidine-rich protein of *Plasmodium falciparum*. *Proceedings of the National Academy of Sciences*, **84**, 7139-7143.

Price,R., van Vugt,M., Phaipun,L., Luxemburger,C., Simpson,J., McGready,R., ter Kuile,F., Kham,A., Chongsuphajaisiddhi,T., White,N.J., Nosten,F., 1999. Adverse effects in patients with acute *falciparum* malaria treated with artemisinin derivatives. *American Journal of Tropical Medicine and Hygiene*, **60**, 547-555.

Prols,F., Mayer,M.P., Renner,O., Czarnecki,P.G., Ast,M., Gassler,C., Wilting,J., Kurz,H., Christ,B., 2001. Upregulation of the cochaperone Mdg1 in endothelial cells is induced by stress and during *in vitro* angiogenesis. *Experimental Cell Research*, **269**, 42-53.

Ramya,T.C.N., Karmodiya,K., Surolia,A., Surolia,N., 2007. 15-Deoxyspergualin Primarily Targets the Trafficking of Apicoplast Proteins in *Plasmodium falciparum*. *Journal of Biological Chemistry*, **282**, 6388-6397.

Ramya,T.N.C., Surolia,N., Surolia,A., 2007. 15-Deoxyspergualin inhibits eukaryotic protein synthesis through eIF2α phosphorylation. *Biochemical Journal*, **401**, 411–420.

Ramya,T.N.C., Surolia,N.N., Surolia,A., 2006. 15-Deoxyspergualin modulates *Plasmodium falciparum* heat shock protein function. *Biochemical and Biophysical Research Communications*, **348**, 585-592.

Reiter,P., 2000. From Shakespeare to Defoe: Malaria in England in the Little Ice Age. *Emerging Infectious Disease*, **6**, 1–11.

Ridder,R., Schmitz,R., Legay,F., Gram,H., 1995. Generation of rabbit monoclonal antibody fragments from a combinatorial phage display library and their production in the yeast *Pichia pastoris*. *Biotechnology*, **13**, 255-260.

Robbins,J., Dilworth,S.M., Laskey,R.A., Dingwall,C., 1991. Two interdependent basic domains in nucleoplasmin nuclear targeting sequence: identification of a class of bipartite nuclear targeting sequence. *Cell*, **64**, 615-623.

Rosenthal,P.J., 2008. Artesunate for the Treatment of Severe *Falciparum* Malaria. *New England Journal of Medicine*, **358**, 1829-1836.

Ross R., 1898. The role of the mosquito in the evolution of the malaria parasite. *Lancet*, **2**, 489.

Rozendaal,J., 2001. Fake antimalaria drugs in Cambodia. *Lancet*, **357**, 890.

Rug,M., Maier,A., 2011. The Heat Shock Protein 40 Family of the Malaria Parasite *Plasmodium falciparum*. *Life*, **63**, 1081-1086.

Sabeti,P., 2008. Natural Selection: Uncovering Mechanisms of Evolutionary Adaptation to Infectious Disease. *Nature education*, **1**, **1**.

Samudzi,R.R., Leman,P.A., Paweska,J.T., Swanepoel,R., Burt,F.J., 2012. Bacterial expression of Crimean-Congo hemorrhagic fever virus nucleoprotein and its evaluation as a diagnostic reagent in an indirect ELISA. *Journal of Virological Methods*, **179**, 70-76.

Sargeant,T., Marti,M., Caler,E., Carlton,J., Simpson,K., Speed,T., Cowman,A., 2006. Lineage-specific expansion of proteins exported to erythrocytes in malaria parasites. *Genome Biology*, **7**, R12.1-R12.22.

Schwaller,M., Wilkinson,B., Gilbert,H.F., 2003. Reduction-Reoxidation Cycles Contribute to Catalysis of disulfide Isomerization by Protein-disulfide Isomerase. *Journal of Biological Chemistry*, **278**, 7154-7159.

Sevier,C.S., Kaiser,C.A., 2002. Formation and transfer of disulphide bonds in living cells. *Nature Reviews Molecular Cell Biology*, **3**, 836-847.

Sharma,YD., 1992. Structure and possible function of heat-shock proteins in *falciparum* malaria. *Comparative Biochemistry and Physiology*, **102**, 437-444.

Shen,J., Chen,X., Hendershot,L., Prywes,R., 2002. ER Stress Regulation of ATF6 Localization by Dissociation of BiP/GRP78 Binding and Unmasking of Golgi Localization Signals. *Developmental Cell*, **3**, 99-111.

Shen,Y., Meunier,L., Hendershot,L.M., 2002. Identification and characterization of a novel endoplasmic reticulum (ER) DnaJ homologue, which stimulates ATPase activity of BiP *in vitro* and is induced by ER stress. *Journal of Biological Chemistry*, **277**, 15947-15956.

Shen,Y., Hendershot,L.M., 2005. ERdj3, a Stress-inducible Endoplasmic Reticulum DnaJ Homologue, Serves as a CoFactor for BiP's Interactions with Unfolded Substrates. *Molecular Biology of the Cell*, **16**, 40-50.

Shen,Y., Meunier,L., Hendershot,L.M. 2002. Identification and characterization of a novel endoplasmic reticulum (ER) DnaJ homologue, which stimulates ATPase activity of BiP *in vitro* and is induced by ER stress. *Journal of Biological Chemistry*, **277**, 15947-15956.

Shonhai,A., Botha,M., de Beer,T.A., Boshoff,A., Blatch,G.L., 2008. Structure-function study of a *Plasmodium falciparum* Hsp70 using three dimensional modelling and *in vitro* analyses. *Protein & Peptide Letters,* **15**, 1117-1125.

Shonhai,A., Boshoff,A., Blatch,G.L., 2007. The structural and functional diversity of Hsp70 proteins from *Plasmodium falciparum*. *Protein Science*, **16**, 1803–1818.

Shonhai,A., Boshoff,A., Blatch,G.L., 2005. *Plasmodium falciparum* heat shock protein 70 is able to suppress the thermosensitivity of an *Escherichia coli* DnaK mutant strain. *Molecular Genetics and Genomics*, **4,** 70-78.

Singh,S.M., Panda,A.K., 2005. Solubilization and refolding of bacterial inclusion body proteins. *Journal of Bioscience and Bioengineering*, **99**, 303-310.

Silva,MD., Cooke,B.M., Guillotte,M., Buckingham,D.W., Sauzet,J.P., *et al*., 2005. A role for the *Plasmodium falciparum* RESA protein in resistance against heat shock demonstrated using gene disruption. *Molecular Microbiology*, **56**, 990-1003.

Sitia,R., Braakman,I., 2003. Quality control in the endoplasmic reticulum protein factory. *Nature*, **426**, 891-894.

Skowronek,M.H., Rotter,M., Haas,I.G., 1999. Molecular characterization of a novel mammalian DnaJ-like Sec63p homolog. *Biological Chemistry*, **380,** 1133–1138.

Šlapeta,J., Keithly,J.S., 2004. *Cryptosporidium parvum* mitochondrial-type Hsp70 targets homologous and heterologous mitochondria. *Eukaryotic Cell*, **3**, 483-494.

Sommer,T., Wolf,D.H., 1997. Endoplasmic reticulum degradation: reverse protein flow of no return. *The FASEB Journal*, **11**, 1227-1233.

Stüber,D., Matile,H., Garotta,G., 1990. System for high-level production in *Escherichia coli* and rapid purification of recombinant proteins: application to epitope mapping, preparation of antibodies and structure–function analysis. *Immunological Methods*, **4**, 121–152.

Suh,W.C., Lu,C.Z., Gross,C.A., 1999. Structural Features Required for the Interaction of the Hsp70 Molecular Chaperone DnaK with Its Cochaperone DnaJ. *Journal of Biological Chemistry*, **274**, 30534-30539.

Surolia,N., Padmanaban,G., 1991. Chloroquine inhibits heme-dependent protein synthesis in *Plasmodium falciparum*. *Proceedings of the National Academy of Sciences*, **88**, 4786–4790.

Szabo,A., Langer,T., Schröder,H., Flanagan,J., Bukau,B., Hartl,F.U., 1994. The ATP hydrolysis-dependent reaction cycle of the *Escherichia coli* Hsp70 system DnaK, DnaJ, and GrpE. *Proceedings of the National Academy of Sciences*, **91**, 10345-10349.

Thomas,J.G., Baneyx,F., 1996. Protein misfolding and inclusion body formation in recombinant *Escherichia coli* cells overexpressing Heat-shock proteins. *Journal of Biological Chemistry*, **271,** 11141-11147.

Thompson,J.D., Higgins,D.G., Gibson,T.J., 1994. CLUSTAL W: improving the sensitivity of progressive multiple sequence alignment through sequence weighting, position-specific gap penalties and weight matrix choice. *Nucleic Acids Research*, **22**, 4673-4680.

Timasheff,S.N., 1998. Control of protein stability and reactions by weakly interacting cosolvents: The simplicity of the complicated. *Advances in Protein Chemistry*, **51**, 355-432.

Tolia,N.H., Joshua-Tor, L., 2006. Strategies for protein coexpression in Escherichia coli. *Nature Methods*, **3**, 55 - 64.

Tortorella,D., Story,C.M., Huppa,J.B., Wiertz,E.J.H.J., Jones,T.R., Ploegh,H.L., 1998. Dislocation of type I membrane proteins from the ER to the cytosol is sensitive to changes in redox potential. *Journal of Cell Biology*, **142**, 365–376.

Trampuz,A., Jereb,M., Muzlovic,I., Prabhu,R., 2003. Critical review: Severe malaria. *Critical Care*, **7 (4)**, 315–323.

Triglia,T., Stahl,H.D., Crewther,P.E., Scanlon,D., Brown,G.V., Anders,R.F., Kemp,D.J., 1987. The complete sequence of the gene for the knob-associated histidine-rich protein from *Plasmodium falciparum*. *EMBO Journal.* **6**: 1413-1419.

Tsai,B., Ye,Y., Rapoport,T.A., 2002. Retro-translocation of proteins from the endoplasmic reticulum into the cytosol. *Nature Reviews Molecular Cell Biology*, **3**, 246–255.

Tsai,J., Douglas,M.G., 1996. A Conserved HPD Sequence of the J-domain Is Necessary for YDJ1 Stimulation of Hsp70 ATPase Activity at a Site Distinct from Substrate Binding. *Journal of Biological Chemistry*, **271**, 9347-9354.

Tu,B.P., Weissman,J.S., 2004. Oxidative protein folding in eukaryotes. *Journal of Cell Biology*, **164**, 341-346.

Tyedmers,J., Lerner,M., Bies,C., Dudek,J., Skowronek,M.H., Haas,I.G., Heim,N., Nastainczyk,W., Volkmer,J., Zimmermann,R., 2000. Homologs of the yeast Sec complex subunits Sec62p and Sec63p are abundant proteins in dog pancreas microsomes. *Proceedings of the National Academy of Sciences*, **97**, 7214-7219.

Ushioda,R., Hoseki,J., Araki,K., Jansen,G., Thomas,D.Y., Nagata,K., 2008. ERdj5 Is Required as a Disulfide Reductase for Degradation of Misfolded Proteins in the ER. *Science*, **321**, 569-572.

Vincensini,L., Richert,S., Blisnick,T., Van Dorsselaer,A., Leize-Wagner,E., Rabilloud, T., Braun Breton,C., 2005. Proteomic analysis identifies novel proteins of the Maurer's clefts, a secretory compartment delivering *Plasmodium falciparum* proteins to the surface of its host cell. *Molecular & Cellular Proteomics*, **4**, 582-593.

Vitale,A., Ceriotti,A., Denecke., 1993. The Role of the Endoplasmic Reticulum in Protein Synthesis, Modification and Intracellular. *Journal of Experimental Botany*, **44**, 1417-1444.

Walter,S., Buchner,J., 2002. Molecular chaperones--cellular machines for protein folding. *Angewandte Chemie, International Edition*, **41**, 1098–1130.

Walsh,P., Bursac,D., Law,Y.C., Cyr,D., Lithgow,T., 2004. The J-protein family: modulating protein assembly, disassembly and translocation. *EMBO Reports*, **5**, 567-571.

Wang,T.F., Chang,J.H., Wang,C., 1993. Identification of the peptide binding domain of hsc70. 18-Kilodalton fragment located immediately after ATPase domain is sufficient for high affinity binding. *Journal of Biological Chemistry*, **268**, 26049-26051.

Watanabe,J., 1997. Cloning and characterization of heat shock protein DnaJ homologues from *Plasmodium falciparum* and comparison with ring infected erythrocyte surface antigen[1]. *Molecular and Biochemical Parasitology*, **88**, 253-258.

White, N., 2004. Antimalarial drug resistance. *Journal of Clinical Investigation*, **113**, 1084-1092.

White,N.J., Looareesuwan,S., Warrell,D.A., 1983. Quinine and quinidine: a comparison of EKG effects during the treatment of malaria. *Journal of Cardiovascular Pharmacology*, **5**, 173-175.

Wittung-Stafshede,P., Guidry,J., Horne,B.E., Landry,S.J., 2003. The J-Domain of Hsp40 Couples ATP Hydrolysis to Substrate Capture in Hsp70. *Biochemistry*, **42**, 4937-4944.

Woodrow,CJ., Haynes,RK., Krishna,S., 2005. Artemisinins. *Postgraduate Medical Journal*, **81**, 71-80.

World Health Organisation. (http://www.who.int/en/)
(Access 6 February 2012)

Wu,Y., Li,J., Jin,Z., Fu,Z., Sha,B., 2005. The Crystal Structure of the C-terminal Fragment of Yeast Hsp40 Ydj1 Reveals Novel Dimerization Motif for Hsp40. *Journal of Molecular Biology*, **346**, 1005-1011.

Yan,W., Frank,CL., Korth,MJ., Sopher,BL., Novoa,I., Ron,D., Katze,M.G., 2002. Control of PERK eIF2alpha kinase activity by the endoplasmic reticulum stress-induced molecular chaperone P58IPK. *Proceedings of the National Academy of Sciences of the United States of America*, **99**,15920-15925.

Yu,M., Haslam,R.H., Haslam,D.B., 2000. HEDJ, an Hsp40 cochaperone localized to the endoplasmic reticulum of human cells. *Journal of Biological Chemistry*, **275**, 24984-24992.

Zahedi,RP., Volzing,C., Schmitt,A., Frien,M., Jung,M., Dudek,J., Wortelkamp,S., Sickmann,A., Zimmermann,R., 2009. Analysis of the membrane proteome of canine pancreatic rough microsomes identifies a novel Hsp40, termed ERj7. *Proteomics*, **9**, 3463-3473.

Zoller,M.J., 1991. New molecular biology methods for protein engineering. *Current Opinion in Biotechnology*, **2**, 526–531.

Zuccala,E.S., Baum,J., 2011. Cytoskeletal and membrane remodelling during malaria parasite invasion of the human erythrocyte. *British Journal of Haematology*, **154**, 680-689.